UNIVERSITA' DEGLI STUDI DI ROMA
"TOR VERGATA"

Facoltà di Ingegneria
Per l'Ambiente e il Territorio

DOTTORATO DI RICERCA IN
INGEGNERIA AMBIENTALE

XXI CICLO

Absolute Risk Analysis Applied to Contaminated Sites

COORDINATORE
Prof. Renato Gavasci

TUTOR
Prof. Renato Baciocchi

DOTTORANDO
Ing. Emiliano Scozza

A. A. 2008/2009

INDEX

ABSTRACT

The instrument 'Risk Analysis' for the assessment of contaminated sites has been used for several years and has received a strong boost in the U.S. in the framework of the Superfund Program and in Italy has gained wider relevance after the introduction of new environmental legislation.

Risk analysis is currently the most advanced procedure for the evaluation of the degree of contamination of an area and to define the priorities and modalities of intervention in the site itself. The risk analysis procedure can be conducted in forward mode or backward mode. The forward mode allows estimating the health risk for the exposed receptor, whether located near the site (on-site) or at some distance (off-site), given the concentration at the source of contamination. Having instead set the level of risk to health considered acceptable to the exposed receptor, the backward mode allows the calculation of the highest concentration at the source compatible with the condition of acceptability of the risk, i.e. the so-called site-specific target level.

The Italian Agency for Environmental Protection (now ISPRA, formerly APAT) has recently issued a guideline document that provides a standard procedure for application of risk analysis to contaminated sites. This guideline document is based on a Tier 2 risk analysis approach, which is based on a series of simplifying assumptions:

- Contaminant transport is described through the analytical equations which are not validated with experimental data or with numerical model results.
- Attenuation of contaminant through biodegradation phenomena is not accounted for;
- Exposure to contaminants through the food chain is neglected.

Besides, when this thesis was started, the document included only the procedure for applying the risk analysis in forward mode.

The work performed within this PhD thesis, supported by APAT, was to upgrade the procedure for application of risk analysis to contaminated sites, including also the unresolved issues listed above.

In chapter 1, after a short background on the fundamentals of risk analysis, a procedure to obtain the threshold risk concentration, as requested by the new Italian legislation (D.M. 152/06) was developed.

In chapter 2 the assumption and the procedure suggested by several technical documents and software on the exposure through the food chain were analyzed and a standard procedure was suggested for implementation in the risk analysis framework.

In chapter 3 the results of the analytical equation selected for tier II risk analysis were compared with those provided by numerical transport models. The validation of the equations for Tier 2 risk analysis was performed on two key transport factors:

- The Leaching Factor, LF, which describes the contaminant transport through the vadose zone;
- The Dilution Attenuation Factor, DAF, which describes the contaminant transport through the acquifer.

In chapter 4 the influence of the vadose zone biodegradation related to the indoor vapour intrusion was studied in order to understand how this phenomena can influence the chemical volatilization to indoor environment.

Besides, in the framework of the PhD activities, a risk analysis software, based on the APAT guidelines, was developed and linked to a database of the chemical and toxicological properties of the contaminants, properly developed.

1 BACKGROUND

1.1 THE HEALTH-ENVIRONMENTAL RISK ANALYSIS

Risk Assessment has been defined in different ways by many authors who have studied this topic (Rowe, 1977, NRC, 1983, OTA, 1993, U.S. EPA, 1984; Bowles et al., 1987; Asante-Duah, 1990); in technical terms, Risk Assessment is defined as "systematic process for assessing all the significant risk factors that exist in circumstances of exposure caused by the presence of dangers ". In less technical terms, risk assessment is the evaluation of the consequences on human health of a potentially damaging event in terms of probability that the same consequences may occur.

The evaluation process, by its nature, provides the degree of importance of potential risks examined in the specific case, compared with a unique baseline set; this one is the typically level of acceptability set in the guidelines established by national or international agencies and organizations involved in environmental planning and protection.

The instrument 'Risk Analysis' for the assessment of contaminated sites has been used for several years and has received a strong boost in the U.S. in the framework of the Superfund Program and in Europe with the increasing problem of remediation of a very wide number of sites. Risk assessment or risk analysis, linked to a polluted site, is at present one of the most advanced procedures for assessing the degree of contamination of an area and to define the priorities and the ways of intervention on the site itself.

This risk assessment is carried out, in general, on sites that represent a chronic danger to humans and/or to environment, estimating a level of risk and, consequently, limit values of concentration, determined on the basis of characteristics of the source of pollution, the transport mechanisms and the targets of contamination.

Risk (R), as originally defined in the industrial safety procedures, is considered as the combination of the probability of occurrence of an event (P) and the degree of damage caused by the same event (D):

$$R = P \cdot D$$

Eq. 1-1

The damage resulting from the incidental event (D), in turn, can be given by a hazard (F_p), related to the entity of the possible damage, and a contact factor (F_e), which is a function of the exposure duration:

$$D = F_p \cdot F_e$$

Eq. 1-2

In the case of polluted sites, the probability (P) of occurrence of the event is $P = 1$, since the event has already taken place; the danger factor is the toxicity of the pollutant (T [mg / kg d]$^{-1}$) whereas the contact factor is given by the actual extent of exposure (E [mg / kg d]). Thus the risk (R) resulting from a contaminated site is given by the following expression:

$$R = E \cdot T$$

Eq. 1-3

Where:

E ([mg / kg d]) is the chronic daily intake of the contaminant, and

T ([mg / kg d] -1) the toxicity of the contaminant.

The calculation of the risk differs if the pollutant has carcinogenic or non-carcinogenic.

For carcinogenic effects, the toxicity T is equal to the slope factor (SF, [mg / kg d]$^{-1}$), i.e. the slope of the line correlating the exposure to a given contaminant with the incremental cancer risk.

Thus, Eq. 1-3 becomes:

$$R = E \cdot SF$$

Eq. 1-4

Where:

R (Risk [---]) is the probability of incremental cases of cancer in course of life, caused by exposure to the substance, compared to usual living conditions.

For non-carcinogenic effects, the Reference Dose (RfD [mg / kg d]) is introduced, defined as the daily average of the exposure that has no appreciable adverse effects on human body during the course of life.

$$HQ = \frac{E}{RfD}$$

Eq. 1-5

Where:

HQ (Hazard Quotient [---]) is a “Hazard index” that indicates how much the exposure to the substance exceeds the tolerable or reference dose.

The procedure of risk analysis can be conducted in forward mode or backward mode (Figure 1.1). The forward mode allows estimating the health risk for the exposed receptor, whether located near the site (on-site) or at some distance (off-site), given the concentration at the source of contamination. Having instead set the level of risk to health considered acceptable to the exposed receptor, the backward mode allows the calculation of the highest concentration at the source compatible with the condition of acceptability of the risk, i.e. the so-called site-specific target level.

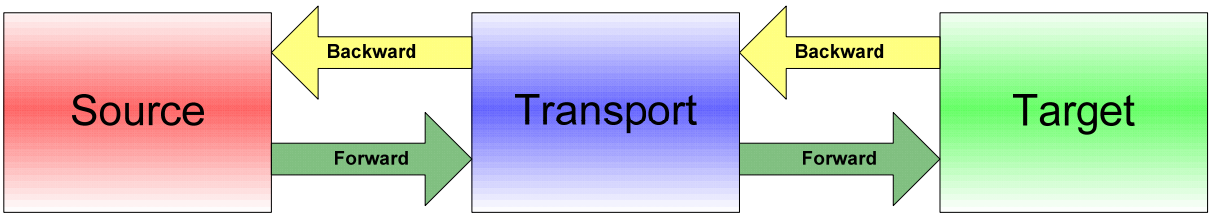

Figure 1.1: Risk analysis application mode.

It seems appropriate to recall the basic principles upon which the procedure is based, valid both for the direct mode and the reverse mode:

- principle of the "Reasonable Worst Case", that concern all the risk analysis procedure steps;
- principle of the “Reasonable Maximum Exposure”, which provides, in relation to the selection of the exposure parameters, the use of reasonably conservative values in order to achieve precautionary results for the protection of human health.

It is also worth noting notes that the absolute risk analysis applies to the assessment of chronic or long-term risks associated with current contamination in environmental matrix (soil surface, deep soil, groundwater, surface water) due to one or more identifiable and delimited sources and not to the assessment of risks from acute exposure or professional exposure in the workplace, which are regulated differently.

1.2 THE RBCA-ASTM TIERED APPROACH

The absolute risk assessment is a scientific process that requires, in its full and strict implementation, a remarkable technical and economic effort, considering the amount of data needed (and thus the investigations, evidence and analysis from which these are derived) and the subsequent mathematical processing. However, notwithstanding the basic principle of the “worst case” that must always lead to choose between alternatives, it’s possible to split the risk evaluation in different levels of analysis, which differ mainly in the timing and in the necessary financial commitment.

The Italian Environmental protection Agency (APAT) has developed a document which provides the methodological principles for conducting a procedure of risk analysis [5], it refers to the procedure RBCA (Risk-Based Corrective Action). This procedure is derived from ASTM (American Society for Testing and Materials) and was published in 1995 under the reference E1739-95 to guide rehabilitation interventions on sites contaminated by hydrocarbons. In 1998 the rule has been updated and supplemented by guidance PS104, which concerns more generally chemicals release(ASTM 1995, ASTM 1998).

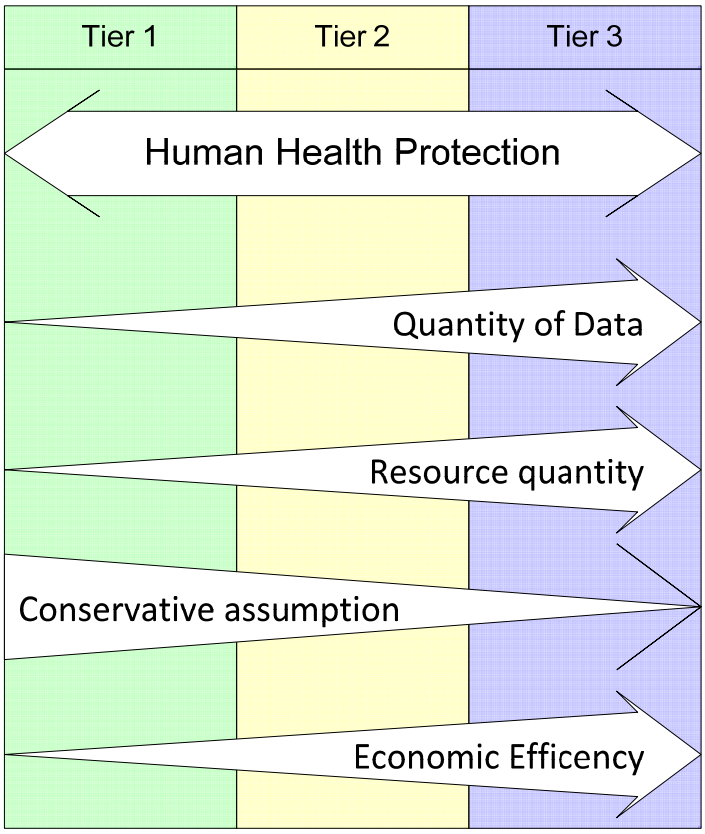

Figure 1.2: Risk Analysis level characterization.

The RBCA procedure refers to a gradual approach based on a three levels assessment referred below.

Tier 1

Risk analysis conducted at this level refers to site-generic conditions and can be used as a screening step. It takes into account direct or indirect exposure paths, conservative exposure factors, analytical solution to transport models nature and on-site receptors.

Applying this level of analysis (“tier 1") the so-called Risk Based Screening Levels (RBSL) are obtained.

Tier 2

This level of analysis refers to site-specific conditions and it is therefore a more detailed evaluation with respect to Tier 1. It involves once again the use of analytical models for estimating the concentration at the point of exposure considering a homogenous and isotropic environmental media. Applying this level of analysis (“tier 2") the Site Specific Target Levels (SSTL) are calculated, and can be considered as remediation targets. Both on-site and off-site receptors are considered.

Tier 3

The level 3 analysis allows a more detailed site-specific evaluation. It uses numerical models and probabilistic analysis that allow to account for the heterogeneity of the system, and for the complex geometry of the pollutant source. Its application requires, however, a deeper knowledge of the physical system and, consequently, a more detailed site characterization.

This thesis essentially refers to a Level 2 analysis. This level, being intermediate between the three proposed by the RBCA procedure, represents, generally, a good compromise between the use of tabular values, corresponding to application of Level 1, and application of complex numerical models, typically used for analysis of level 3. A fundamental assumption of a level 2 analysis concerns the use of analytical models for the description of transport of contaminants through the different environmental compartments. This means an extreme simplification of the conceptual model of the site, namely:

- simplification of the geometry of the site;
- simplification of the physical properties of environmental compartment through which migration occurs (e.g., assumptions of homogeneity);
- simpler definition of the geology and the hydrogeology of the site;
- Steady-state conditions;
- simplified representation of the mechanisms of transport and dispersion.

The main advantages of analytical models are the simplicity of implementation, the need to input a limited number of parameters, their numerical stability.

The simplifying assumption behind the analytical models cause the following limitation:

- the impossibility of representing the properties of an heterogeneous media;
- the inability to consider the temporal variability of the simulated events;
- the inability to consider the presence of multiple sources of contamination;
- the inability to consider the irregularities related to the geometry of the site and the source of contamination.

1.3 EXPOSURE ROUTES AND TARGETS

The exposure routes are those by which the potential target comes into contact with the chemical contaminants species.

There is a direct exposure if the exposure pathways coincides with the source of contamination; there is an indirect exposure if the receptor contact with the pollutant occurs as a result of its migration from the source to the receptor and therefore occurs at a certain distance from the source.

In general, the routes of exposure can be divided into four categories:

- surface soil (SS);
- outdoor air (AO);
- indoor air (AI);
- ground water (GW).

For each source of contamination it is possible to match more than one way of exposure, and therefore in different sites there are several combinations, depending on the specific features of the site itself.

To implement a health risk analysis the considered targets of contamination are only humans. These receptors are differentiated according to:

- their location: targets are defined as on-site if located at the source of contamination and off-site if located at a certain distance from it, but shell within the potential influence of the contaminated site.
- the intended use of the soil: in this thesis, the types of soil use are differentiated into:
    - Residential, where human targets are both adults and children;
    - Recreational, where human targets are both adults and children;
    - Industrial / Commercial, where targets are only adults.

Site-specific information are required to define the exposure route pathways for the different soil use . This information includes:

- the use of the current site and the intended use provided by urban development tools;
- soil use around the site (residential, industrial, commercial, recreational);
- the presence of wells for drinking water use;
- the distribution of the resident population and other human activities.

In particular, if the current and future uses of the site are different, it is appropriate to conduct a risk analysis for each of them and then select the more precautionary result in terms of risk. Whenever the future site use is not known, risk analysis must be performed in relation to the current situation, considering that it is always necessary to conduct an integrative risk assessment at the time of the change of destination and / or use of the site. Results related to conducted risk analysis should be maintained as instruments of urban planning.

1.3.1 Calculation of Effective Exposure Rate

Exposure E [mg (kg d)$^{-1}$] is given by the product between the concentration of the contaminant in an environmental matrix (surface soil, indoor air, outdoor air), calculated at the C_{poe} (point of exposure) and the effective exposure rate EM, defined as the daily amount of contaminated matrix to which the receptors are exposed, per unit of body weight:

$$E = C_{poe} \cdot EM$$

Eq. 1-6

For the determination of both terms it is necessary to define the conceptual model of the site. The evaluation of the effective exposure rate EM is reflected in the estimation of the daily dose of the considered environmental matrix, which can be uptaken from human receptors identified in the conceptual model.

The general equation for calculating the effective exposure rate EM [mg / kg / day] is the following:

$$EM = \frac{CR \cdot EF \cdot ED}{BW \cdot AT}$$

Eq. 1-7

Where:

AT indicates the average time of exposure of an individual to a substance;

BW is the body weight [Kg];

CR is the contact rate;

ED is the exposure duration[years]

EF is the Exposure Frequency[day/years].

For carcinogenic compounds, exposure is calculated on the average length of life (AT = 70 years), while for non-carcinogenic ones it is mediated on the actual period of exposure (AT = ED). In this way the risk for carcinogenic compounds is not related to the period of time of direct exposure, but to life duration.

1.4 ABSOLUTE RISK ANALYSIS IN BACKWARD MODE

The aim of this section is to describe the procedure to calculate the risk threshold concentration (CSR) for soil and groundwater with the application of the Tier 2 absolute risk analysis in backward mode, as outlined by APAT [6].

The calculation of the Risk Threshold Concentration (in Italian " Concentrazione soglia di Rischio, CSR) is performed by applying the risk analysis procedure in backward mode, using the same equations applied for the calculation of risk. The following procedure can be followed.

STEP 1: Calculation of acceptable exposure

The risk to human health is differentiated between individual and cumulative:

- Individual Risk: Risk due to single contaminant for one or more routes of exposure.
- Cumulative Risk: Risk due to the cumulation of the effects of several substances for one or more routes of exposure.

For carcinogenic substances, the values of risk considered acceptable are:

- TR = 10^{-6} (individual value)
- TR_{CUM} = 10^{-5} (cumulative value)

For non-carcinogenic substances, the value of risk considered tolerable (for individual risk and cumulative) is:

- THQ = 1 (individual value)
- THQ_{CUM} = 1 (cumulative value)

Given the tolerable risk, it is possible to derive the acceptable exposure (E_{ACC}) for each contaminant, using the following equations for carcinogenic and non carcinogenic effects, :

$$E_{acc} = \frac{TR}{SF}$$

Eq. 1-8

$$E_{acc} = THQ \cdot RfD$$

Eq. 1-9

STEP 2: Calculation of the concentration at the point of exposure

Given the acceptable exposure, it is possible to derive the acceptable concentration at the point of exposure (C_{poe}) through the application of the following equation:

$$C_{poe,acc} = \frac{E_{acc}}{EM}$$

Where EM is the effective exposure rate.

The exposure routes related to each contamination source are shown in Table 1-1.

Table 1-1: Methods of exposure for each contamination source

Source	Pathways
Surface soil	• Dermal contact • Soil ingestion • Outdoor and indoor vapor inhalation • Outdoor and indoor particulate inhalation
Deep Soil	• Outdoor and indoor vapor inhalation • Water ingestion due to leaching
Groundwater	• Water ingestion • Outdoor and indoor vapor inhalation

STEP 3: Calculation of the remediation goals

Once the acceptable exposure and the concentration at the point of exposure are established, it is possible to identify the target remediation value (Threshold Risk Concentration, CSR) by the following relationship:

$$CSR = \frac{C_{poe,acc}}{FT}$$

Where FT is the transport factor which takes in account the mitigation phenomena that occur during the migration of contaminants between the source and the target.

By combining the relationships of the three steps of this procedure, it is possible to determine the risk threshold concentration (CSR) as:

- for carcinogenic substances

$$CSR = \frac{C_{poe,acc}}{FT} = \frac{E_{acc}}{EM \cdot FT} = \frac{TR}{SF \cdot EM \cdot FT}$$

Eq. 1-10

- for non carcinogenic substances

$$CSR = \frac{C_{poe,acc}}{FT} = \frac{E_{acc}}{EM \cdot FT} = \frac{THQ \cdot RfD}{EM \cdot FT}$$

Eq. 1-11

It is worth pointing that the values of threshold risk concentrations (CSR), resulting from the procedure, are referred to the wet soil; then this concentration values have to be converted on a dry basis to perform a comparison with the screening value concentration.
Conversion can be performed with the expression below:

$$C_w = C_{dry} \cdot (1 - \alpha)$$

Where:

$$\alpha = \frac{\theta_w}{\rho_s}$$

In order to calculate the risk threshold concentrations (CSR): the toxicological parameters (Reference Dose-RFD; Slope Factor-SF), the effective exposure rate (EM), the transport factors (FT) and the criteria for cumulating individual substances due to multiple exposure routes have to be established.

1.5 EFFECTIVE EXPOSURE RATE

Estimating the effective exposure rate, EM, requires evaluating the daily dose of the contaminated matrix that is assumed by the human receptors identified in the conceptual model. The general form of the equation used to estimate the effective exposure rate EM [mg/kg/day] has been presented in the previous chapter (Eq. 1-7):

$$EM = \frac{CR \cdot EF \cdot ED}{BW \cdot AT}$$

The selection of the values of the different exposure parameters included in Eq. 1-7 is discussed in the next sections.

1.5.1 Effective Exposure Duration

In this section the different values found for the effective exposure duration in different texts will be discussed. The analyzed documents are: *Users' guide and background technical document for U.S.EPA Region 9's Preliminary Remediation Goals (PRG) table [EPA 2004]*, *Standard Guide for Risk-Based Corrective Action Applied at Petroleum Release Sites [ASTM 1995]* and *Criteri metodologici per l'applicazione dell'analisi assoluta di rischio ai siti contaminati [APAT 2005 rev.0].*

Table 1-2 and Table 1-3 summarize the ED values, provided for the different approaches for residential and industrial receptors, respectively.

Table 1-2: Effective Exposure Duration, Residential

Effective Exposure Duration –Residential						
	Carcinogenic			Non Carcinogenic		
Source	APAT (2005 REV.0)	REGION 9 (EPA 2004)	RBCA (ASTM 1995)	APAT (2005 REV.0)	REGION 9 (EPA 2004)	RBCA (ASTM 1995)
Surface Soil	30	24+6	30	30	6	30
Deep Soil	30	(*)	30	30	(*)	30
Groundwater	30	24+6	30	30	30	30

(*) there is no distinction between surface and deep soil

Table 1-3: Effective Exposure Duration, Industrial

Effective Exposure Duration –Industrial						
Source	Carcinogenic			Non Carcinogenic		
	APAT (2005 REV.0)	REGION 9 (EPA 2004)	RBCA (ASTM 1995)	APAT (2005 REV.0)	REGION 9 (EPA 2004)	RBCA (ASTM 1995)
Surface Soil	30	25	25	30	25	25
Deep Soil	30	(*)	25	30	(*)	25
Groundwater	30	25	25	30	25	25

(*) there is no distinction between surface and deep soil

As it is possible to see, Table 1-2 and Table 1-3 show a clear difference between the effective Exposure Duration provided by the APAT approach and the EPA approach, respectively. In order to identify the most appropriate value for the exposure duration (ED) the Effective Exposure rate was calculated using both approaches for the different exposure scenario and the obtained results compared, as shown in the next section.

1.5.2 Effective Exposure rate calculation

The possible pathways in industrial and residential scenario are reported below with the corresponding equations:

1. Dermal soil contact

$$EM\left[\frac{mg}{Kg \cdot d}\right] = \frac{SA \cdot AF \cdot ABS \cdot EF \cdot ED}{BW \cdot AT}$$

Eq. 1-12

2. Soil ingestion

$$EM\left[\frac{mg}{Kg \cdot d}\right] = \frac{IR \cdot FI \cdot EF \cdot ED}{BW \cdot AT}$$

Eq. 1-13

3. Water ingestion

$$EM\left[\frac{l}{Kg \cdot d}\right] = \frac{IR_w \cdot EF \cdot ED}{BW \cdot AT}$$

Eq. 1-14

4. Outdoor vapor and particulate inhalation

$$EM\left[\frac{m^3}{Kg \cdot d}\right] = \frac{B_o \cdot EF_{go} \cdot EF \cdot ED}{BW \cdot AT}$$

Eq. 1-15

5. Indoor vapor and particulate inhalation

$$EM\left[\frac{m^3}{Kg \cdot d}\right] = \frac{B_i \cdot EF_{gi} \cdot EF \cdot ED}{BW \cdot AT}$$

Eq. 1-16

With the following symbols notations :

SA : Exposed skin area [cm^2];

AF : Soil dermal adherence factor [mg/cm^2-d];

ABS: Dermal Adsorption factor [dimensionless];

IR : Soil ingestion rate [mg/d];

FI : Fraction of ingested soil [dimensionless];

IR_w : Water ingestion rate [l/d];

B_o : Outdoor inhalation [m^3/d];

EF_{go}: Daily outdoor frequency exposure [h/d]

B_i : Indoor inhalation [m^3/d];

EF_{gi}: Daily indoor frequency exposure [h/d]

The values chosen for the exposure parameters were the default data provided in the APAT guidelines [APAT, 2005]. The values of EM for different exposure routes obtained with the exposure

duration values taken from APAT and EPA Region9 guidelines are shown in Table 1-4 and in Table 1-5, respectively.

Table 1-4: Effective Exposure Rate – APAT approach

EFFECTIVE EXPOSURE RATE (EM) – APAT APPROACH					
Exposure	**Target**	**Residential**		**Industrial**	
		Carcinogenic	**Non Carcinogenic**	**Carcinogenic**	**Non Carcinogenic**
Water ingestion [l / Kg_d]	Adult	1,17E-02	2,74E-02	4,19E-03	9,78E-03
	Child	-	-	-	-
Outdoor inhalation [m^3 / Kg_d]	Adult	*3,17E-02*	*7,40E-02*	*8,39E-02*	*1,96E-01*
	Child	-	-	-	-
Indoor inhalation [m^3 / Kg_d]	Adult	9,51E-02	2,22E-01	3,02E-02	7,05E-02
	Child	-	-	-	-
Soil Ingestion [mg / kg_d]	Adult	5,87E-01	1,37E+00	2,10E-01	4,89E-01
	Child	-	-	-	-
Dermal contact Organic compound [mg / kg_d]	Adult	5,05E+00	1,18E+01	3,61E+00	8,41E+00
	Child	-	-	-	-
Dermal contact Inorganic compound [mg / kg_d]	Adult	5,05E-01	1,18E+00	3,61E-01	8,41E-01
	Child	-	-	-	-

Table 1-5: Effective Exposure Rate – EPA approach

EFFECTIVE EXPOSURE RATE (EM) – EPA (REGION 9) APPROACH					
Exposure	**Target**	**Residential**		**Industrial**	
		Carcinogenic	**Non Carcinogenic**		
Water ingestion [l / Kg_d]	Adult	9,39E-03	2,74E-02	3,49E-03	9,78E-03
	Child	5,48E-03	6,39E-02	-	-
Outdoor inhalation [m^3 / Kg_d]	Adult	2,54E-02	7,40E-02	6,99E-02	1,96E-01
	Child	2,30E-02	2,68E-01	-	-
Indoor inhalation [m^3 / Kg_d]	Adult	7,61E-02	2,22E-01	2,52E-02	7,05E-02
	Child	6,90E-02	8,05E-01	-	-
Soil Ingestion [mg / kg_d]	Adult	4,70E-01	1,37E+00	1,75E-01	4,89E-01
	Child	1,10E+00	1,28E+01	-	-
Dermal contact Organic compound [mg / kg_d]	Adult	4,04E+00	1,18E+01	3,01E+00	8,41E+00
	Child	2,19E+00	2,56E+01	-	-
Dermal contact Inorganic compound [mg / kg_d]	Adult	4,04E-01	1,18E+00	3,01E-01	8,41E-01
	Child	2,19E-01	2,56E+00	-	-

In order to correctly compare the APAT and EPA [Region 9-US.EPA] approaches for residential use and carcinogenic compounds, it is worth noting that in the latter one the exposure routes corresponding to 6 years exposure as child and 24 years exposure as adult, shall be added.

That is, an adjusted Exposure rate is defined as:

$$EM_{adj} = EM_{child} + EM_{adult}$$

Eq. 1-17

Where:

EM_{child} is the exposure rate calculated with child default data;

EM_{adult} is the exposure rate calculated with adult default data;

The EM_{adj} can then be fairly compared to the EM calculated using the APAT approach for 30 years exposure as adult.

The results of this comparison relevant to exposure to surface soil, shown in Figure 1.3, Figure 1.4 and Figure 1.5 for carcinogenic and non-carcinogenic compounds allow to make the following consideration:

- With the carcinogenic compounds in residential scenario(Figure 1.3), the EPA method returns values of effective exposure rate higher than the APAT method, resulting more conservative.

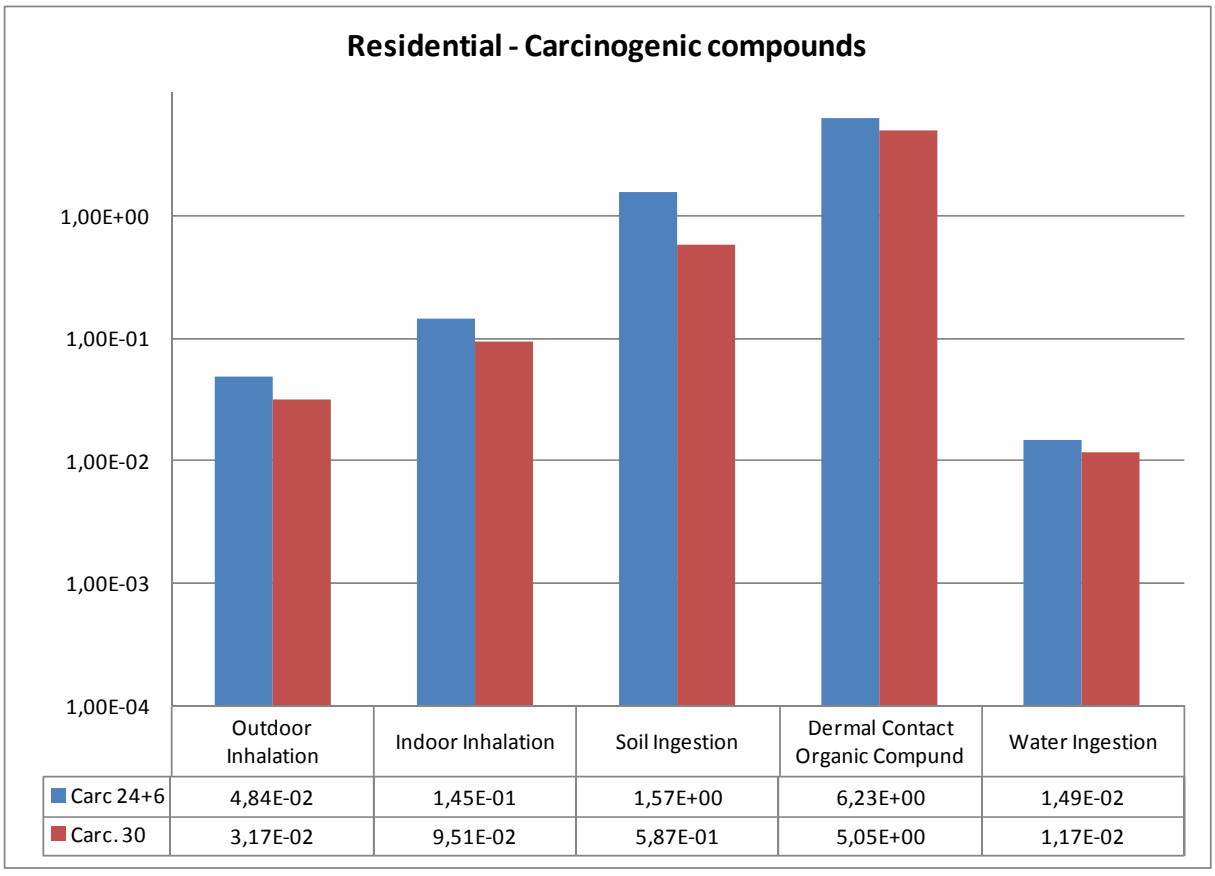

	Outdoor Inhalation	Indoor Inhalation	Soil Ingestion	Dermal Contact Organic Compund	Water Ingestion
Carc 24+6	4,84E-02	1,45E-01	1,57E+00	6,23E+00	1,49E-02
Carc. 30	3,17E-02	9,51E-02	5,87E-01	5,05E+00	1,17E-02

Figure 1.3: Effective Exposure Rate comparison – Residential Scenario, carcinogenic compounds

- For non carcinogenic compounds the EM value is independent from the exposure duration. Nevertheless, as shown in Figure 1.4, different values of EM are obtained relating the two approaches. This difference arises since the EPA approach considers exposure of a child (BW = 15 kg), where the APAT considers exposure of an adult (BW = 70 kg).

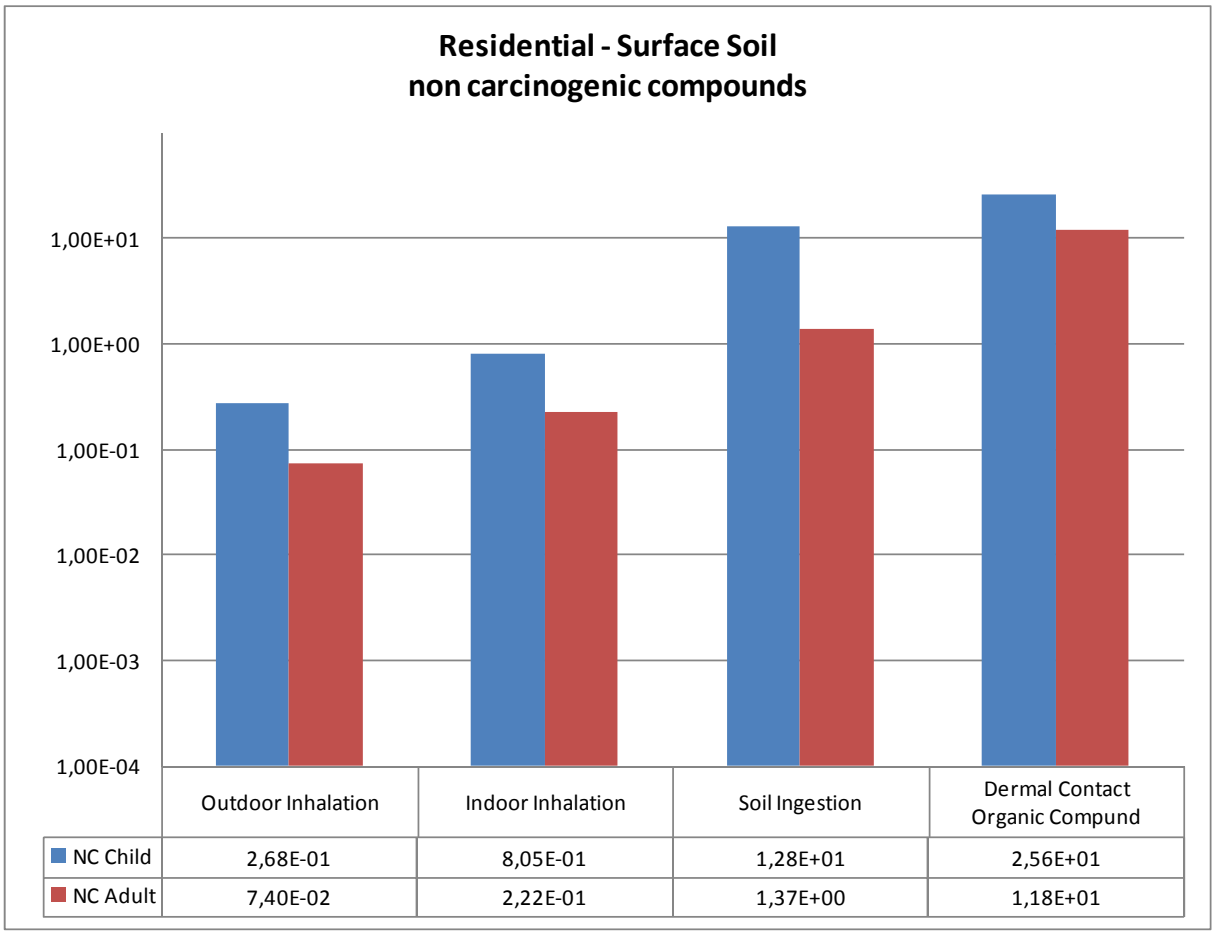

Figure 1.4: Effective Exposure Rate comparison – Residential Scenario, surface soil, non-carcinogenic compounds

- Finally as shown in Figure 1.5 corresponding to carcinogenic compounds in industrial scenario, the APAT approach gives values of effective exposure rate higher than the EPA approach, resulting more conservative for human health.

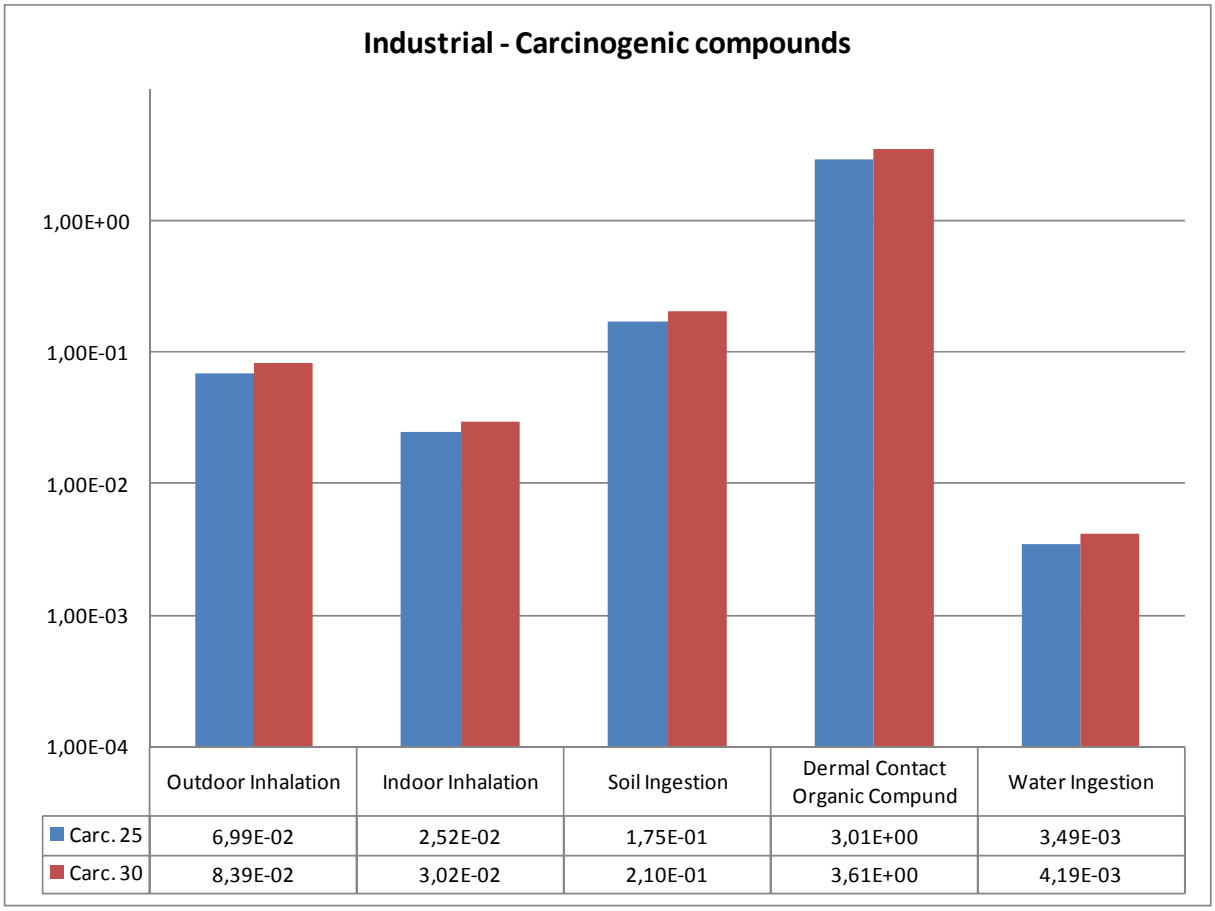

	Outdoor Inhalation	Indoor Inhalation	Soil Ingestion	Dermal Contact Organic Compund	Water Ingestion
Carc. 25	6,99E-02	2,52E-02	1,75E-01	3,01E+00	3,49E-03
Carc. 30	8,39E-02	3,02E-02	2,10E-01	3,61E+00	4,19E-03

Figure 1.5: Effective Exposure Rate comparison – Industrial Scenario, carcinogenic compounds

According to the values obtained and their comparison, it was then decided to select the EPA approach for the residential area, since more conservative for the residential scenario. For consistency, the same approach has been chosen also for the industrial scenario, although slightly less conservative than the APAT method [2005 Rev.0]. In this way, for both soil use, the average exposure of an adult either as a worker (25 years) or as a resident (24 years) are very similar.

1.6 RISK THRESHOLD VALUE CALCULATION

In this chapter the procedure required to calculate the risk threshold value (CSR) for single contaminant related to one or more exposure routes, will be discussed.

Calculation of Target Risk Concentration (CSR) through Eq. 1-10 and Eq. 1-11, becomes more complex as more than one exposure pathways are active.

1.6.1 Risk Threshold value for single exposure route.

The CSR obtained considering individually the different exposure routes have been calculated using the procedure outlined above and considering all the default parameters provided in the APAT document, so to get the so-called site-generic screening level, CSRg.

The results are summarized in Figure 1.6, Figure 1.7 and Figure 1.8, for the different environmental compartments, with reference to residential use only. The following considerations can be done:

- For the lesser volatile compounds the lowest screening concentrations are those corresponding to direct exposure, i.e. soil ingestion and dermal contact (for surface soil) and water ingestion (for deep soil and groundwater).
- For the more volatile compounds the lowest screening concentration is that related to indoor inhalation.

It is therefore very important to establish the appropriate cumulating criteria, since according to the choice, the results are significantly different.

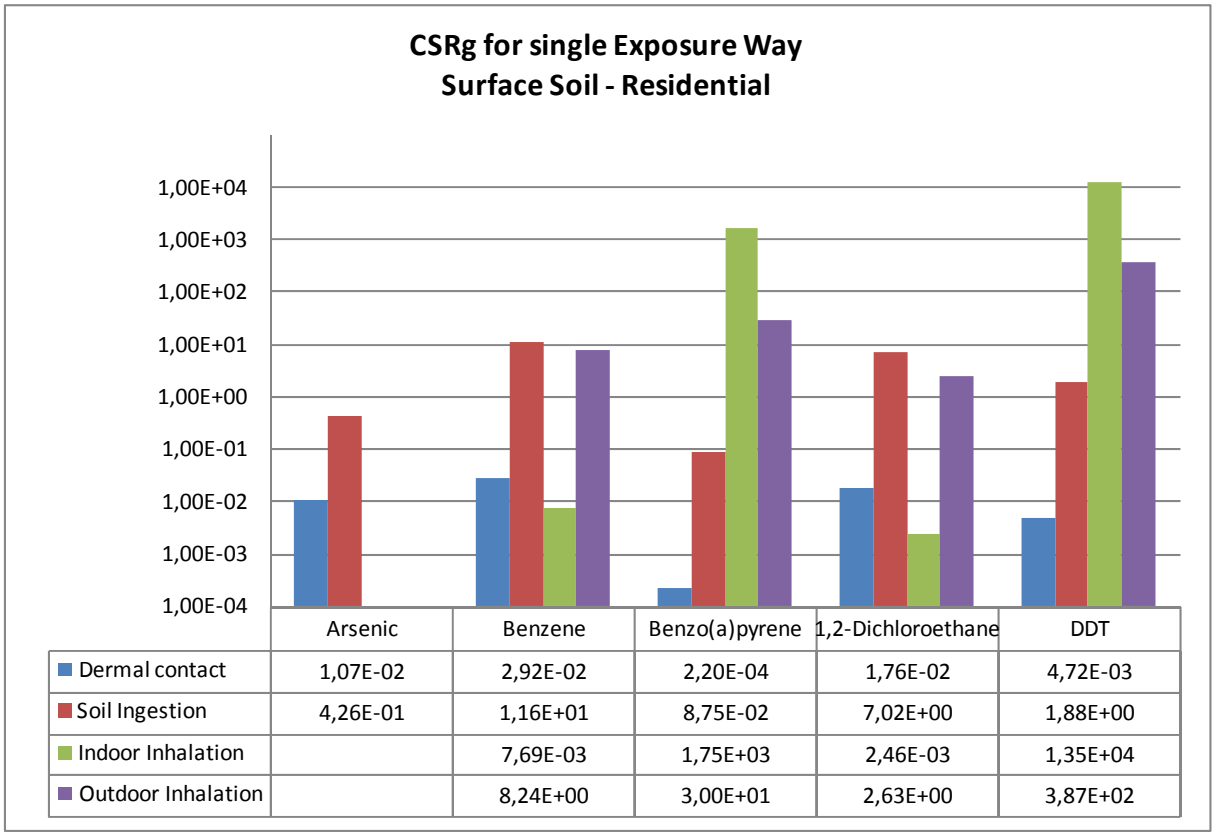

	Arsenic	Benzene	Benzo(a)pyrene	1,2-Dichloroethane	DDT
Dermal contact	1,07E-02	2,92E-02	2,20E-04	1,76E-02	4,72E-03
Soil Ingestion	4,26E-01	1,16E+01	8,75E-02	7,02E+00	1,88E+00
Indoor Inhalation		7,69E-03	1,75E+03	2,46E-03	1,35E+04
Outdoor Inhalation		8,24E+00	3,00E+01	2,63E+00	3,87E+02

Figure 1.6: Comparing of CSRg for single Exposure Way, Residential, Surface soil

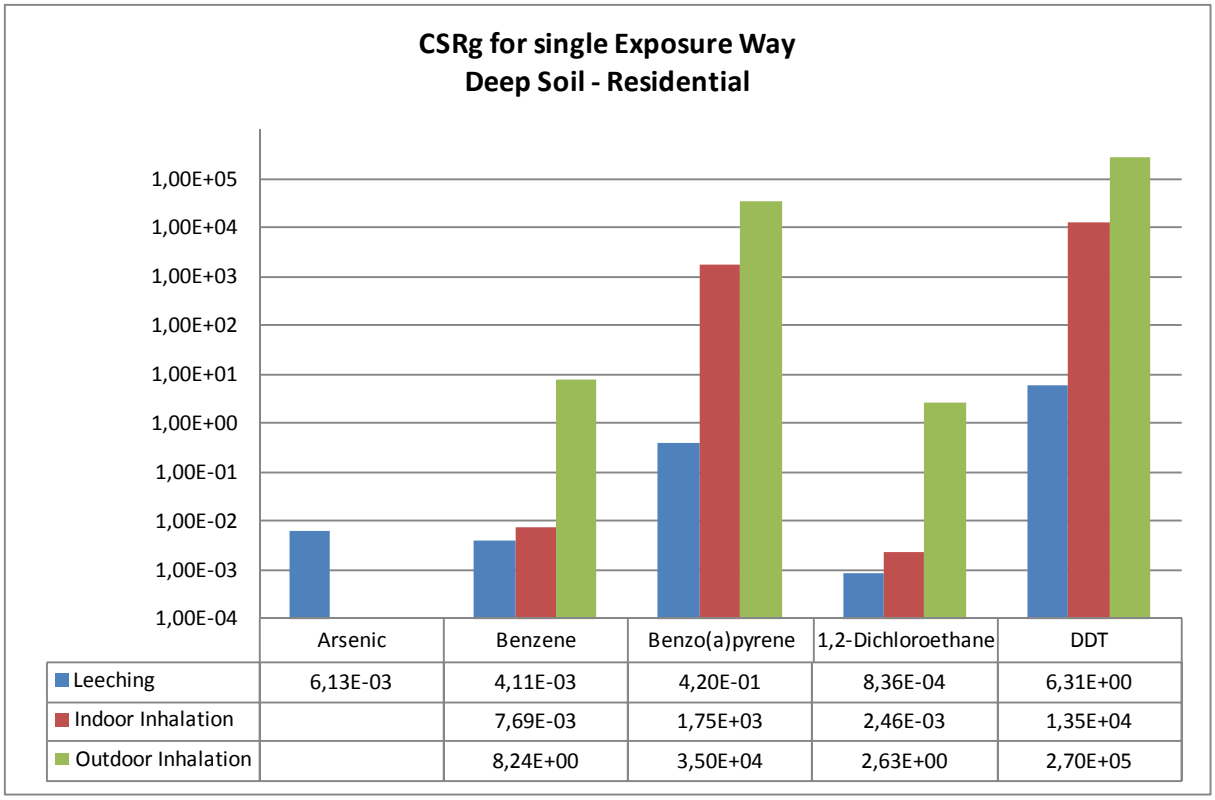

	Arsenic	Benzene	Benzo(a)pyrene	1,2-Dichloroethane	DDT
Leeching	6,13E-03	4,11E-03	4,20E-01	8,36E-04	6,31E+00
Indoor Inhalation		7,69E-03	1,75E+03	2,46E-03	1,35E+04
Outdoor Inhalation		8,24E+00	3,50E+04	2,63E+00	2,70E+05

Figure 1.7: Comparing of CSRg for single Exposure Way, Residential, Deep soil

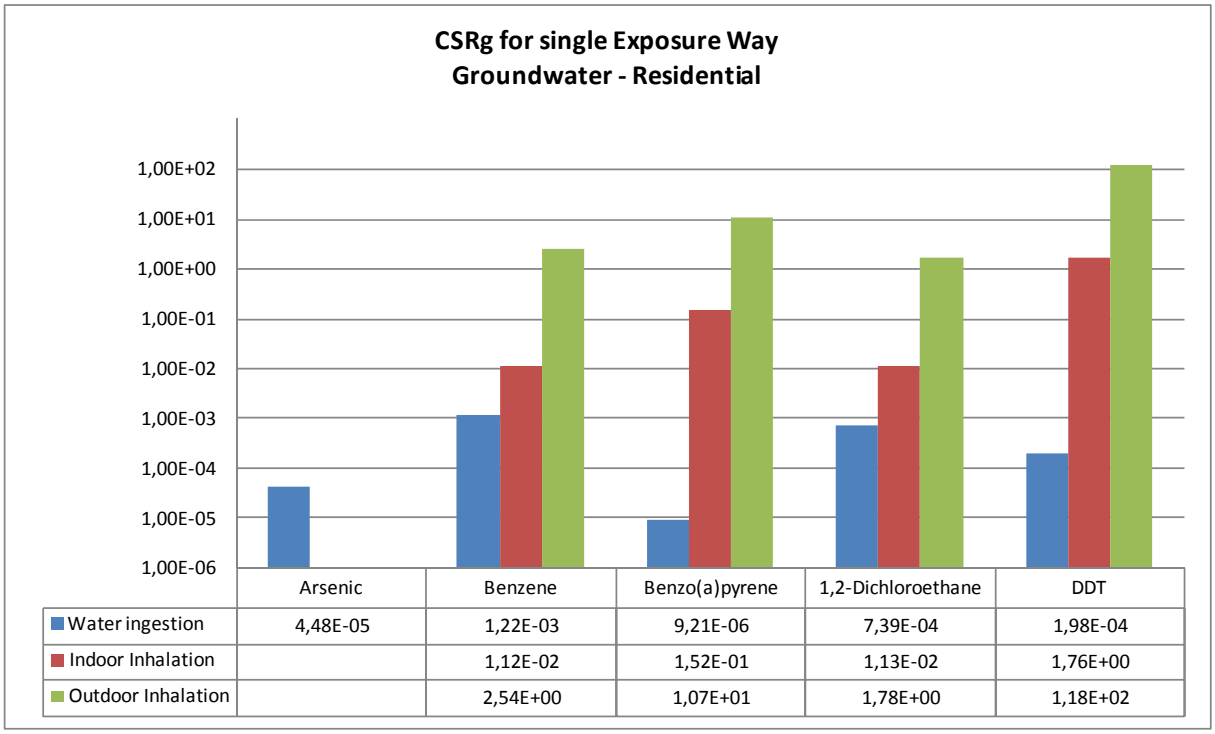

	Arsenic	Benzene	Benzo(a)pyrene	1,2-Dichloroethane	DDT
Water ingestion	4,48E-05	1,22E-03	9,21E-06	7,39E-04	1,98E-04
Indoor Inhalation		1,12E-02	1,52E-01	1,13E-02	1,76E+00
Outdoor Inhalation		2,54E+00	1,07E+01	1,78E+00	1,18E+02

Figure 1.8: Comparing of CSRg for single Exposure Way, Residential, Groundwater

1.6.2 Risk Threshold concentration for multiple exposure routes.

When more than one exposure pathway is active, as it is often the case, the effects deriving from the different exposure pathways need to be cumulated with a given criteria. In this section, we discuss in detail the selection of a criteria for the cumulation of the effects in the case of exposure from surface soil, where basically all direct (ingestion, dermal contact) and indirect (indoor and outdoor vapor and dust inhalation) exposures are active.

The main problem arises on how discriminating between indoor and outdoor exposure. Table 1-6 (residential scenario) and Table 1-7 (industrial scenario) summarize the possible approaches that can be used, proposed in literature.

The results provided by following the three different scenarios are reported in Figure 1.9 and Figure 1.10 for residential and industrial scenario, respectively.

Analyzing the obtained risk threshold concentration for generic site (CSRg) it can be noted that the differences are related to the contaminant properties, as seen before in section 1.6.1.

As far as the residential use is concerned (Figure 1.9), for non-volatile substances the three different approaches give the same results because the main exposure pathway is by dermal contact, which is only an outdoor exposure route. For the volatile substances the main exposure is the indoor inhalation; the Risk Threshold Concentration obtained with the application of the scenario 2 are more conservative than the ones obtained for the application of scenario 3

For the industrial area, concentrations corresponding to scenario 1 and 2 are the same; even in this case, as for the residential area, the less conservative Risk Threshold Concentrations value are the one obtained by the application of the scenario 3.

Table 1-6: Residential Scenarios for CSRg calculation;

Residential Scenarios – 24 hours				
Scenarios	**Outdoor**	**Indoor**	**Cumulating Criteria**	**Approach**
SCENARIO 1	6 hours	18 hours	It combine the indoor and outdoor effects	APAT [2005 REV.0]
SCENARIO 2	24 hours	24 hours	Choose the most conservative between indoor and outdoor exposure	ASTM
SCENARIO 3	24 hours	-	Is considered only the outdoor exposure	PRG (REGION 9/ EPA)

Table 1-7: Industrial Scenarios for CSRg calculation

Industrial Scenarios – 8 working hours				
Scenarios	**Outdoor**	**Indoor**	**Cumulating Criteria**	**Approach**
SCENARIO 1 SCENARIO 2	8 ore	8 ore	Choose the most conservative between indoor and outdoor exposure	ASTM
SCENARIO 3	8 ore	-	Is considered only the outdoor exposure	PRG (REGION 9/ EPA)

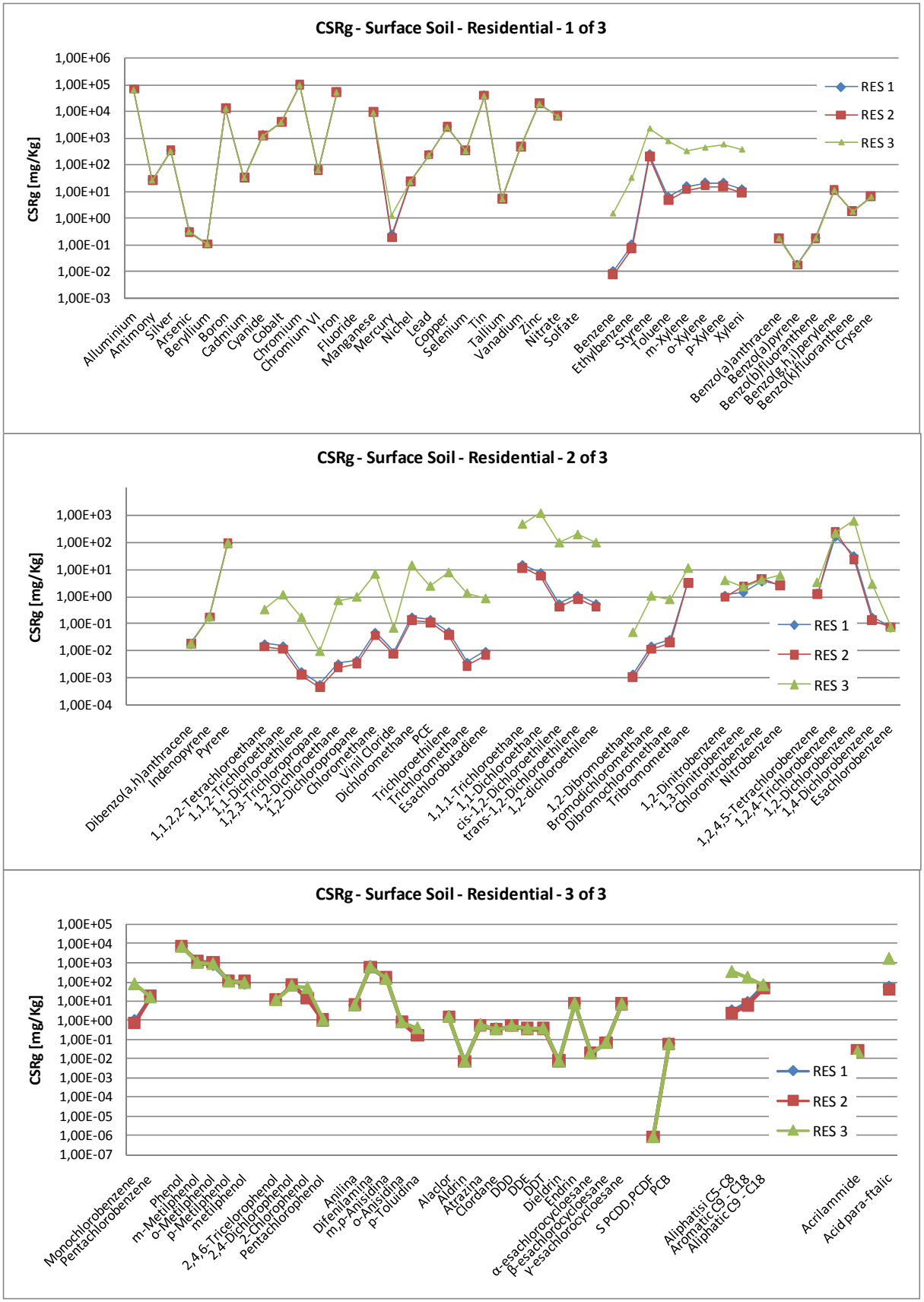

Figure 1.9: CSRg comparison for the surface soil for the 3 scenario – Residential use.

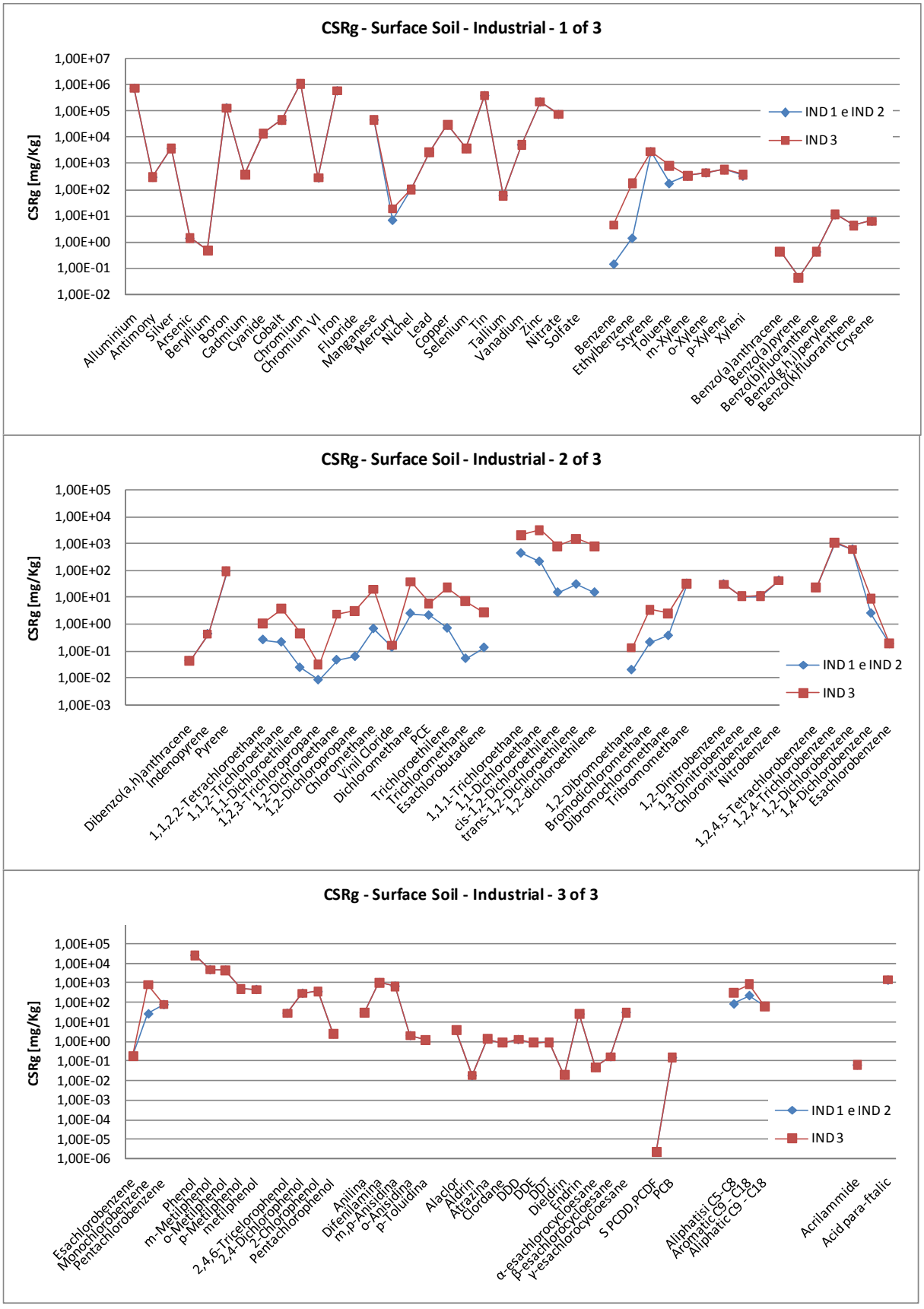

Figure 1.10: CSRg comparison for the surface soil for the 3 scenario – Industrial use.

2 HUMAN HEALTH RISK ASSOCIATED TO THE VEGETABLE CHAIN

2.1 BACKGROUND

Ingestion of contaminated fruits and vegetables is a potential condition of human exposure to toxic chemicals. Fruits and vegetables may become contaminated with toxic chemicals by several different pathways. Environment pollutants from the air may be deposited on or absorbed by the plants, or dissolved in rainfall or irrigation waters that come in contact with the plants. Pollutants may also be absorbed through plant roots from contaminated soil and ground water. The addition of pesticides, soil additives and fertilizers may also result in food contamination.

In this chapter a description of the vegetables will be given together with the main processes necessary to the plant life. Then a short description of the technical documents and software including the ingestion of vegetables as exposure route to contaminants is given

2.1.1 Plants

2.1.1.1 Roots

The root can be defined as a part of a plant that bears no leaves, and therefore also lacks nodes. There are also important internal structural differences between stems and roots. The two major functions of roots are:

1) absorption of water and inorganic nutrients;
2) anchoring of the plant body to the ground.

In response to the concentration of nutrients, roots also synthesize cytokine, that indicate how fast the roots can grow. Roots often function as storage of food and nutrients.

Plant roots gain nutrients from the soil using three mechanisms (refer to Figure 2.1). As water drops from the leaf surface, it moves in the soil via mass flow towards the root (arrow 1). As the root tips grow, the living cells of the root intercept nutrients that may be bound in the soil (arrow 2). Nutrients must be dissolved to flow in the soil water and to cross the cells of the root, they must be dissolved. Accordingly, the major plant nutrients (nitrogen, potassium, phosphorus, sulphur, calcium, magnesium) must be in the inorganic state, and must be soluble in the soil water. Organic acids secreted by root tips into the soil (arrow 3) may change the chemical state of nutrients on contact, improving their uptake into the root tissues.

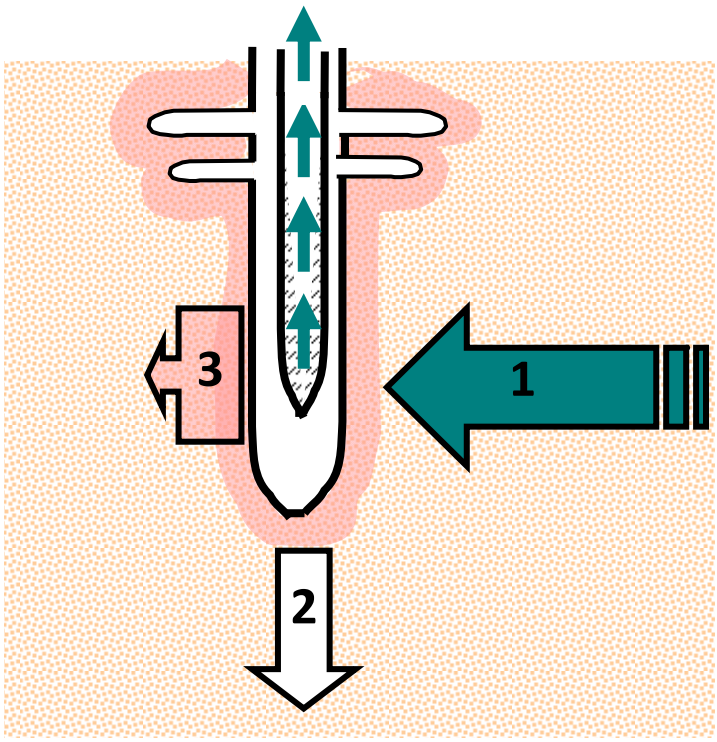

Figure 2.1: Nutrient Uptake by roots growing in soil

2.1.1.2 Leaves

The surface of the leaf is specialized for trapping energy from light (photosynthesis) and storing it as sugars and starch. Therefore the upper leaf surface must be angled to face the sun, reaching surface temperatures of more than 10^0C above environment air temperature. To control water loss under such conditions, most leaves have a thick, water resilient waxy layer (the cuticle: refer to Figure 2.2). The specialized openings that control the rate of water loss (stomates) tend to be more numerous on the lower side of the leaf.

Accordingly, leaves are not adapted for taking up nutrients. The specialized ion carriers within the walls of the leaf cells are not as numerous as on root hairs and root tips, and water is less likely to be in contact with leaf cells due to the presence of the protective waxy cuticle at the surface.

Comparatively, mass flow of solutes from the soil to the roots provides the greatest amount of nutrients for plants. Moreover, root tips branch prolifically when they intercept concentrated pockets of nutrients in the soil. However plants need only micronutrients such as manganese, zinc, iron, boron, copper and molybdenum in trace amounts, which can be applied successfully as a foliar spray to leaves.

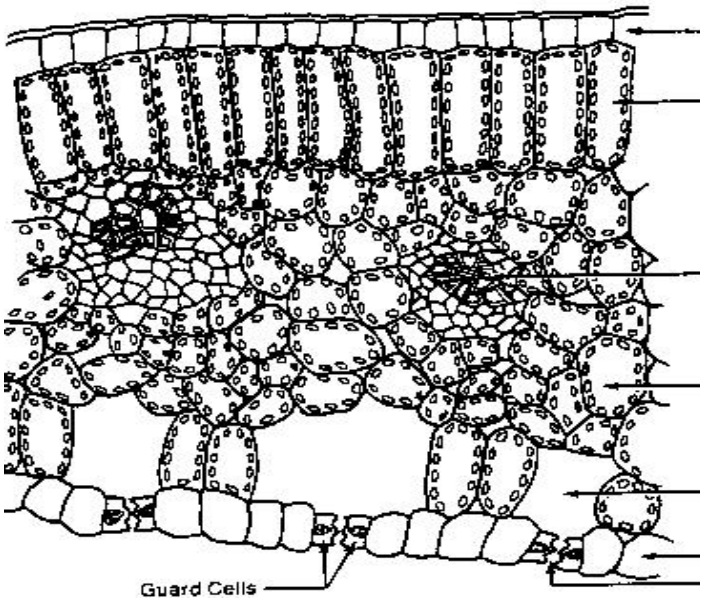

Figure 2.2: Cross section of the structure of a leaf.

2.2 METHODOLOGY

This section reports and compares the approaches provided by several document for evaluating the risk for the human health due to vegetables assumption.

2.2.1 Soil Screening Guidance: Technical Background Documents

The US.EPA document "Soil Screening Guidance: Technical Background Documents" provides the following equation for estimating the Risk Based Screening Level for soil-plant-human ($RBSL_v$) pathway (Eq. 2-1):

$$RBSL_v = RBSL_s \cdot BCF_{vs} \quad \text{Eq. 2-1}$$

Where:

$RBSL_s$= soil risk based screening level [mg/kg];

BCF_{vs}= Bioconcentration Factor soil-vegetable, (discussed below in the document);

This equation can be applied to the above-ground vegetables and to the root vegetables. Eq. 2-1 can be specified for carcinogenic and non carcinogenic compounds, as follow:

Carcinogenic

$$RBSL_s^c = \frac{TR \cdot BW \cdot AT}{F \cdot ED \cdot EF \cdot (CR_{vs} \cdot BCF_{vs}^{ss} + CR_{vr} \cdot BCF_{vs}^{sr}) \cdot SF} \quad \text{Eq. 2-2}$$

Non Carcinogenic

$$RBSL_s^{nc} = \frac{THQ \cdot BW \cdot AT \cdot RfD}{F \cdot ED \cdot EF \cdot (CR_{vs} \cdot BCF_{vs}^{ss} + CR_{vr} \cdot BCF_{vs}^{sr})}$$

Eq. 2-3

Where:

CR_{vs} and CR_{vr}= Vegetables consumption rate for above-ground and below-ground vegetable, respectively; (discussed below)

F = Vegetables contaminated Fraction (discussed below)

BCF_{vs}^{ss} and BCF_{vs}^{sr} = Vegetable Bioconcentration Factor for above-ground and below-ground vegetable, respectively;

And all other parameters are defined as above in the document.(See section 1.3.1)

The same methodology can be applied to a forward mode to calculate chemical concentration in vegetables:

$$C_v = C_s \cdot BCF_{vs}$$

Eq. 2-4

Using Eq. 2-4 with the extended terms for carcinogenic and non carcinogenic compounds:

Carcinogenic

$$R = \frac{C_s^c \cdot (CR_{vs} \cdot BCF_{vs}^{ss} + CR_{vr} \cdot BCF_{vs}^{sr}) \cdot SF \cdot F \cdot ED \cdot EF}{BW \cdot AT}$$

Eq. 2-5

Non Carcinogenic

$$HQ = \frac{C_s^c \cdot (CR_{vs} \cdot BCF_{vs}^{ss} + CR_{vr} \cdot BCF_{vs}^{sr}) \cdot F \cdot ED \cdot EF}{BW \cdot AT \cdot RfD}$$

Eq. 2-6

Where all parameters are defined as above in the document.

Table 2-1 shows the default value of the main parameters given in the document

Table 2-1: default value for specific parameters in SSG

Parameter	Default Value		Unit
	Above ground Vegetables and Fruit	Root vegetables	
CR_{vs}	0,0197	---	$Kg_{plant\ dw}/d$
CS_{vr}	---	0,0024	$Kg_{plant\ dw}/d$
F	0,4	0,4	
α	0,15	0,085	Kg_{dw}/Kg_{ww}

2.2.2 Food Chain Models for Risk Assessment [RAIS '05]

This section describes the document developed by the Risk Assessment Information System [RAIS] to set food chemicals concentration and the parameters default value.

Parameters can depend on different vegetables type or different agricultural practice (plowing, irrigation). Plant models consider leafy or nonleafy vegetables and the following contamination pathways:

- Root uptake;
- Irrigation with contaminated water;
- Aerial deposition
- Resuspension contribution.

As noted previously, the general model for estimating contaminant concentrations in and on plants includes root uptake and foliar deposition from air and resuspended soil. Where irrigation is a significant management practice, components accounting for root uptake and resuspension of contaminants originating in irrigation water and direct deposition of irrigation water on plant surfaces can be added.

Therefore, the comprehensive plant model for a site where irrigation is performed, is:

$$C_v = C_{v-asr} + C_{v-dda} + C_{v-rs} + C_{v-ari} + C_{v-ddw} + C_{v-rw} \quad \text{Eq. 2-7}$$

Where:

- C_v = concentration in and on plant estimated based on root uptake and foliar deposition (mg/kg),
- $C_{v\text{-}asr}$ = concentration in plant tissue resulting from root uptake from soil (mg/kg),
- $C_{v\text{-}dda}$ = concentration in edible parts of plant as a result of direct deposition of airborne contaminants (mg/kg),
- $C_{v\text{-}rs}$ = concentration in edible parts of plant as a result of resuspension of contaminants associated with soil (mg/kg),
- $C_{v\text{-}ari}$ = concentration in plant tissue associated with root uptake of contaminants resulting from irrigation (mg/kg),
- $C_{v\text{-}ddw}$ = concentration in edible parts of plant as a result of direct deposition of contaminants in irrigation water (mg/kg),
- $C_{v\text{-}rw}$ = concentration in edible parts of plant as a result of resuspension of contaminants associated with irrigation water (mg/kg).

The last three terms of this model are set to zero if irrigation is not performed. If airborne contamination is not considered, the direct deposition term may also be set to zero

The following section provides details on the estimation of each of the terms presented in Eq. 2-7.

$C_{v\text{-}asr}$: is the concentration of a contaminant in plant tissue as a result of root uptake from soil. It can be estimated through the following equation:

$$C_{v-asr} = C_s \cdot BCF_{vs}$$
Eq. 2-8

where:

$C_{v\text{-}asr}$ = concentration in plant tissue from root uptake from soil (mg/kg),

C_s = concentration in the upper 15 cm of soil (mg/kg dry soil)

BCF_{vs} = transfer factor from soil to plant tissue (mg/kg dry plant per mg/kg dry soil).

The BCF_{vs} parameter is the combination of BCF_{vs}^{ss} and BCF_{vs}^{sr}, i.e. the bioconcentration factor for the above-ground and the root vegetables respectively. More details are given below in the document.
The soil concentration used as input into this model should be derived from data relevant to the root zone soil. Depending on plant type and site conditions, plant roots depths may vary from several centimeters to more than a meter. The bulk of roots that are actively engaged in the uptake of water and minerals occur in the upper 15-100 cm [21]. Under plowed agricultural conditions, the root zone would nearly always be expected to be greater than 15 cm. The default value recommended for root zone soil in this report is the concentration corresponding to the upper 15 cm of soil.

$C_{v\text{-}dda}$: The aerial deposition component accounts for direct deposition of airborne contaminants onto plant surfaces. A general model for deposition of contaminants onto plant surfaces from air pathways is:

$$C_{v-dda} = \frac{d \cdot f_R \cdot T}{Y} \cdot \frac{\left(1 - e^{(-\lambda_E \cdot t_s)}\right)}{\lambda_E}$$
Eq. 2-9

Where:
d = deposition rate of contaminant from air to ground surface [mg/m^{2}d]. Calculated as the product of the air concentration ($C_{s\text{-}air}$) [mg/m^3] and a chemical-specific average deposition velocity (v_{dep}) [m/d]:

$$d = C_{s-air} \cdot v_{dep}$$
Eq. 2-10

The air concentration can be measured at the height of the vegetation or at a reference height (i.e., 1 m), or it can be calculated using the air mass loading parameter. Using this parameter, the air

concentration of the contaminant is the product of the soil contaminant concentration and the concentration of soil particles in the air (Eq. 2-11).

$$\boldsymbol{C_{s-air} = MLF_{air} \cdot C_s}$$
Eq. 2-11

f_R = interception fraction. The fraction of deposited material intercepted and retained on foliage [unitless]. A range of 0.02-0.82 is defined for various grasses. The midpoint of this range (0.42) is suggested as the default value.

T = translocation factor. This factor accounts for translocation of externally deposited contaminants to edible parts of plants [unitless]. The edible portion of leafy vegetables and pasture grasses are the leaf surfaces, so the translocation factor is set to 1.0 for these plant types and set to 0.1 for nonleafy vegetables

Y = standing plant biomass at harvest above a unit surface area or yield of crop [kg(wet weight)/m^2]. If site-specific data are unavailable, a default value of 2.0 can be used for leafy and nonleafy vegetables

λ_E = the effective removal constant for given constituent from plant [per day]. λ_E = i + 0.693/t_w, where: t_w = weathering half-life, and i = the radioactive decay constant for radionuclides,

ts = time of above-ground exposure of plant to contamination during the growing season [d]. 60 days represents the approximate growing time for vegetable crops.

$C_{v\text{-}rs}$: Contaminants in surface soil layers can be resuspended in air by wind or mechanical disturbances. Resuspended particles may then be deposited on plant surfaces. Contaminant concentrations are usually higher in soil than in plants, so even small amounts of soil on plant surfaces can significantly affect ingestion exposures.

The plant mass loading approach involves determining the mass of soil on vegetation per mass of dry vegetation. If directly measured plant concentrations are missing, mass loading factors (MLF) can be multiplied by the concentration in the resuspendable soil fraction at the site to provide the plant concentration. Using the plant mass loading approach, the contribution of resuspension from soil to the plant contaminant load can be estimated as the product of the measured soil concentration and the plant mass loading factor:

$$C_{v-rs} = MLF_{sv} \cdot C_s$$
Eq. 2-12

where:

$C_{v\text{-}rs}$ = concentration in edible parts of plant as a result of direct deposition of airborne contaminants resulting from resuspension from soil [mg/kg],

C_s = concentration of the contaminant measured in resuspendable soil fraction (mg/kg);

MLF_{sv} = plant mass-loading factor (kg soil/kg dry plant). The plant mass loading factor is defined as the ratio of the mass of soil on vegetation per mass of dry vegetation. The value of 0.26 kg soil/kg plant is selected as the default for leafy vegetables and the suggested default for nonleafy vegetables is 0.11 kg soil/kg plant.

$C_{v\text{-}ari}$: The following equation determines the contaminant uptake by plant roots as a result of irrigation:

$$C_{v-ari} = \frac{C_w \cdot I_r \cdot I_p \cdot BCF_{vs}}{\rho_{sr}} \cdot \frac{\left(1 - e^{(-\lambda_B \cdot t_b)}\right)}{\lambda_B}$$

Eq. 2-13

where:

C_{v-ari} = concentration in plant tissue from root uptake due to irrigation (mg/kg),

C_w = concentration in water used for irrigation (mg/L);

I_r= irrigation rate (L/m^2/d)

I_p = irrigation period, i.e. is the fraction of year plants during which are irrigated (unitless)

The irrigation rate and irrigation period define the amount and duration of water applied to crops. A default irrigation period of 0.25 is selected assuming crops will be irrigated three months out of the year. These defaults correspond to irrigation rates of approximately 32.5 cm per growing season.

BCF_{vs} = transfer factor from soil to plant tissue (mg/kg dry plant per mg/kg dry soil),

ρ_{sr} = root zone soil density (kg/m^2). While plant rooting depths vary depending on species and soil conditions, a typical depth used in a number of exposure models is 15 cm. This is considered a typical depth for the plow layer. Soil density [kg/m^3] is multiplied by the rooting depth to obtain the root zone soil density, or areal soil density, in kg dry soil/m^2. The recommended default value is 240 kg/m^2

λ_B = the effective removal constant for given constituent from soil [per day]. The default value is :

$$\lambda_B = r_i + 0{,}000027$$

Eq. 2-14

Where r_i is the radioactive decay constant in case of radionuclides.

t_b = long-term deposition and buildup (d). The time for buildup of contaminants in soil depends on the duration of deposition; this should be determined on a site-specific basis. The default suggested here is 10,95 days, but site-specific values are preferred.

$C_{v\text{-}ddw}$: The concentration of a contaminant in plant tissue as a result of irrigation water deposited on the plant surface is similar to that for direct deposition from air. However, the deposition rate is the product of the concentration in the irrigation water and the irrigation rate rather than the air concentration times the deposition velocity:

$$C_{v-ddw} = \frac{C_w \cdot I_r \cdot I_p \cdot f_R \cdot T}{Y} \cdot \frac{\left(1 - e^{(-\lambda_B \cdot t_s)}\right)}{\lambda_E}$$

Eq. 2-15

where:

f_R= in this case the recommended value for the interception fraction of particles deposited by spray irrigation is 0.25,

λ_E = the effective removal constant for given constituent from plant (per day), and the other symbols have the same meaning described before.

$C_{v\text{-}rw}$: A resuspension component exists for the irrigation scenario which incorporates the irrigation rate and decay and leaching loss rate into the model for resuspension from soil. Essentially, the concentration in soil resulting from irrigation is used as input into the model for resuspension from soil.

$$C_{v-rw} = MLF_{sv} \cdot C_w \cdot \frac{I_r \cdot I_p}{\rho_{sr}} \cdot \frac{\left(1 - e^{(-\lambda_B \cdot t_b)}\right)}{\lambda_B}$$

Eq. 2-16

2.2.3 Software Risc 4.0 [July 2001]

The model included in this software make the assumption that contaminant uptake in vegetables may occur from the contaminated soil when they grow or from being irrigated with contaminated groundwater. There are other mechanisms that can also contaminate vegetables, such as particulate deposition, however these mechanisms are not modeled in RISC. The vegetables are classified as root vegetables and above-ground (or leafy) vegetables.

As seen in section 2.2.1, either the forward mode approach or the backward mode approach can be used.

INGESTION OF HOME-GROWN VEGETABLES GROWN IN CONTAMINATED SOIL

Software RISC 4.0 uses the same equation proposed by the SSG document, taking into account the different contribution for the root vegetables and the above-ground vegetables. The Risk Based screening Level and the Risk/hazard quotient can be then calculated either for carcinogenic or non carcinogenic compounds.

BACKWARD MODE

Carcinogenic

$$RBSL_s^c = \frac{TR \cdot BW \cdot AT}{F \cdot ED \cdot EF \cdot (CR_{vs} \cdot BCF_{vs}^{ss} + CR_{vr} \cdot BCF_{vs}^{sr}) \cdot SF}$$

Eq. 2-17

Non Carcinogenic

$$RBSL_s^{nc} = \frac{THQ \cdot BW \cdot AT \cdot RfD}{F \cdot ED \cdot EF \cdot (CR_{vs} \cdot BCF_{vs}^{ss} + CR_{vr} \cdot BCF_{vs}^{sr})}$$

Eq. 2-18

FORWARD MODE

Carcinogenic

$$R = \frac{C_s^c \cdot (CR_{vs} \cdot BCF_{vs}^{ss} + CR_{vr} \cdot BCF_{vs}^{sr}) \cdot EF \cdot ED \cdot F \cdot SF}{BW \cdot AT}$$

Eq. 2-19

Non Carcinogenic

$$HQ = \frac{C_s^c \cdot (CR_{vs} \cdot BCF_{vs}^{ss} + CR_{vr} \cdot BCF_{vs}^{sr}) \cdot EF \cdot ED \cdot F}{BW \cdot AT \cdot RfD}$$

Eq. 2-20

INGESTION OF HOME-GROWN VEGETABLES IRRIGATED WITH GROUNDWATER

Concentrations in the root and above-ground vegetables are calculated by multiplying the concentration in groundwater by the root concentration factor, *RCF,* or the above-ground vegetable concentration factor, *ABCF*.

BACKWARD MODE

Carcinogenic

$$RBSL_s^c = \frac{TR \cdot BW \cdot AT}{F \cdot ED \cdot EF\,(CR_{vs} \cdot ABCF + CR_{vr} \cdot RCF) \cdot SF}$$

Eq. 2-21

Non Carcinogenic

$$RBSL_s^{nc} = \frac{THQ \cdot BW \cdot AT \cdot RfD}{F \cdot ED \cdot EF\,(CR_{vs} \cdot ABCF + CR_{vr} \cdot RCF)}$$

Eq. 2-22

FORWARD MODE

Cancerogenic

$$R = \frac{C_w^c \cdot (CR_{vs} \cdot ABCF + CR_{vr} \cdot RCF) \cdot EF \cdot ED \cdot F \cdot SF}{BW \times AT}$$

Eq. 2-23

Non Cancerogenic

$$HQ = \frac{C_w^c \cdot (CR_{vs} \cdot ABCF + CR_{vr} \cdot RCF) \cdot EF \cdot ED \cdot F}{BW \cdot AT \cdot RfD}$$

Eq. 2-24

The Bioconcentration Factors (ABCF,RCF, BCF) are discussed below in the document.

The ingestion rate (CR_{vs} and CR_{vr}) have different value depending on the target; if the target is a children the default values are 55,8 $g_{plant\ TQ}$/d (CR_{vs}) and 48,5 $g_{plant\ TQ}$/d (CR_{vr}); otherwise, for adult targets, the default values are 127 $g_{plant\ TQ}$/d (CR_{vs}) and 87,5 $g_{plant\ TQ}$/d (CR_{vr}).

The fraction of the contaminated ingested vegetables (F) has a default value of 0,1 [unitless]

2.3 ANALYSIS OF THE PARAMETERS

The purpose of this paragraph is to analyze the key parameters used in the vegetable chain risk analysis:

- Bioconcentration Factor;
- Ingestion Rate;
- Fraction of the contaminated ingested vegetables.

2.3.1 Bioconcentration factor

When a chemical enters the food chain it becomes potentially dangerous for the life species. The food chain concentrates chemicals, so every different trophic level is subjected to an increased dose level.

The bioconcentration factor has been introduced and investigated in several studies to account for this phenomena. A short discussion on the different approaches follows.

2.3.1.1 Bioconcentration of Organics in Beef, Milk, and Vegetation (Trevis and Arms, 1988)

This is the first study performed on the bioconcentration factor, where food chain is considered as the primary source of human exposure to a large class of environmental organics.

Assessing the magnitude of human exposure to some organics depends largely on the ability to predict the extent of their bioaccumulation in the aquatic and terrestrial food chains. The octanol-water partition coefficient (K_{ow}) has thus proven a valuable tool for making such predictions. Travis and Arms (1988) developed correlations between K_{ow} and the bioconcentration of organics in beef, cow milk, and vegetation.

The traditional measure of a chemical's potential to accumulate in an organism is the bioconcentration factor (BCF), which is defined as the chemical's concentration in an organism or

tissue divided by its concentration in water (for aquatic organisms) or in food (for terrestrial organisms).

The bioconcentration factor for vegetation *(BCF_{vs})* is defined as the ratio between the concentration in aboveground parts (mg of compound/kg of dry plant) and the concentration in soil (mg of compound/kg of dry soil).

Travis and Arms (1988) elaborated an equation to calculate the bioconcentration factors for vegetables:

$$\log BCF_{vs} = 1{,}588 - 0{,}578 \cdot \log K_{ow}$$

Eq. 2-25

i.e., in other terms:

$$BCF_{vs} = 4{,}89 \cdot {K_{ow}}^{-0{,}578}$$

Eq. 2-26

Thus, the vegetation bioconcentration factor is inversely proportional to the square root of K_{ow}. The inverse proportionality is not surprising since transport from soil to aboveground plant parts is dependent on the chemical's solubility in water, which is inversely proportional to K_{ow}.

The study of Travis and Arms (1988) does not distinguish between vegetables type, i.e. root or above-ground respectively.

2.3.1.2 Food chain models for risk assessment, Appendix F [RAIS, 2005]

Transfer coefficients reported in the literature can vary widely because of the effects of different soil and vegetation types and environmental conditions involved in their estimation (IAEA 1994). Management practices such as plowing, liming, fertilizing, and irrigating can also affect uptake. Therefore, site-specific values are preferred over literature values that may have been derived under conditions dissimilar to those at the site under investigation.

Soil-to-plant transfer coefficients for organic chemicals are less widely available. Where possible, actual measured values should be used. In the absence of measured data, uptake of contaminants by above-ground plant parts can be estimated through the bioconcentration factor, that can be estimated through the following equation (Travis and Arms 1988), as modified by McKone (1994):

$$BCF_{vs}^{ss} = 7{,}7 \cdot {K_{ow}}^{-0{,}578}$$

Eq. 2-27

where:

BCF_{vs}^{ss} = measure of uptake into above-ground vegetation expressed as mg contaminant/kg above-ground plant (fresh weight) over mg contaminant/kg root zone soil (dry weight),

K_{ow} = octanol-water partitioning coefficient for the organic chemical.

For uptake by edible root crops, McKone (1994) modified the original Travis and Arms (1988) equation to incorporate information on uptake by plant roots described in other studies:

$$BCF_{vs}^{sr} = 270 \cdot {K_{ow}}^{-0,578}$$

Eq. 2-28

where

BCF_{vs}^{sr} = measure of uptake into plant roots expressed as mg contaminant/kg plant roots (fresh weight) over mg contaminant/kg root zone soil (dry weight),

K_{ow} = octanol-water partitioning coefficient for the organic chemical.

2.3.1.3 Soil Screening Guidance: Technical Background Document [EPA, 1996]

This document does not present any default value for the soil-to-plant bioconcentration factors (BCF_{vs}) for either aboveground or belowground plants. They must be identified from empirical studies because, according to this document, the relationship between soil concentration and plant concentration has not been described adequately to provide a mathematical framework for modeling.

2.3.1.4 Software Risc 4.0, july 2001

ORGANIC COMPOUNDS

The equations used in Risc 4.0 for the organic compound are empirical, and in this case are derived from Briggs' experiments of growing barley shoots in water containing various compounds. Briggs actually provides a series of equations to derive concentrations in different parts of the plant. The soil-root uptake factor (BCF_{vs}^{sr}) is given by [USEPA (1993)]:

$$BCF_{vs}^{sr} = \frac{0,01 \cdot RCF}{K_d}$$

Eq. 2-29

Where:

RCF is the root concentration factor [mg chemical/kg product per mg chemical/l water]

$$RCF = 10^{(0,788 \times \log K_{ow} - 1,52)} + 0,82$$

Eq. 2-30

K_d is the soil equilibrium partitioning coefficient [l/Kg or ml/g]] calculated as product between the organic carbon partitioning coefficient (K_{oc}) and the fraction of organic carbon (f_{oc}).

The soil-to-above-ground vegetable concentration factor, BCF_{vs}^{ss}, is calculated from:

$$BCF_{vs}^{ss} = e^{(1,588 - 0,578 \cdot \log K_{ow})}$$

Eq. 2-31

Finally, the irrigation water-to-above-ground vegetable concentration factor, *ABCF*, is calculated from Eq. 2-32 assuming equilibrium partitioning:

$$ABCF = BCF_{vs}^{ss} \times K_d = e^{(1{,}588-0{,}578\cdot\log K_{ow})} \cdot K_d$$

Eq. 2-32

INORGANIC COMPOUNDS

An uptake model based on K_{ow} is clearly inapplicable to inorganic compounds. As an alternative, the USEPA has in several guidance documents recommended the use of a set of "default" uptake factors published by Baes, et al (1984). For the most part, Baes et al (1984), report the geometric mean of observed soil-to-plant concentration ratios, although some values are extrapolated from one element to another within the same periodic groups. The geometric mean uptake factor will over- or underestimate the uptake, depending on the concentration of the element at the specific site. Nonetheless, the Baes et al (1984) data are generally accepted, and their use is recommended in RISC for metals. In Table 2-2 the default value for eleven inorganic compounds are reported.

Table 2-2 Default values for BCF, RCF and ABCF for inorganic compounds in Risc 4.0

Compounds	Parameters			
----	BCF_{vs}^{ss}	BCF_{vs}^{sr}	RCF	ABCF
	$\frac{mg_{chem}/Kg_{veg(dw)}}{mg_{chem}/Kg_{soil(dw)}}$		$\frac{mg_{chem}/Kg_{veg(dw)}}{mg_{chem}/l_{water)}}$	
Arsenic	0,267		7,743	
Barium	1		30	
Beryllium	0,067		113,9	
Cadmium	3,67		403,7	
Copper	2,67		93,45	
Mercury	6		492	
Nickel	0,27		23,76	
Selenium	0,167		0,7181	
Silver	2,67		197,58	
Vanadium	0,0367		36,7	
Zinc	10		750	

2.3.2 Consumption Rate

Consumption rate is defined as the quantity of fruits and vegetables consumed by individuals, adults and children, who ate these food items during the survey period [2]. Two separate uptake factors are considered in this approach; the first one is relevant to determine plant uptake in roots; the other one for above-ground plants. This means that the exposure calculations use separate ingestion rate

values for each plant "type", root or above-ground respectively. In the following, the consumption rate provided by the different standard document are discussed.

2.3.2.1 Soil Screening Guidance: Technical Background Document [EPA 1996]

The default values for total fruit and vegetable consumption rates (CR) cited in the *Exposure Factors Handbook* are 0.140 and 0.2 kg/d fresh weight, respectively. Assuming that the homegrown fraction is roughly 0.25 to 0.40, EPA estimated fresh weight consumption rates of:

(1) 0.088 kg/d of aboveground unprotected fruits,

(2) 0.076 kg/d of aboveground unprotected vegetables, and

(3) 0.028 kg/d of unprotected belowground vegetables (U.S. EPA, 1994).

The consumption rates for fruits and vegetables are converted to dry weight based on the average fresh-to-dry conversion of 0.15 for fruits and 0.085 for vegetables. For unprotected belowground vegetables, the consumption rate (CR) is calculated by multiplying the fresh weight consumption rate (0.028 kg FW/d) by the average conversion factor of 0.085 resulting in a CR of 0.0024 kg DW/d. Using this same method, dry weight consumption rates of 0.0132 and 0.0065 kg DW/d were calculated for unprotected aboveground fruits and vegetables, respectively. Consequently, the overall consumption rate (CR) for aboveground, unprotected fruits and vegetables is 0.0197 kg DW/d.

2.3.2.2 Food chain models for risk assessment, Appendix F [RAIS, 2005]

RAIS does not provide any value for the consumption rate. It stop its analysis to the evaluation of the vegetable chemical concentration only.

2.3.2.3 Software Risc 4.0, July 2001

The values suggested from Risc 4.0 are presented in Table 2-3

Table 2-3 Vegetable ingestion rate in Risc 4.0

	Mean Adult Ingestion Rate (g_{WW}/Kg_{BW} d)	Mean Small Child Ingestion Rate (g_{WW}/Kg_{BW} d)[2]
Above Ground Vegetables[1]	1,82	3,72
Root Vegetables	1,25	3,23
Fruit	3,40	11,84

(1) Above ground vegetables calculated as the sum of protected and unprotected vegetables

(2) 1-2 years old child. Rate calculated from total vegetable ingestion rate multiplied by the proportions of vegetable types in adults

These values can then be converted to dry weight basis using the proper correction factors.

2.3.3 Contaminated Fraction

This is the fraction of consumed vegetables actually grown on contaminated soil or irrigated with contaminated water. This is typically a site-specific data depending on specific dietary data. Nevertheless some studies provide values as described below.

2.3.3.1 Soil Screening Guidance: Technical Background Document [EPA 1996]

For home gardeners, a high-end dietary fraction of 0.40 is assumed for the ingestion of contaminated fruits and vegetables grown onsite.

2.3.3.2 Food chain models for risk assessment, Appendix F [RAIS, 2005]

RAIS does not provide any value for the contaminated fraction because its analysis stop to the evaluation of the chemical concentration only.

2.3.3.3 Software Risc 4.0, July 2001

A default value of 0,1 is provided by the Risc manual for vegetables grown on contaminated soil or irrigated with contaminated water.

2.4 RISK CALCULATION

This section compares the values of risk calculated using Eq. 2-19, Eq. 2-20, Eq. 2-23 and Eq. 2-24. Data sheet using the different input parameters discussed above, with the aim of selection the most proper values. The default value for all the other risk analysis parameters (BW,AT, EF, ED) were taken from the APAT document rev. 1.

Different chemicals were selected to perform the analysis. The choice was based upon:

- Wide presence in contaminated sites;
- Danger for the human health;
- Bioaccumulation on the vegetable chain.

On this basis the chemicals chosen were:

- Arsenic;
- Cadmium;
- Mercury;
- Zinc;
- α-, β-, γ – hexachlorocyclohexane;
- Dioxin;
- PCBs.

The following sections report the results of a sensitivity analysis of the different input parameters on risk calculation.

2.4.1 Influence of the contaminated fraction (F)

The influence of the contaminated fraction F on the calculated risk is reported in Figure 2.3 and Figure 2.4 with reference to adult and children receptors, respectively.

The following values for the parameter F were considered:

- 0,1 [Risc 4.0 , 2001]
- 0,106 [EPA, 2002], home production, root vegetables
- 0,173 [EPA, 2002] industrial production, root vegetables
- 0,233 [EPA, 2002] home production, above-ground vegetables
- 0,4 [EPA, 1996]
- 0,42 [EPA, 2002] industrial production, above-ground vegetables

As expected from Eq. 2-19 there is a linear relationship between risk and contaminated Fraction F; which is not evident from Figure 2.3 and Figure 2.4, where a logarithmic scale was adopted.

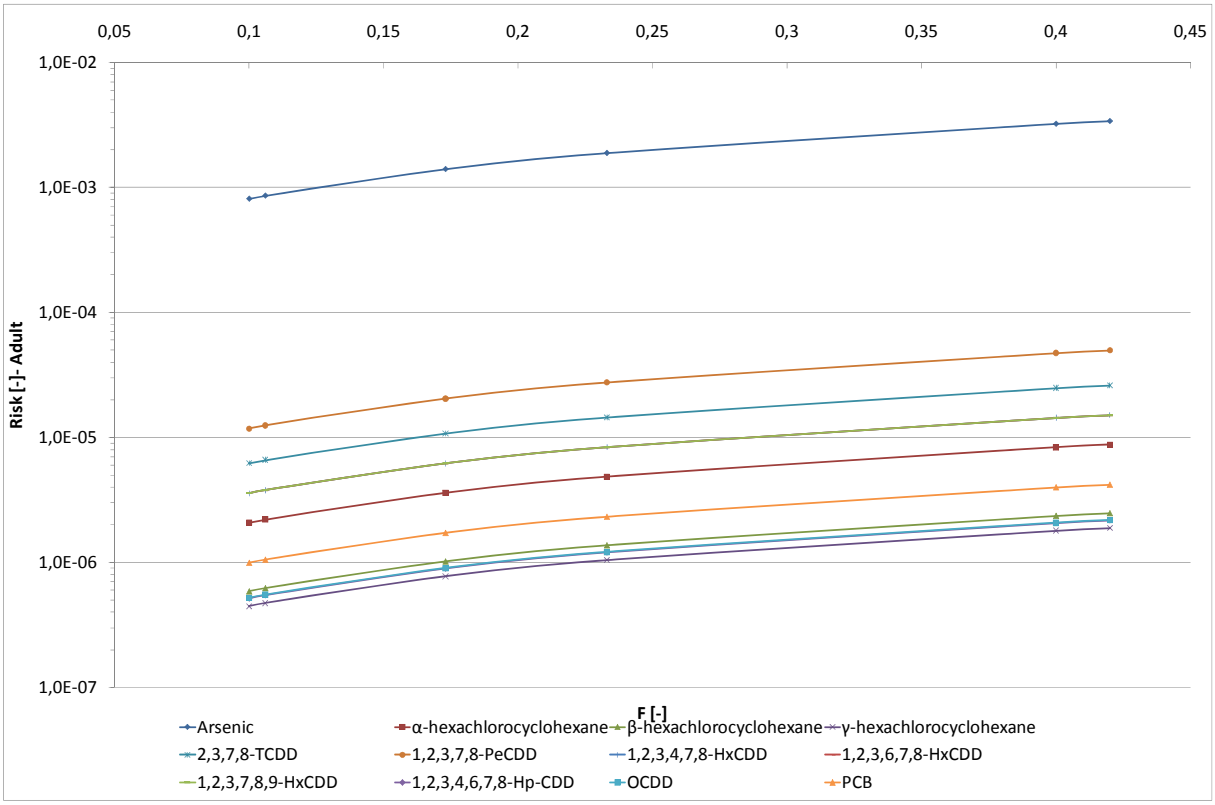

Figure 2.3: Risk Trend for Contaminated Fraction variation (adult).

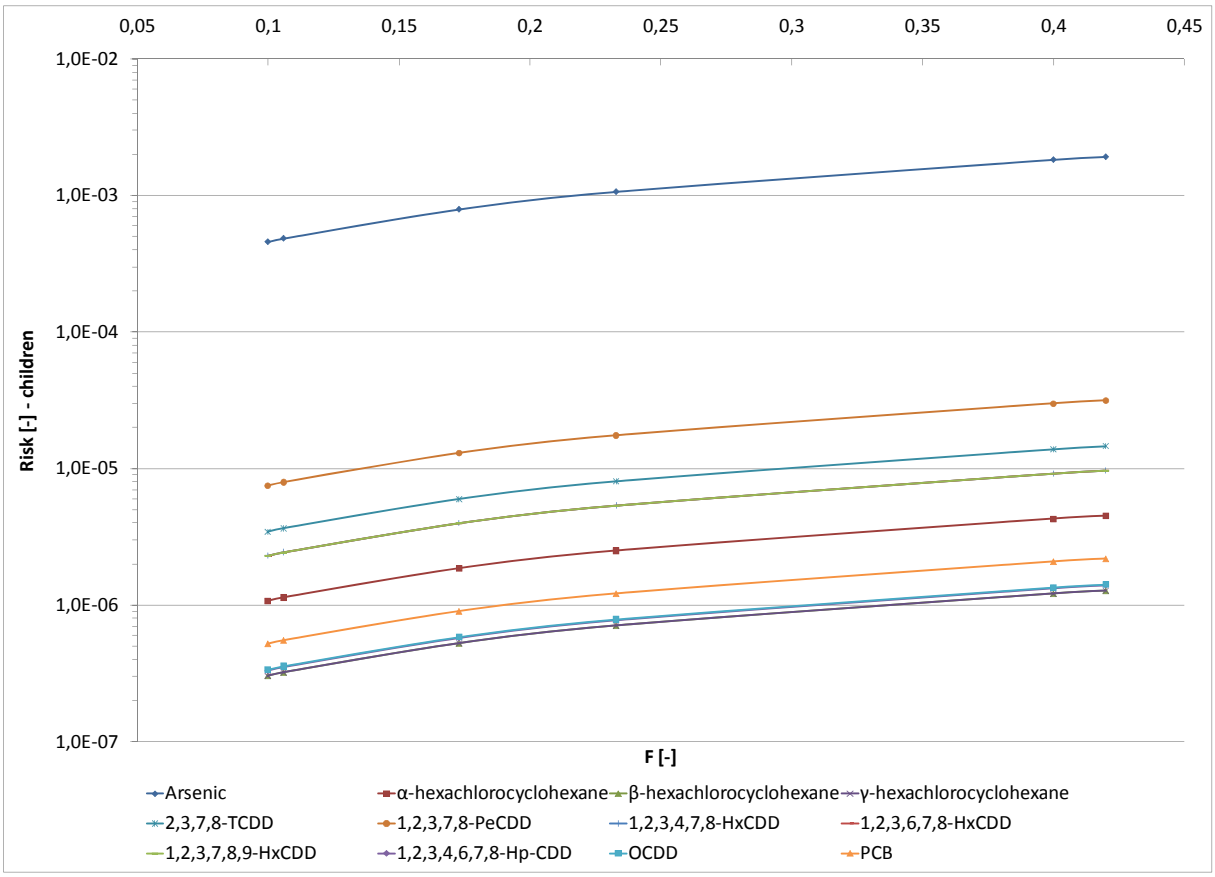

Figure 2.4: Risk Trend for Contaminated Fraction variation (Children).

This sensitivity analysis study allowed to select F=0,42 as default value, since it responds to the following criteria:

- It provides the most conservative result for the human health;
- It is the most updated data.

2.4.2 Influence of the consumption rate (CR)

In this case it was impossible to study directly the relation between Risk and consumption rate, CR, because the latter one is related to the BCF as shown in Eq. 2-19, Eq. 2-20, Eq. 2-23 and Eq. 2-24.

For this reason the sensitivity analysis shown in Figure 2.5 and Figure 2.6 was made with reference to the combination of the consumption rate and BCF factors.

The following different consumption rate values were used:

Adults:

- CR_{vs}:
  - $1{,}27 \times 10^{-1}$ $Kg_{plant\ dw}/d$ [Risc 4.0 , 2001]
  - $1{,}97 \times 10^{-2}$ $Kg_{plant\ dw}$ /d [EPA, 1996]
  - $1{,}06 \times 10^{-1}$ $Kg_{plant\ dw}/d$ [EPA, 1997]
  - $7{,}80 \times 10^{-2}$ $Kg_{plant\ dw}/d$ [CDPHE, 2004]
- CR_{vr}:

- $8{,}75\times10^{-2}$ $Kg_{plant\ dw}/d$ [Risc 4.0 , 2001]
- $2{,}40\times10^{-3}$ $Kg_{plant\ dw}/d$ [EPA, 1996]
- $8{,}12\times10^{-2}$ $Kg_{plant\ dw}/d$ [EPA, 1997]
- $1{,}20\times10^{-2}$ $Kg_{plant\ dw}/d$ [CDPHE, 2004]

Children:

- CR_{vs}:
  - $5{,}58\times10^{-2}$ $Kg_{plant\ dw}/d$ [Risc 4.0 , 2001]
  - $1{,}97\times10^{-2}$ $Kg_{plant\ dw}/d$ [EPA, 1996]
  - $2{,}28\times10^{-2}$ $Kg_{plant\ dw}/d$ [EPA, 1997]
- CR_{vr}:
  - $4{,}85\times10^{-2}$ $Kg_{plant\ dw}/d$ [Risc 4.0 , 2001]
  - $2{,}40\times10^{-3}$ $Kg_{plant\ dw}/d$ [EPA, 1996]
  - $1{,}74\times10^{-2}$ $Kg_{plant\ dw}/d$ [EPA, 1997]

Where the same values for the BCF parameters were used.

The obtained results show that there is a proportional dependence of risk from the term obtained by combining consumption rate and bioconcentration factor.

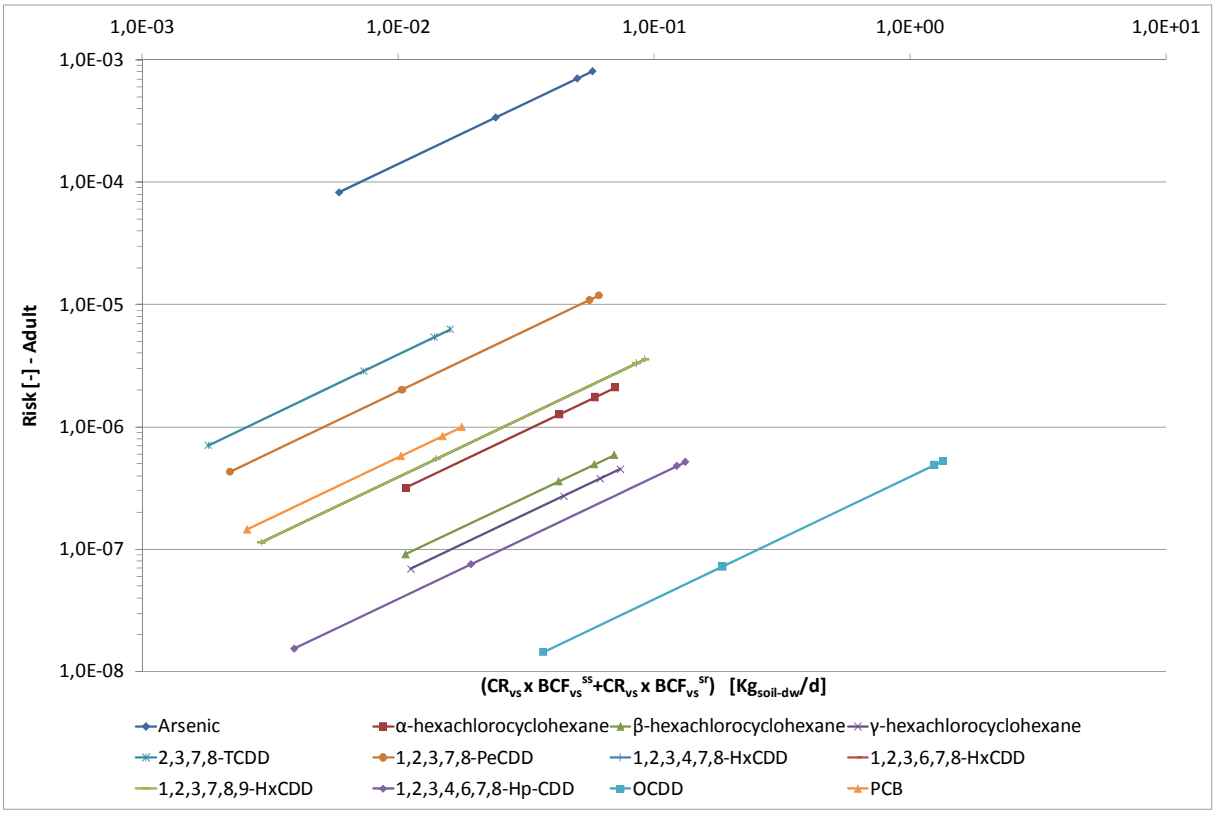

Figure 2.5: risk trend for consumption rate variation (Adult)

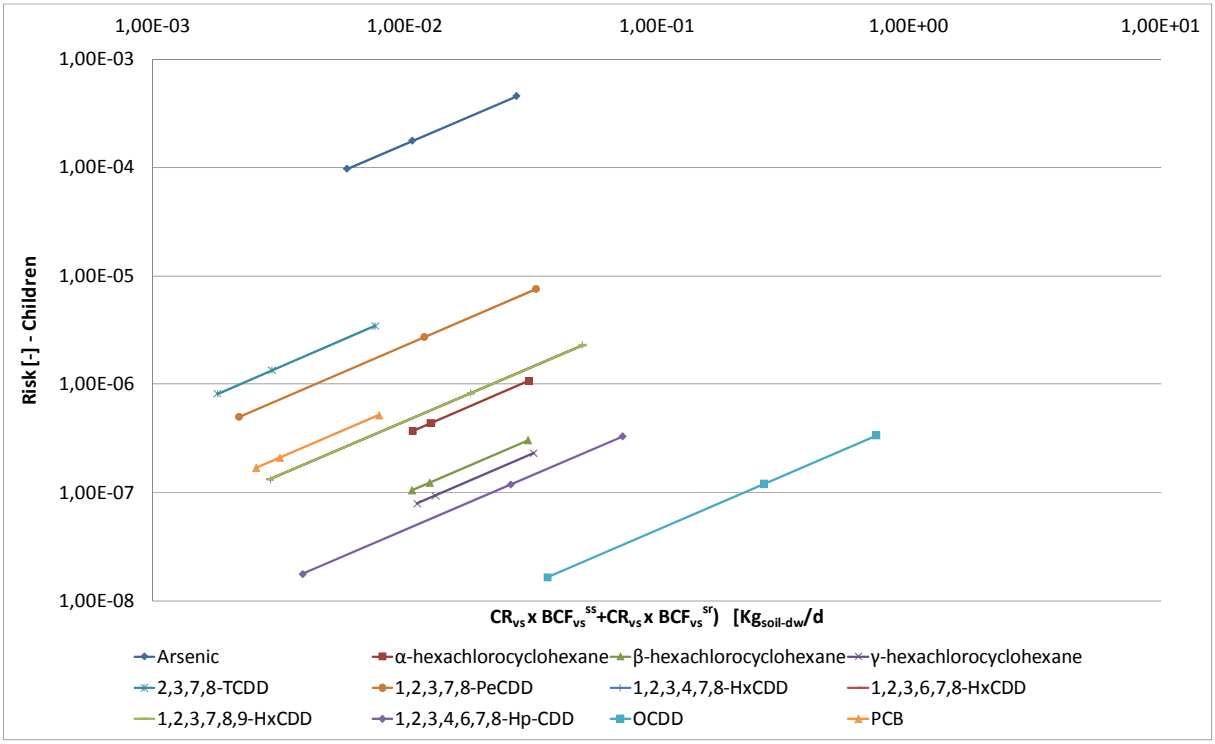

Figure 2.6: risk trend for consumption rate variation (Children)

Also in this case the values selected as default correspond to those resulting in the obtained risk values, i.e.:

Adults:

$CR_{vs} = 1{,}27 \times 10^{-1}$ $Kg_{plant\ dw}/d$ [Risc 4.0 , 2001]

$CR_{vr} = 8{,}75 \times 10^{-2}$ $Kg_{plant\ dw}/d$ [Risc 4.0 , 2001]

Childrens

$CR_{vs} = 5{,}58 \times 10^{-2}$ $Kg_{plant\ dw}/d$ [Risc 4.0 , 2001]

$CR_{vr} = 4{,}85 \times 10^{-2}$ $Kg_{plant\ dw}/d$ [Risc 4.0 , 2001]

2.4.3 Influence of the Bioconcentration Factor (BCF)

Also in this case, as seen in the previous section, the sensitivity analysis shown in Figure 2.7 and Figure 2.8 was made with reference to the combination of the consumption rate and BCF. In this case, a constant value of consumption rate was selected whereas the different BCF values shown in Table 2-4 were used.

Table 2-4: BCF values used in the simulation

Chemicals	Bioconcentration Factors			
	RAIS, 2005		Risc 4.0, 2001	
	BCF_{vs}^{ss}	BCF_{vs}^{sr}	BCF_{vs}^{ss}	BCF_{vs}^{sr}
Arsenic	ND	ND	2,67E-01	2,67E-01
Cadmium	ND	ND	3,67E+00	3,67E+00
Marcury	ND	ND	6,00E+00	6,00E+00
Zinc	ND	ND	1,00E+01	1,00E+01
α-esachlorocycloexane	8,50E-01	2,98E+01	5,44E-01	1,60E-02
β-esachlorocycloexane	8,45E-01	2,96E+01	5,41E-01	1,34E-02
γ-esachlorocycloexane	8,85E-01	3,10E+01	5,67E-01	1,85E-02
2,3,7,8-TCDD	1,31E-01	4,60E+00	8,46E-02	5,99E-02
1,2,3,7,8-PeCDD	5,13E-02	1,80E+00	3,32E-02	6,45E-01
1,2,3,4,7,8-HxCDD	3,73E-02	1,31E+00	2,41E-02	1,02E+00
1,2,3,6,7,8-HxCDD	3,73E-02	1,31E+00	2,41E-02	1,02E+00
1,2,3,7,8,9-HxCDD	3,73E-02	1,31E+00	2,41E-02	1,02E+00
1,2,3,4,6,7,8-Hp-CDD	2,79E-02	9,78E-01	1,81E-02	1,49E+00
OCDD	2,33E-02	8,17E-01	1,51E-02	1,53E+01
PCB	2,00E-01	7,03E+00	1,29E-01	1,50E-02

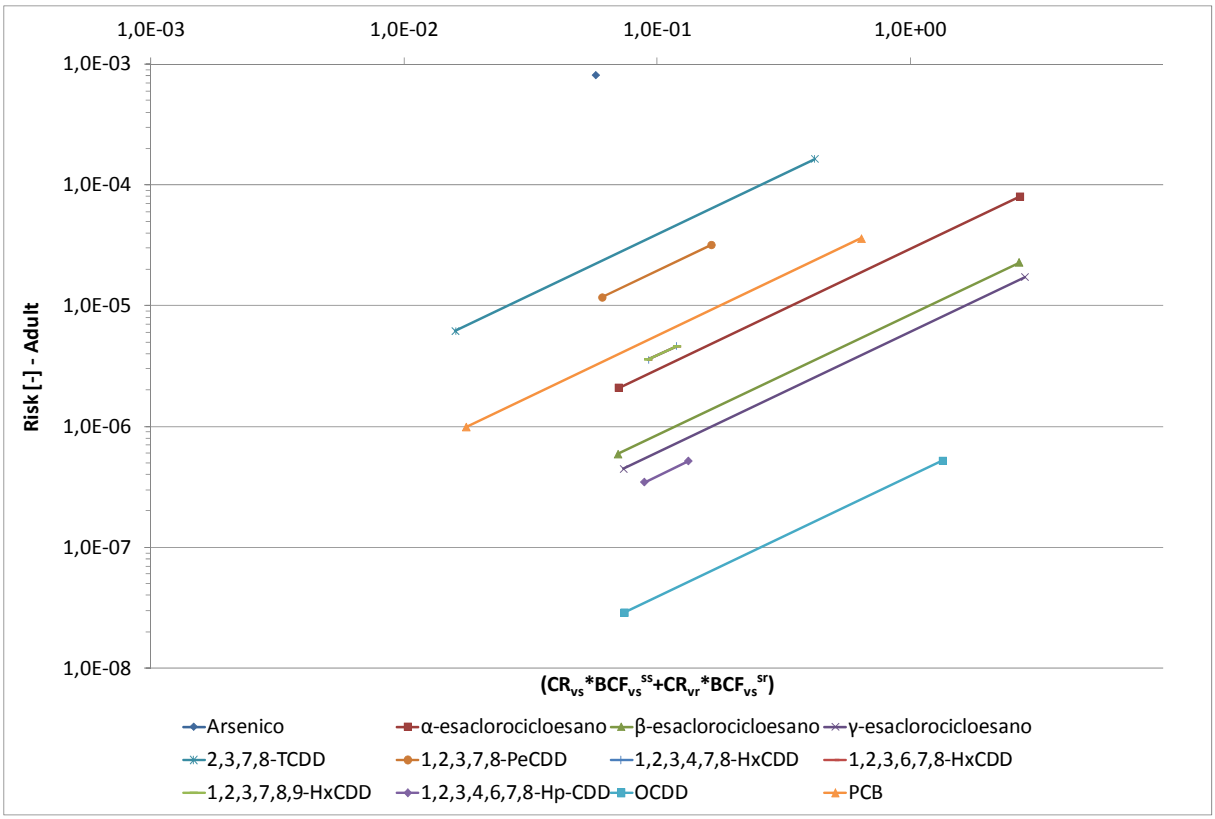

Figure 2.7: risk trend for bioconcentration factor variation (Adult)

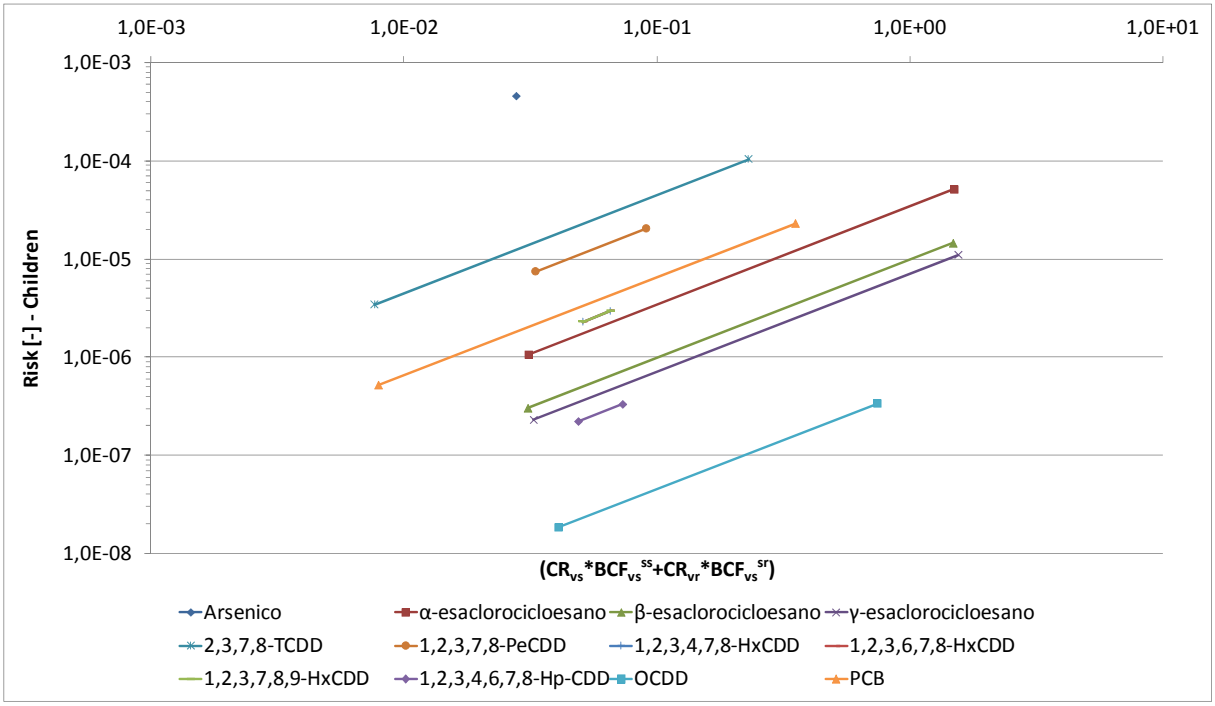

Figure 2.8: risk trend for bioconcentration factor variation (Children)

The selection for the bioconcentration value was performed through a comparison with a case study as shown in the next section.

2.4.4 Bioconcentration factor in a case study

The case study is relative to the Caffaro factory located in Brescia (IT); Data were collected from ARPA (Italian regional environmental protection agency) and ASL (Italian Local Sanitary Agency), and were taken from public document available on-line.

Two maps have been prepared, one with the sampling point performed by ARPA (Figure 2.9) and another one with the sampling point performed by ASL (Figure 2.10). Both of them correspond to the spring time, i.e. the harvesting period.

Figure 2.9: ARPA soil data map.

Figure 2.10: ASL vegetables data map (spring).

These maps have been matched in order to obtain cross data and locate some area (and data) where the BCF could be calculated and their prediction compared to actual data. Figure 2.11 shows the area where data were available for both soil and vegetables. The vegetables concentration were calculated through BCFs and soil concentration data by ARPA and compared with the field vegetables concentration data provided by ASL.

First of all, the ARPA soil concentration data were treated using the following procedure, taken from the one reported by risk analysis APAT rev. 1 document:

1. Analysis of the data set extension;
2. Identification of the outlier separating “real outlier” and false outlier:
    a. Real Outlier: depends on human or instrumental error.
    b. False Outlier: are real extreme value usually hot spot.
3. Identification of the density function distribution, between the following ones:
    a. Normal;
    b. Log normal
    c. Gamma
    d. No parametric
4. Application of statistical method to obtain a value representative of the whole data set, usually an upper confidential limit.

Figure 2.11: Map with cross data (soil and vegetables)

Since the ARPA data set was made of only 10 data points this statistical approach could be used and the representative concentration calculated. The selected value and the corresponding distribution function for superficial and radical soils are referred in Figure 2.12 and Figure 2.13, respectively.

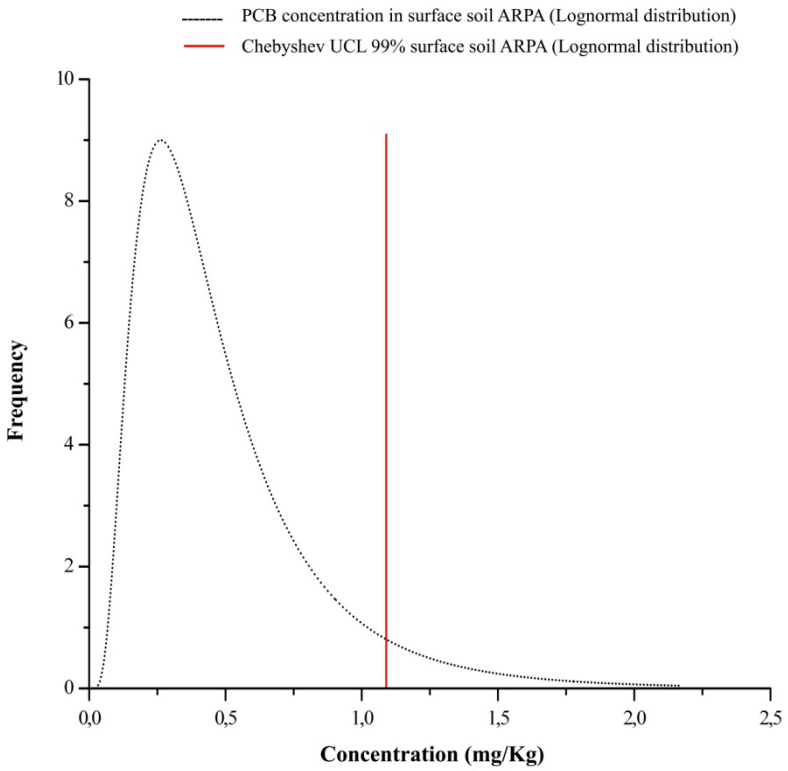

Figure 2.12: Concentration Distribution of PCB in superficial soil.

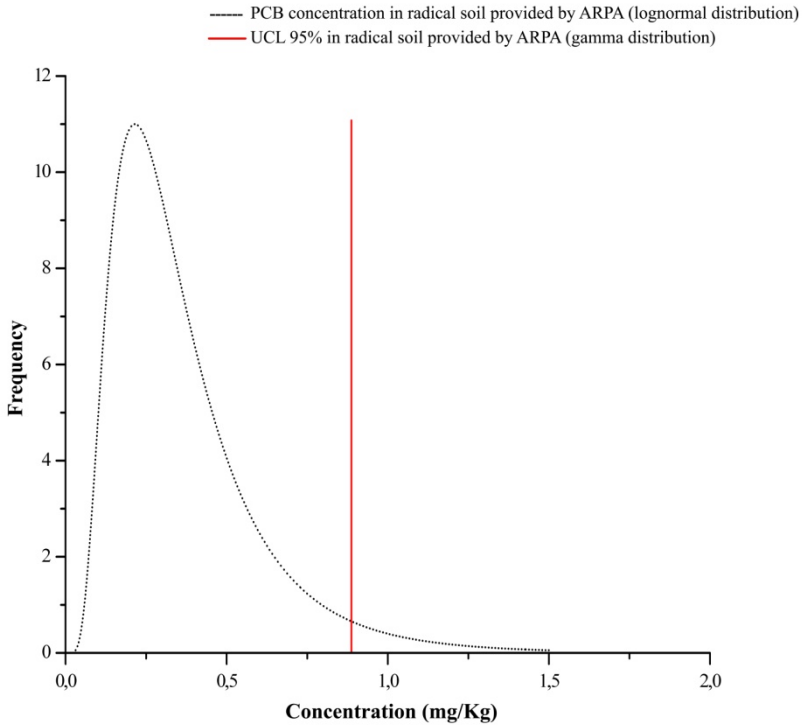

Figure 2.13: Concentration Distribution of PCB in radical soil.

As shown in Figure 2.12 and Figure 2.13 data distribution is log-normal for both data sets, whereas the representative concentration value is the Chebyshev UCL99% for the surface soil and the UCL 95% (gamma type) for the radical soil.

These data were then used in different BCF models (RISC and RAIS), to predict the chemical concentration in vegetables. The results and the comparison with actual vegetables data are represented below for the two models.

RISC MODEL

Figure 2.14 reports the following information:

- the ASL above-ground vegetables concentration data (ASL sample n°1, n°2, n°3, n°4);
- the distribution curve for the vegetables PCB concentration obtained with the RISC model
- The vegetables PCB concentration data calculated using the UCL 99% Chebyshev superficial soil concentration data.

The model seems to have a normal distribution (Black curve) but, analyzing the parameter distribution (

Table 2-5), the model shows a log-normal distribution, confirmed by observing that the median value is lower than the arithmetic mean.

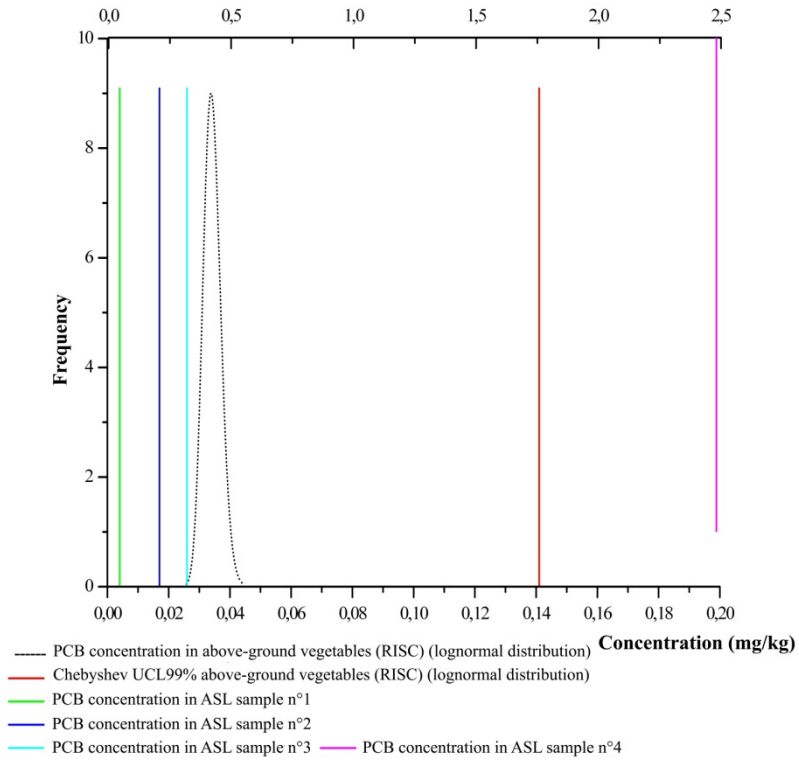

Figure 2.14: PCB concentration distribution in above ground vegetables.

Table 2-5: distribution parameters for Risc model (above ground vegetables)

Above Ground Vegetables			
	Mean	Median	Standard Deviation
Risc	0.03385	0.0058	0.08361

Although the available data base is too small to allow general and robust conclusions, looking at Figure 2.14, it can be observed that the values predicted by the model are higher than three of four vegetables concentration data, and the ASL n°4 data can be considered as an outlier.

For the root vegetables a comparison was impossible because no ASL data were available.

RAIS MODEL

Figure 2.15 reports the following information:

- the ASL above-ground vegetables concentration data (ASL sample n°1, n°2, n°3, n°4);
- the distribution curve for the vegetables PCB concentration obtained with the RAIS model
- The vegetables PCB concentration data calculated using he UCL 99% Chebyshev surface soil concentration data.

The model seems to have a normal distribution (Black curve) but, analyzing the parameter distribution (Table 2-6), the model shows a log-normal distribution, confirmed by observing that the median value is lower than the arithmetic mean.

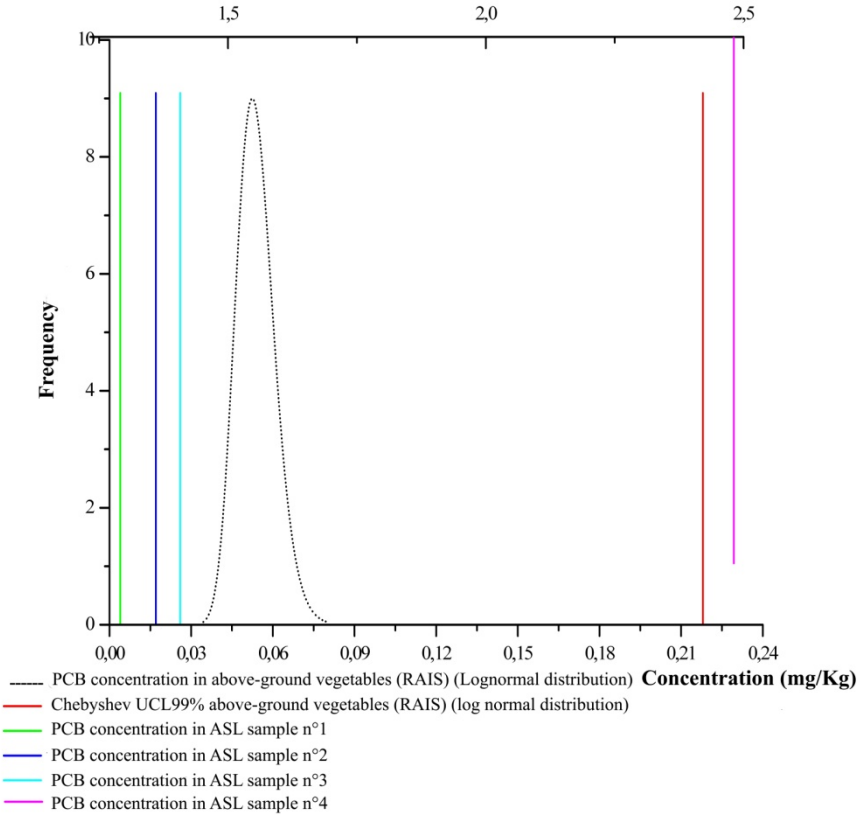

Figure 2.15: PCB concentration distribution in above-ground vegetables (RAIS).

Table 2-6: distribution parameters for RAIS model

Above-ground Vegetables			
	Mean	Median	Standard Deviation
Risc	0.05248	0.009	0.12963

Using the RAIS model to evaluate the chemical concentration in the above ground vegetable, looking at Figure 2.15 it can be derived the same conclusions obtained for the RISC model. The value predicted by the model are higher than three of four vegetables concentration data, and the ASL n°4 data can be considered as an outlier.

In order to choice between the two different models, in the next section a comparison in term of risk for human health will be performed.

2.4.5 Risk comparison

This chapter compares the risk through the vegetables chain obtained applying different BCF models (Risc and RAIS) and the risk for soil ingestion, both calculating assuming the same soil concentration, i.e. the soil concentration limit for residential use. All the parameter used were defined above. Results are shown in Figure 2.16

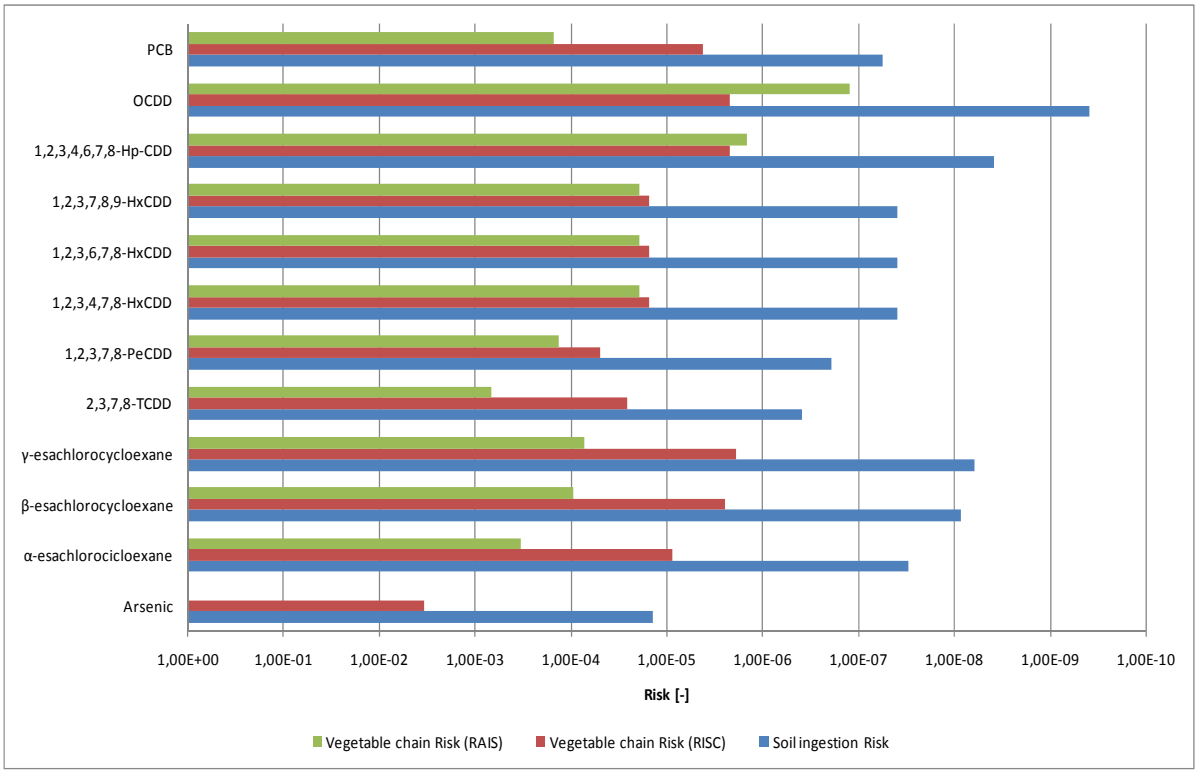

Figure 2.16: risk comparison

By comparing the results provided in Figure 2.16 the following conclusion can be drawn:

- The risk obtained using the RAIS model is about three order of magnitude higher than the one provided by the Risc model. This great difference is due to the different equations used in these models to evaluate the BCF. This is especially true for the BCF_{vs}^{sr}, i.e.:

  RAIS:

$$BCF_{vs}^{sr} = 270 \cdot K_{ow}{}^{-0,58}$$

Eq. 2-33

  Risc:

$$BCF_{vs}^{sr} = \frac{0,01 \cdot \left[10^{(0,778 \cdot logK_{ow} - 1,52)} + 0,82\right]}{K_d}$$

Eq. 2-34

- The soil risk ingestion, obtained by applying the common equations used in a Tier2 risk analysis approach, is lower than the one given by the vegetables chain models. Using these models, indeed, a screening concentration value in soil can lead to an unacceptable risk for human health (higher than 10^{-6}). This situation can be explained by the use of bioconcentration factors that have a magnifying effect, and by the high typical vegetables consumption rate.

3 VALIDATION OF THE ANALYTICAL EQUATIONS

In the tier 2 risk analysis approach the concentration at the point of exposure is calculated through the application of analytical models which provide a solution to contaminants' transport models, under simplifying assumptions. In this section a validation of the chosen models has been performed through a comparison with numerical models. The results provided by these simplified equations are compared with those obtained through numerical models, in order to get a sort of validation

3.1 CHEMICALS TRANSPORT IN VADOSE ZONE

In this chapter the leaching of contaminants from the vadose zone to ground water will be considered. The process by which water on the ground surface enters the soil is the infiltration process. Infiltration rate is defined as the rate at which soil is able to absorb rainfall or irrigation. If the precipitation rate exceeds the infiltration rate, runoff will usually occur unless there is some physical barrier. Infiltrability (or infiltration capacity) is the rate at which water will infiltrate soil when the rate is limited by soil factors only.

Water that flows through the soil and comes into contact with contaminants generates an eluate that percolates through the vadose zone and reaches the ground water table where dilution, transport and dispersion processes occur. Infiltration rate is regulated by the energy associated to the liquid mass, water flow in soil and potential difference from high energy point to another point with lower energy.

The water potential (Φ) is given by:

$$\Phi = \Psi_v + \Psi_g + \Psi_p + \Psi_s$$

Eq. 3-1

Where:

Ψ_v =kinetic energy, related to the fluid velocity;

Ψ_g = potential energy related to geodetic elevation;

Ψ_p = potential energy related to liquid pressure;

Ψ_s = potential energy related to adsorption processes.

With the usual measuring technique, it is impossible to differentiate between the pressure potential (Ψ_p) and the adsorption potential (Ψ_s) thus a new term needs to be introduced:

$$\Psi = \Psi_p + \Psi_s$$

Eq. 3-2

Where:

Ψ = is the matrix potential that represent the force that the soil exerts (pulls) on water;

The terms contained in Eq. 3-1 can be written in another form:

- Geometric elevation ($\Psi_g = Z_A$);
- Pressure elevation $\left(\Psi_p = \frac{p}{\rho \cdot g}\right)$;
- Velocity elevation $\left(\Psi_v = \frac{v^2}{2g}\right)$.

The sum of these three terms is the total hydraulic head.

$$Z_A + \frac{p}{\rho g} + \frac{v^2}{2g} = H$$

Eq. 3-3

For a saturated or unsaturated soil the energy related to liquid velocity is negligible compared to the other energy terms, and the water potential simplifies to:

$$\Phi = \Psi + z$$

Eq. 3-4

So the water potential that controls the infiltration process depends by the energy related to the gravity, the pressure and the adsorption.

With the Darcy equation, that describes the water flow in unsaturated soil:

$$q = -k(\theta)\nabla\Phi = -k(\theta)\nabla(\Psi + z)$$

Eq. 3-5

Where:

q = water flow in the unsaturated soil (infiltration rate);

k = k(θ) is the hydraulic conductivity in the vadose zone

θ = soil water content;

Ψ = matrix potential.

And the continuity equation:

$$\frac{\partial\theta}{\partial t} = \frac{\partial q}{\partial z}$$

Eq. 3-6

It is possible to obtain the Richards equation that represents the movement of water in unsaturated soils:

$$\frac{\partial\theta}{\partial t} = \frac{\partial}{\partial z}\left(-k(\theta)\frac{\partial}{\partial z}(\Psi + z)\right) = \frac{\partial}{\partial z}\left(k(\theta)\frac{\partial\Psi}{\partial z}\right) - \frac{\partial k(\theta)}{\partial z}$$

Eq. 3-7

Eq. 3-7 shows that the soil textures have great importance for the water movement in unsaturated soil. For this study an analytical model (Soil Leachability Model) and two numerical models (VS2DTI and Chemflow software) were used to investigate the soil texture contribution to water movement in unsaturated zone.

3.1.1 Analytical Model (Soil Leachability Model)

3.1.1.1 Model description

The Soil Leachability Model (SLM) is based on the Green-Ampt equation and for this reason it is usually called Green-Ampt Model. Green and Ampt (1911) derived the first physically based equation describing the infiltration of water into a soil. The Green-Ampt model has been the subject of considerable developments in applied soil physics and hydrology owing to its simplicity and satisfactory performance for a great variety of hydrological problems. For many hydrological problems the use of more sophisticated approaches (*e.g.*, the models based on the nonlinear Richards equation,) is both impractical and inefficient due to more information on soil hydraulic parameters (*e.g.* water retention and hydraulic conductivity functions) being required. In these methods, the entire soil moisture-pressure profile is generally evaluated, even though the main quantity of interest is the flux at one or both of the boundaries.

Green and Ampt assumed a plug-flow water profile (Figure 3.1) with a well-defined wetting front. The plug-flow profile assumes the soil is saturated at a volumetric water content of θ_s (except for entrapped air) down to the wetting front. At the wetting front, the water content drops abruptly to value of θ_0, which is the initial water content. The soil-water pressure head at the wetting front is assumed to be h_f (negative). Soil-water pressure at the surface, h_s, is assumed to be equal to the depth of the ponded water.

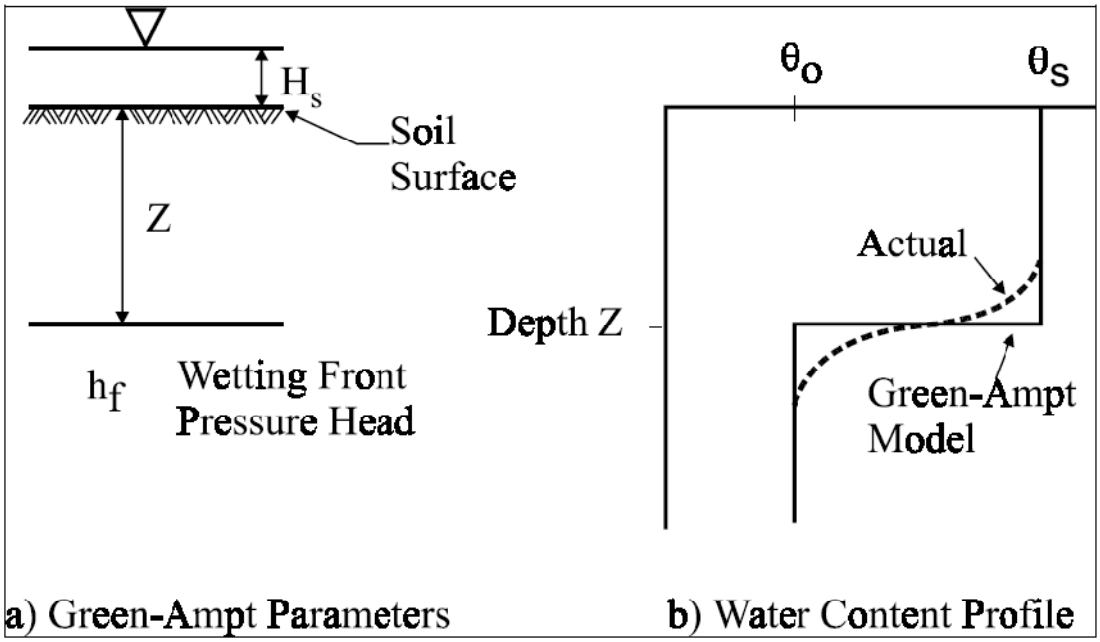

Figure 3.1: Illustration of Green-Ampt parameters and the conceptualized water content profile, which demonstrates the sharp wetting front.

3.1.1.2 Equation Analysis

As noticed before, the SLM model is based on Green-Ampt equations where the leaching process is represented considering an horizontal wet profile in which the soil, isotropic and homogeneous, has constant humidity and constant hydraulic conductivity. The time(t_w) required for the wet profile to reach the groundwater table is given by:

$$t_w[s] = \frac{\theta_a}{K_{su}} \cdot \left(L_{sgw} - (H_w - \Psi) \cdot \ln\left[\frac{H_w + L_{sgw} - \Psi}{H_w - \Psi} \right] \right)$$

Eq. 3-8

Where:

θ_a = air soil content;

K_{su} = vadose zone hydraulic conductivity [cm/s];

H_w = average annual recharge [cm];

L_{sgw} = distance between the bottom of the source and the groundwater [cm];

Ψ = matrix potential [cm].

Once this time is defined, it is possible to calculate the vertical infiltration velocity (V_s):

$$V_s \left[\frac{cm}{s} \right] = \frac{L_{sgw}}{t_w}$$

Eq. 3-9

Contaminant uses more time to reach groundwater compared to the water and this delay is accounted by introducing the retardation factor, R:

$$R = 1 + \frac{\rho_s}{\theta_T} \cdot K_s$$

Eq. 3-10

The velocity of a given contaminant is:

$$V_c \left[\frac{cm}{s}\right] = \frac{V_s}{R}$$

Eq. 3-11

The time required by the contaminant to reach the groundwater table is given by:

$$t_{gw}[s] = \frac{L_{sgw}}{V_c}$$

Eq. 3-12

3.1.1.3 Model parameters

SLM model has been applied to a site contaminated by benzene. The parameters values used to calculate the time required to reach groundwater table have been reported in Table 3-1.

Table 3-1: site default value

Symbol	Parameter	Unit measures	value	References
f_{oc}	Organic carbon fraction in vadose zone	g-C/g-soil	0,01	APAT 2006 rev. 1
L_F	Vadose zone thickness	cm	300	APAT 2006 rev. 1
d	Source thickness in vadose zone	cm	100	APAT 2006 rev. 1
ρ_s	Soil density	g/cm^3	1,7	APAT 2006 rev. 1
H_w	average annual recharge	cm	25	
K_s	Soil-water partition coefficient	cm^3/g	62	ISS-ISPESL database

Some parameters, depending on the soil texture, are reported in Table 3-2. In our study the vadose zone has been assumed as saturated so $K_{su} = K_{sat}$

Table 3-2: parameters depends by soil texture

	K_{sat}	θ_T	θ_r	θ_e	θ_a	θ_w
Texture	[cm/s]	[-]	[-]	[-]	[-]	[-]
Sand	8,25E-03	0,43	0,045	0,385	0,317	0,068
Loamy Sand	4,25E-03	0,41	0,057	0,353	0,25	0,103
Sandy Loam	1,23E-03	0,41	0,065	0,345	0,151	0,194
Sandy Clay Loam	3,64E-04	0,39	0,1	0,29	0,112	0,178
Loam	1,25E-04	0,43	0,078	0,352	0,139	0,213
Silt Loam	7,22E-05	0,45	0,067	0,383	0,128	0,255
Clay Loam	7,22E-05	0,41	0,067	0,383	0,128	0,255
Silty Clay Loam	1,94E-5	0,41	0,095	0,315	0,115	0,2
Silty Clay	5,56E-06	0,36	0,07	0,29	0,016	0,274
Silt	6,94E-05	0,46	0,034	0,426	0,148	0,278
Sandy Clay	3,33E-05	0,38	0,1	0,28	0,052	0,228
Clay	5,56E-05	0,38	0,068	0,312	0,008	0,304

3.1.1.4 Matrix potential

As described before the matrix potential is defined as

$$\Psi = \Psi_p + \Psi_s$$

For an unsaturated soil there is a capillary pressure characterized by $p_w<p_{atm}$ so the matrix potential will be negative (see. Figure 3.2). Instead in the saturated zone there is hydrostatic pressure so $p_w>p_{atm}$ and the matrix potential will be positive (see Figure 3.2).

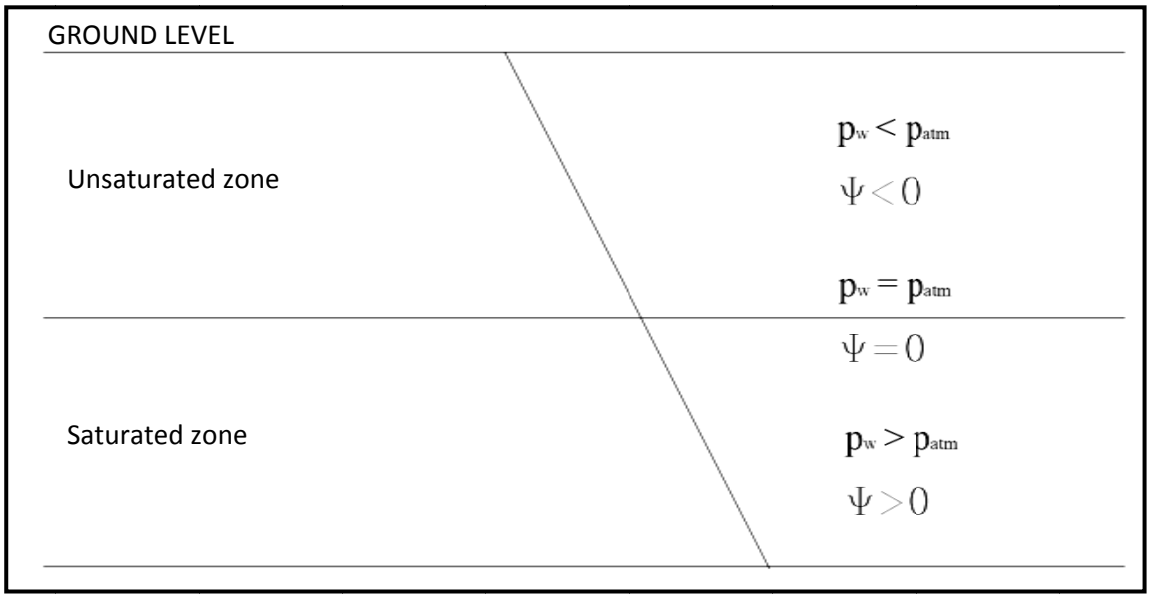

Figure 3.2: soil matrix potential trend

In this study the following methods, for the estimation of the matrix potential, were used:

- Graphic method (SCRBCA)
- Analytical method (Brooks Corey)

Graphic method (SCRBCA)

The document *South Carolina Risk-Based Corrective Action For Petroleum Releases* provides a graphic method to estimate the matrix potential, through a scheme based on Rawl and Brakensiek values, reported in Figure 3.3.

In

Table 3-3 the matrix potential value for the different soil textures have been reported. The highlighted soil textures were out of the validity range in the scheme of Figure 3.3. So, for this textures, as suggested in the document *South Carolina Risk-Based Corrective Action For Petroleum Releases*, the nearest maximum or minimum values have been used.

Table 3-3: Matrix potential values

Texture	Ψ [cm]
Sand	8,25E-03
Loamy Sand	4,25E-03
Sandy Loam	1,23E-03
Sandy Clay Loam	3,64E-04
Loam	1,25E-04
Silt Loam	7,22E-05
Clay Loam	7,22E-05
Silty Clay Loam	1,94E-5
Silty Clay	5,56E-06
Silt	6,94E-05
Sandy Clay	3,33E-05
Clay	5,56E-05

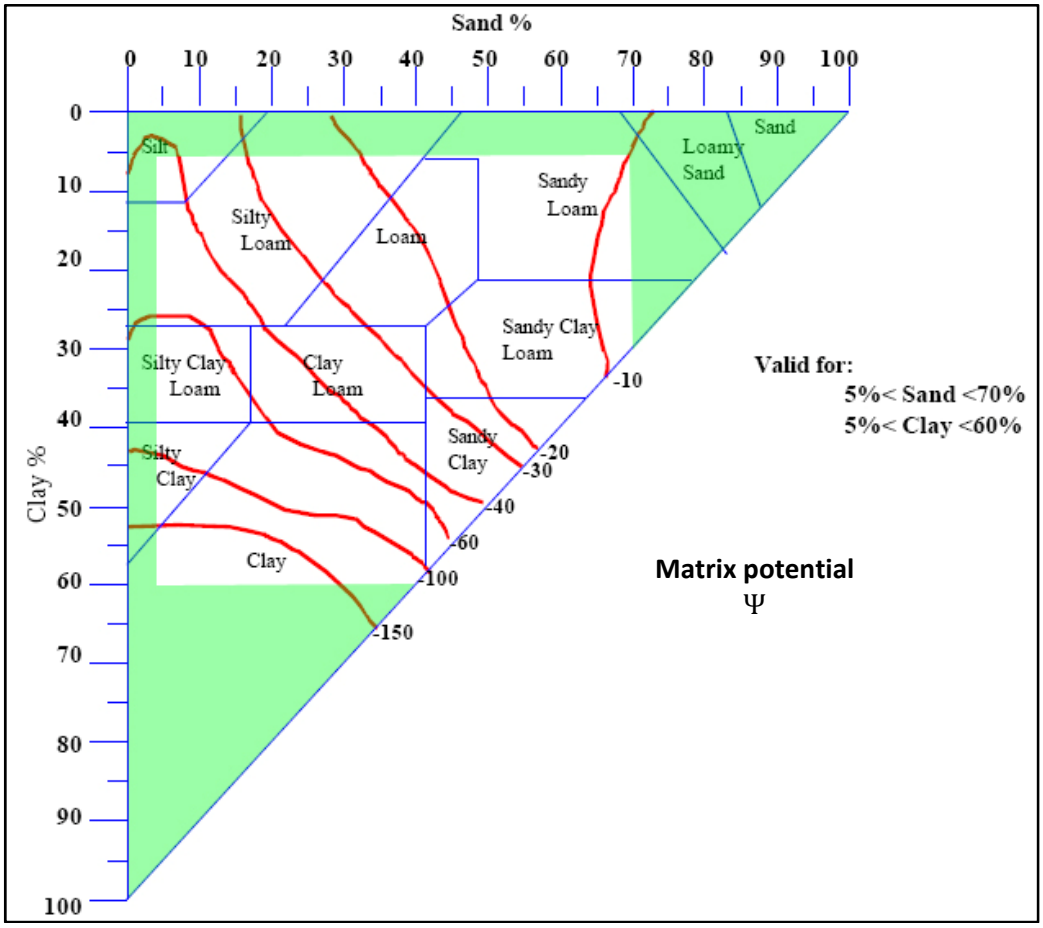

Figure 3.3: Matrix potential extract from *"Carolina Risk-Based Corrective Action For Petroleum Releases"*

Analytical Method (Brooks Corey)

This approach has been proposed in the document "*Estimation of Infiltration Rate in the Vadose Zone: Application of Selected Mathematical Models Volume II (U.S.EPA 1998)*" and is based on the Brooks and Corey equation.

The equation proposed to calculate the matrix potential is:

$$\Psi[cm] = \frac{\eta}{\eta - 1} h_e$$

Eq. 3-13

Where:

η = is the exponent of the Brooks-Corey conductivity model defined as

$$\eta = 2 + 3\lambda_{BC}$$

Eq. 3-14

Where:

λ_{BC} = is the exponent of the Brooks-Corey water retention model

h_e = is the air exit head defined as

$$h_e = -\frac{h_b}{2}$$

Eq. 3-15

Where:

h_b = is the air entry head, or the bubbling pressure head

The parameters necessary for the calculation of h_{cr} are reported in Table 3-4 and Table 3-5

Table 3-4: Typical values of air-entry head (h_e)(cm).

Texture	Brakensiek et al. (1981)	Panian. (1987)	Carsel and Parrish (1988)
Sand	35,30	3,58	6,90
Loamy Sand	15,85	1,32	8,06
Sandy Loam	29,21	9,01	13,33
Sandy Clay Loam	46,28	7,85	16,95
Loam	50,94	19,61	27,78
Silt Loam	69,55	31,25	50,00
Clay Loam	42,28	31,25	52,63
Silty Clay Loam	57,78	30,30	100,00
Silty Clay	41,72	15,87	200,00
Clay	63,96	10,00	125,00

The matrix potential values calculated for the different soil textures (using Carsel and Parrish values) are reported in Table 3-6, except for Silt and Sandy Clay textures for which values for λ_{BC} are not available.

Table 3-5: Typical values of pore size index (λ_{BC}).

Texture	Brakensiek et al. (1981)	Panian. (1987)	Carsel and Parrish (1988)
Sand	0,57	0,47	1,68
Loamy Sand	0,46	0,47	1,28
Sandy Loam	0,40	0,52	0,89
Sandy Clay Loam	0,37	0,44	0,48
Loam	0,26	0,40	0,56
Silt Loam	0,22	0,42	0,41
Clay Loam	0,28	0,40	0,31
Silty Clay Loam	0,18	0,36	0,23
Silty Clay	0,21	0,38	0,09
Clay	0,21	0,41	0,09

Table 3-6: matrix potential with Carsel & Parrish

Texture	h_b [cm]	h_e [cm]	λ [---]	η [---]	Ψ [cm]
Sand	6,9	-3,45	1,68	7,04	-4,02
Loamy Sand	8,06	-4,03	1,28	5,84	-4,86
Sandy Loam	13,33	-6,665	0,89	4,67	-8,48
Sandy Clay Loam	16,95	-8,475	0,48	3,44	-11,95
Loam	27,78	-13,89	0,56	3,68	-19,07
Silt Loam	50	-25	0,41	3,23	-36,21
Clay Loam	52,63	-26,315	0,31	2,93	-39,95
Silty Clay Loam	100	-50	0,23	2,69	-79,59
Silty Clay	200	-100	0,09	2,27	-178,74
Silt	---	---	---	---	---
Sandy Clay	---	---	---	---	---
Clay	125	-62,5	0,09	2,27	-111,71

3.1.1.5 Calculation of the time required to reach the groundwater table

As discussed above, in this study the SLM model has been used to calculate the time required for the contaminants to reach the groundwater table. Table 3-7 and Figure 3.4 report the results for the two different approach, i.e. the analytical and graphic one, respectively.

The data are very similar for the two approaches, but the analytical method is more accurate and fast compared with the graphic one. The analytical method, indeed, can be easily implemented in a data sheet and it is not subject to errors in the graphic interpretation.

Table 3-7: time necessary to reach groundwater for the two different method

	Graphics Method (SCRBCA)		Analytical Method (Brooks-Corey)	
	Ψ [cm]	t_{gw} [h]	Ψ [cm]	t_{gw} [h]
Sand	-10	5	-4,02	5
Loamy Sand	-10	8	-4,86	9
Sandy Loam	-11	16	-8,48	16
Sandy Clay Loam	-12	42	-11,95	42
Loam	-20	132	-19,07	133
Silt Loam	-30	190	-36,21	183
Clay Loam	-35	177	-39,95	172
Silty Clay Loam	-60	456	-79,59	414
Silty Clay	-100	253	-178,74	190
Silt	-40	212	---	
Sandy Clay	-30	189	---	
Clay	-150	10	-111,71	12

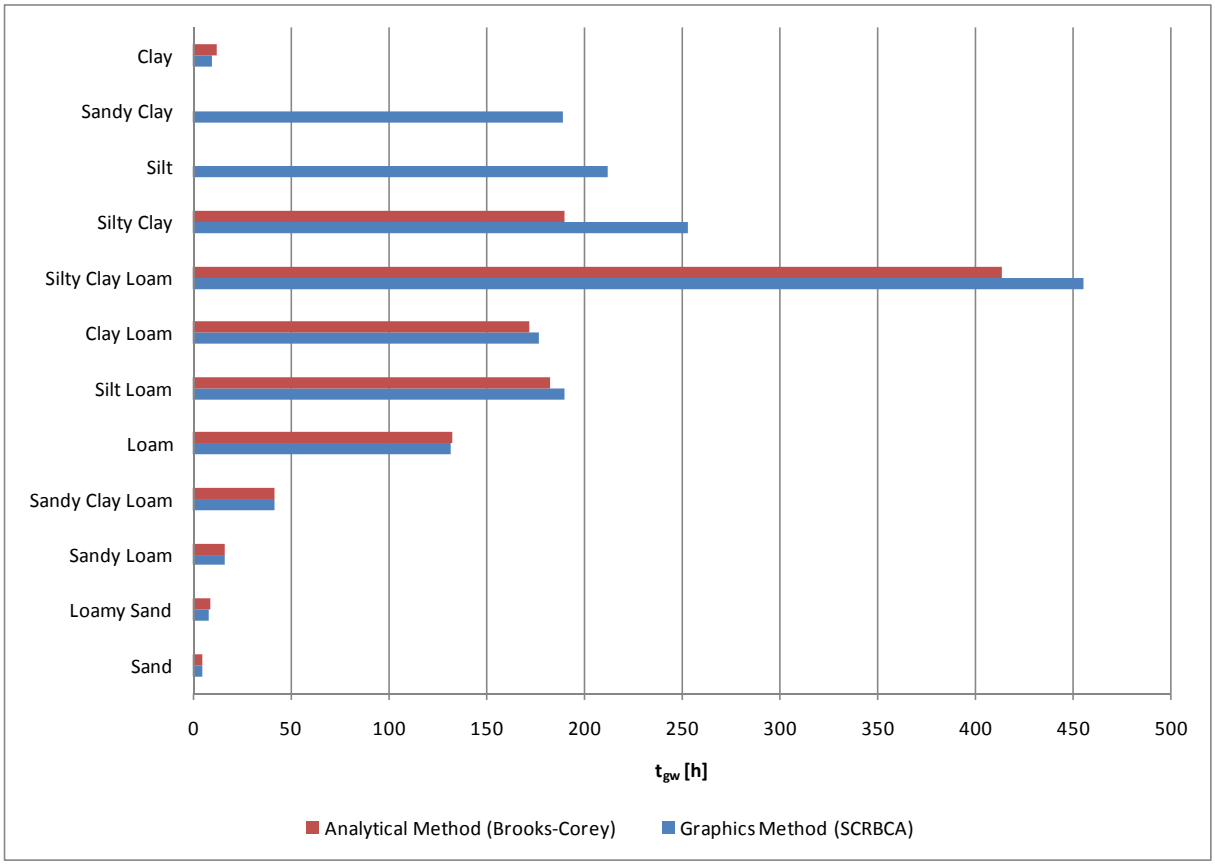

Figure 3.4: comparison from soil textures and time to reach groundwater.

As from the above results, an increase in the fine soil fraction and in the soil heterogeneity leads to an increase of the time required for the contaminant to reach the groundwater table. This fact is related to the different capillary fringe height, since the capillarity phenomena hinders the soil

infiltration process. Thus, for soil textures characterized by small values of the capillary fringe height (e.g. Sand, Loamy Sand), the contaminant needs less time to reach the groundwater table than in the case of soils with higher capillary fringe height (e.g. Silty Clay Loam).

3.1.2 Numerical Models

In this section the two numerical models used in this study, Chemflo™ 2000 and VS2DTI, will be discussed and the results obtained from their application analyzed. The numerical models present some advantages with respect to the analytical ones, since they allow for the following features:

- Simulation of complex physical system;
- Simulation of multi dimensional system;
- Complex boundary conditions;
- Input data spatial variability;
- Transient or steady state simulation;
- Output given as spatial or time distribution.

However, the numerical models present also some disadvantages:

- Long calculation time;
- Larger amount of input data;
- Problems deriving from numerical instability.

3.1.2.1 Chemflo™ 2000

Chemflo™ 2000 was written by D.L. Nofziger and Jinquan Wu of the Department of Plant and Soil Sciences ,Oklahoma State University. This software was written to enhance our understanding of the flow and transport processes. It was written primarily as an educational tool. As a result, it is highly interactive and graphics oriented. This version of the software, used in this study, is an extension of the original one developed by Nofziger et al. (1989) by providing a graphical user interface and other enhancements. The software enables users to define water and chemical transport systems. The software then solves mathematical models of these systems and displays the results graphically.

Using the notation of Nofziger et al. (1989), the differential equation used by the software to describe the water monodimensional transport is the Richards equation:

$$\frac{\partial \theta}{\partial t} = \frac{\partial}{\partial x}\left[K(h)\left(\frac{\delta h}{\delta x} - \sin(A)\right)\right] \quad \text{Eq. 3-16}$$

Introducing the following function $C(h)$:

$$C(h) = \frac{\partial \theta}{\partial h}$$
Eq. 3-17

And coupling Eq. 3-16 and Eq. 3-17, the following equation is obtained:

$$C(h)\frac{\partial h}{\partial t} = \frac{\partial}{\partial x}\left[K(h)\left(\frac{\delta h}{\delta x} - \sin(A)\right)\right]$$
Eq. 3-18

Where:

$\theta = \theta(h)$ is the volumetric water content;

$h = h(x,t)$ is the matrix potential;

x is the distance in the direction parallel to flow;

t is the time;

$\sin(A)$ is the sine of the angle A between the direction of flow and the horizontal direction;

$K(h)$ is the hydraulic conductivity of the soil at matrix potential h;

$C(h)$ is the specific water capacity

Transport and degradation of chemicals in this model are described by the convection-dispersion equation:

$$\frac{\partial}{\partial t}(\theta c + \rho S) = \frac{\partial}{\partial x}\left(\theta D \frac{\partial c}{\partial x} - qc\right) - \alpha\beta S + \gamma\theta$$
Eq. 3-19

where :

$c = c(x,t)$ is the concentration of chemical in the liquid phase;

$S = S(x,t)$ is the concentration of chemical in the solid phase;

$D = D(x,t)$ is the dispersion coefficient;

$\theta = \theta(x,t)$ is the volumetric water content;

$q = q(x,t)$ is the flux of water;

$\rho = \rho(x,t)$ is the soil bulk density;

$\alpha = \alpha(x)$ is the first-order degradation rate constant in the liquid phase;

$\beta = \beta(x)$ is the first-order degradation rate constant in the solid phase;

$\gamma = \gamma(x)$ is the zero-order production rate constant in the liquid phase.

Below the principal characteristics and limitations of Chemflo™ are summarized:

1. The models used in this software assume flow and transport in the soil is strictly one-dimensional.
2. The water flow model does not include any source or sink terms;
3. The Richards equation [Richards, 1931] for water movement is based on the Darcy-Buckingham equation [Buckingham, 1907] for water movement in unsaturated soils. This

equation is usually a good descriptor of water movement in soils, but exceptions exist. No provision is made in the model for swelling soils. No provision is made in this model for preferential flow of water through large pores in contact with free water. Therefore, it will not accurately represent flow in soils with large cracks that are irrigated by flooding. The model assumes that hysteresis in the wetting and drying processes can be ignored. It also assumes that the hydraulic properties of the soil are not changed by the presence of the chemical;

4. Partitioning of the chemical to the vapor phase is ignored in this model;
5. Limitations in the convection-dispersion equation have been observed. Clearly, any inadequacy in simulating water movement will impact the simulation of chemicals. In addition, partitioning of the chemical between the solid and liquid phases may not be proportional as assumed here. The model also assumes that this partitioning is instantaneous and reversible. Partitioning and movement of the chemical in the vapor phase is ignored in this model.
6. Chemflo™ could work under homogeneous or not homogeneous condition (e.g. humidity could change with the soil deep)
7. The simulated results depend upon the initial conditions specified. If the specified initial conditions do not match the real conditions, the calculated values may be incorrect. The user may want to analyze the sensitivity of the results of interest to the specified initial conditions.
8. The predictions of the model can be quite sensitive to the specified boundary conditions. If the specified ones do not match the actual conditions, large errors may be made. In some cases, the errors may be due to a lack of knowledge of the real boundary conditions. In other cases, the software may not be flexible enough to accommodate the real conditions. Hopefully, this will not be a major problem since boundary conditions can be changed during a simulation.
9. Limitations in the results due to approximating derivatives by finite differences, as well as other approximations used in solving the partial differential equations, are subtle and are often difficult to detect. Mass balance errors for water and chemicals are calculated to detect net computational error. Small mass balance errors are simply essential conditions for a valid solution, but they do not guarantee accurate solutions. In general, discretization errors tend to decrease as the mesh sizes decrease, so the user may want to compare solutions for different mesh sizes.
10. There are some limitation to the input data: values could vary between 0 and 1000.

3.1.2.2 VS2DTI

VS2DT is a finite-difference model that solves Richard's equation for fluid flow, and the advection-dispersion equation for solute transport. The model can analyze problems in one or two dimensions using either cartesian or radial coordinate systems. The numerical models used for flow and transport calculations are the U.S. Geological Survey's computer models VS2DT (Healy, 1990; Lappala and others, 1987).

The equations used by this software to describe the water and chemicals flow are the same described for the Chemflo™ software (Eq. 3-16, Eq. 3-17, Eq. 3-18 and Eq. 3-19)

Below the principal characteristics and limitations of VS2DTI are reported:

- Characterized by two step: pre-processor to initialize the conceptual model and post-processor for the calculation flow and transport.
- Use of finite elements to solve the Richards equation and the convection-dispersion equation.
- The model can analyze problems in one or two dimensions;
- Either cartesian or radial coordinate systems can be used;
- Initial hydraulic condition can be specified as static equilibrium, specified pressure head, or specified moisture content;
- Boundary conditions include specified pressure or total head, specified flux, infiltration with ponding, evaporation, plant transpiration, and seepage faces.
- Solute transport processes include advection, dispersion, first-order decay, adsorption, and ion exchange.

3.1.2.3 Comparison between the numerical models

In this section, the results provided by comparing the two numerical models, VS2DTI and Chemflo™, are summarized:

- Both software use Richards equations as transport equation;
- Transport processes used are the same (additionally VS2DTI uses ion exchange);
- VS2DTI considers chemical partitioning in three phases (solid, liquid and vapor) while Chemflo™ does not consider the vapor phase;
- VS2DTI can simulate transport in one dimension (as Chemflo™) or two dimension;
- VS2DTI provides numerical output (as Chemflo™) and graphic solution

Looking at the considerations reported above, the comparison with the analytical model will be limited to the VS2DTI model.

3.1.3 Application of transport model in unsaturated zone

3.1.3.1 Conceptual model

In order to apply the transport models it was required to define a site conceptual model, and to select representative chemicals and the representative source concentration.

The conceptual model proposed in the APAT document [5] for a tier 1 risk analysis was employed. This model includes the site geometry, the source geometry and the soil properties.

Benzene has been selected as representative chemical (physical properties in Table 3-8) with a source concentration value one hundred time higher than the screening value set by the Italian legislation[D.Lgs 152/06].

Table 3-8: Benzene physical properties

Chemical	S [mg/L]	P_v [mmHg]	H [---]	K_{oc}/K_d [mL/g]	$logk_{oc}$ [---]	D_a [cm^2/sec]	D_w [cm^2/sec]
Benzene	1,75E+03	9,53E+01	2,28E-01	6,20E+01	2,13E+00	8,80E-02	9,80E-06

In the current simulation the chemical migration in soil is caused by rainfall and infiltration. Rainfall intensity was evaluated applying the general hydrological balance:

$$I_{eff} = P - (ET + S)$$

Where:

P = Rainfall [mm/year];

ET = Evotraspiration [mm/year];

S = is the surface runoff [mm/year];

Assuming homogeneous soil, the annual infiltration was estimated as function of average annual precipitation for the main soil textures (Sand, Silt, Clay) through the following empirical relationship:

$$I_{eff} = 0{,}0018 \cdot P_{eff} \quad \text{For Sand soil}$$

$$I_{eff} = 0{,}0009 \cdot P_{eff} \quad \text{For Silt soil}$$

$$I_{eff} = 0{,}00018 \cdot P_{eff} \quad \text{For Clay soil}$$

3.1.3.2 Input data parameters

In this section the input data parameters used for the simulation with VS2DTI are reported, where a 1 meter thick benzene source in the surface soil was considered. The soil textures are referred to the USDA classification as reported in APAT document [5]. Table 3-9 and Table 3-10 show the input data.

Table 3-9: Soil parameters value

	K_{zz}/K_{hh} [---]	K_{hh} (=K_{sat}) [m/h]	θ [---]	RMC [---]	θ_w [---]	α [m^{-1}]	β [---]
Sand	1	0,297	0,43	0,045	0,068	14,5	2,68
Loamy Sand	1	0,1458	0,41	0,057	0,103	12,4	2,28
Sandy Loam	1	0,04428	0,41	0,065	0,194	7,5	1,89
Sandy Clay Loam	1	0,013104	0,39	0,1	0,178	5,9	1,48
Loam	1	0,0045	0,43	0,078	0,213	3,6	1,56
Silt Loam	1	0,0025992	0,45	0,067	0,255	2	1,41
Clay Loam	1	0,0025992	0,41	0,095	0,2	1,9	1,31
Silty Clay Loam	1	0,0006984	0,43	0,089	0,246	1	1,23
Silty Clay	1	0,0002002	0,36	0,07	0,274	0,5	1,09
Silt	1	0,0024984	0,46	0,034	0,278	1,6	1,37
Sandy Clay	1	0,0011988	0,38	0,1	0,228	2,7	1,23
Clay	1	0,0020016	0,38	0,068	0,304	0,8	1,09

Table 3-10: input data for VS2DTI simulation

Simbol	parameter	Unit measures	Value
	Site parameters		
α_x	horizontal dispersion	m	0,1
α_y	vertical dispersion	m	0,033
d_s	source thickness	m	1
L_F	unsaturated zone thickness	m	3
ρ_s	soil bulk density	g/m^3	1,70E+06
P	Precipitation	m/h	1,47E-04
	chemical (Benzene) parameters		
K_s	partitioning coefficient	m^3/g	6,20E-07
D_w	Water diffusion coefficient	m^2/h	3,50E-06
S_s	Field capacity	---	0,00E+00
λ	first order degradation constant	m^{-1}	0,00E+00
C_s	chemical source concentration	mg/kg	2,00E+02

Since the VS2DTI software requires as input data the concentration in the eluate, this was calculated from the soil concentration, C_s, trhough the following equations:

$$C_{L1} = C_s \cdot K_{sw}$$

Where:

$$K_{sw} = \frac{\rho_s}{\theta_w + \rho_s \cdot K_s + H \cdot \theta_a}$$

Eq. 3-20

Table 3-11 reports the different chemical source concentrations in liquid phase obtained with Eq. 3-20 for the different soil textures:

Table 3-11: Chemical source concentration for different soil textures

	ρ_s [g/cm^3]	K_s [cm^3/g]	H [---]	θ_w [---]	θ_a [---]	C_s [mg/kg]	K_{sw} [g/cm^3]	C_{L1} [g/m^3]
Sand	1,7	6,20E-01	2,28E-01	0,068	0,317	200	1,42	285
Loamy Sand	1,7	6,20E-01	2,28E-01	0,103	0,25	200	1,4	280
Sandy Loam	1,7	6,20E-01	2,28E-01	0,194	0,151	200	1,33	265
Sandy Clay Loam	1,7	6,20E-01	2,28E-01	0,178	0,112	200	1,35	270
Loam	1,7	6,20E-01	2,28E-01	0,213	0,139	200	1,31	262
Silt Loam	1,7	6,20E-01	2,28E-01	0,255	0,128	200	1,27	254
Clay Loam	1,7	6,20E-01	2,28E-01	0,2	0,115	200	1,33	266
Silty Clay Loam	1,7	6,20E-01	2,28E-01	0,246	0,095	200	1,29	257
Silty Clay	1,7	6,20E-01	2,28E-01	0,274	0,016	200	1,28	255
Silt	1,7	6,20E-01	2,28E-01	0,278	0,148	200	1,24	249
Sandy Clay	1,7	6,20E-01	2,28E-01	0,228	0,052	200	1,31	263
Clay	1,7	6,20E-01	2,28E-01	0,304	0,008	200	1,25	250

3.1.3.3 Software Output

In this section the VS2DTI simulation output obtained for the different soil textures are reported and discussed. Figure 3.5 shows the chemical concentration vs. time at a soil depth of 300 cm (i.e. the water table depth) for the different soil textures. As already noticed for the analytical approach, it is worth noting that increasing fine fraction in soil leads to an increase of the time needed to reach the water table. As explained in section 3.1.1.5 this fact is related to the capillary fringe height, since the capillarity phenomena hinders the soil infiltration process. Thus, for soil textures characterized by small values of the capillary fringe height (e.g. Sand, Loamy Sand), the contaminant needs less time to reach the groundwater table than in the case of soils with higher capillary fringe height (e.g. Silty Clay Loam). Moreover, when the clay percentage in soil increases a more evident bowing can be observed.

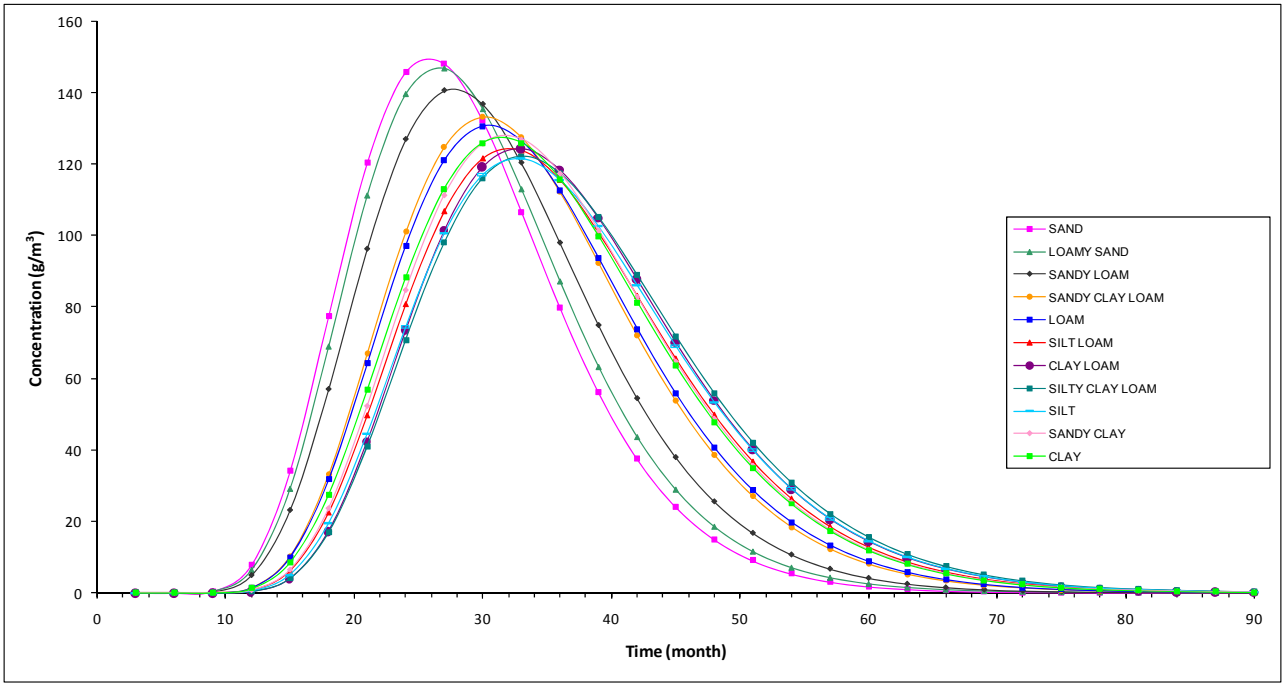

Figure 3.5: chemical concentration at the top of groundwater for the different soil textures

3.1.4 Risk evaluation for transport in the unsaturated zone

In this section, the result provided by the numerical model VS2DTI for an application on a site characterized by soil contamination with benzene, are compared to those provided by the analytical equation commonly used in Tier 2 risk analysis approach, and based on the concept of transport factors.

3.1.4.1 Analytical model

As discussed in chapter 1, in Tier 2 risk analysis the concentration at the point of exposure (C_{poe}) is predicted from the source concentration (C_s), by:

$$C_{poe} = FT \cdot C_s$$

Eq. 3-21

where FT is the transport factor, that takes in account the physical and chemical properties of the constituent, the mechanism of releases of constituents to environmental media, physical and chemical properties of the media through which migration occurs and interactions between the constituent and medium along the migration pathway. The transport factor used for describing the contaminant transport in the unsaturated zone is LF, i.e. the soil to groundwater Leaching Factor.

The Leaching factor (LF) allows the prediction of the attenuation phenomena involved in the contaminant transport from the source located in the vadose zone to the groundwater table due to its infiltration through the vadose zone and the subsequent dilution in groundwater. This factor is simply defined as the ratio between the contaminant's concentration in the groundwater right below the contamination source located in the vadose zone (C_{lmf}) and the concentration in the

contamination source itself (C_s) (see Figure 3.6), which represents also the concentration at point of exposure [APAT, 2006]:

$$LF = \frac{C_{lmf}}{C_s}\left[\frac{\frac{mg}{l - H_2O}}{\frac{mg}{Kg - soil}}\right]$$

Eq. 3-22

The equation for estimating *LF* is given by:

$$LF = \frac{k_{ws} \cdot SAM}{LDF}$$

Eq. 3-23

Where k_{ws} is the coefficient which takes in account the partition of the contaminant between the aqueous, air and solid phase:

$$k_{ws} = \frac{C_{L1}}{C_s}\left[\frac{{}^{mg}/_{l - H_2O}}{{}^{mg}/_{kg - soil}}\right] = \frac{\rho_s}{\theta_w + k_s\rho_s + H\theta_a}$$

Eq. 3-24

Where θ_w and θ_a are the water-filled and air-filled porosity, ρ_s the soil density, H the contaminant's Henry constant and k_s the soil-water partition coefficient. With reference to Figure 3.6, SAM (Soil Attenuation Model) is the attenuation coefficient accounting for the distance the contaminant has to travel before reaching the water table:

$$SAM = \frac{C'_{L1}}{C_{L1}}[adim] = \frac{d_s}{L_F}$$

Eq. 3-25

where d_s is the contamination source thickness and L_F is the distance between the top of the contamination source and the water table.

Making reference to Figure 3.6, LDF (Leachate Diluition Factor) takes in account the dilution of the contaminant's concentration when the contaminant is transferred from the leachate to groundwater, and is given by:

$$LDF = \frac{C'_{L1}}{C_{Lmf}}[adim] = 1 + \frac{V_{gw} \cdot \delta_{gw}}{I_{ef} \cdot W}$$

Eq. 3-26

where V_{gw} is the Darcy's velocity, δ_{gw} is the depth of groundwater contamination, I_{ef} the effective infiltration rate and W the contamination source dimension in the vadose zone longitudinal to the groundwater flow.

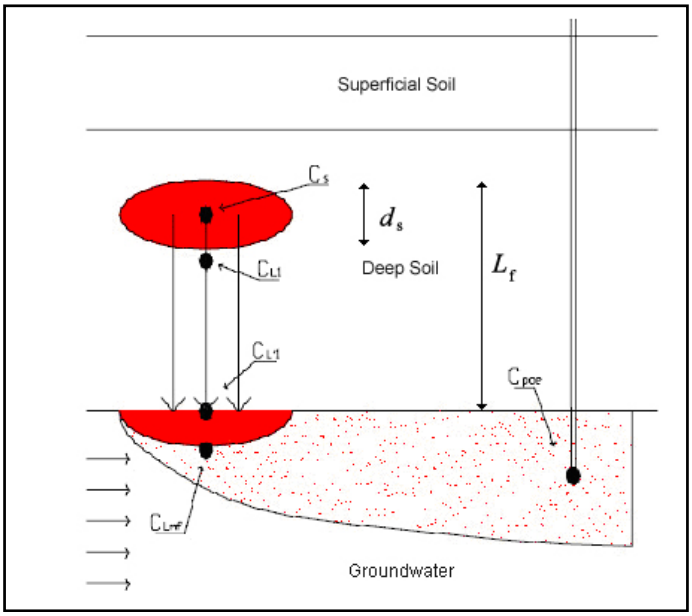

Figure 3.6: *Conceptual model of the leaching process*

3.1.4.2 Input parameters

In this section the values of the parameters used in the risk analysis procedure for water ingestion, are reported.

Table 3-12 reports the saturated soil characteristic

Table 3-12: saturated zone physical parameters

Symbol	Value	Unit
W	4500	Cm
v_{gw}	2500	cm/year
δ_{gw}	200	cm

Table 3-13 reports the parameters used to estimate the exposure rate.

Table 3-13: default value for exposure parameters

Symbol	Value	Unit
IR_w	1	l/day
EF	250	day/year
ED	25	year
BW	70	Kg
AT	70	year

Table 3-14 reports the parameters needed for the risk evaluation.

Table 3-14: parameter for risk evaluation

Symbol	Value	Unit
SF	5,50E-02	$(mg/Kg\ day)^{-1}$
EM	3,50E-03	l/ Kg day

3.1.4.3 Result of the analytical model

For the risk evaluation two cases have been considered:

- SAM = 1;
- SAM ≠ 1;

Benzene leaching from contaminated soil to groundwater was modeled under three conditions, characterized by a different thickness of the contamination source, that is 3cm, 1m and 2m, respectively. Contamination was always assumed to start from the top soil, whereas the water table was always assumed to be 3m deep. The analytical model with SAM=1 (blue column in Figure 3.7) provides the same risk values, whichever contamination thickness value is given. This result, which has a poor physical meaning, can be corrected by introducing the SAM parameter. In this case, the risk value increases with increasing contamination thickness (red column in Figure 3.7). This observation suggests the use of the SAM parameter for a more correct estimation of the LF parameter.

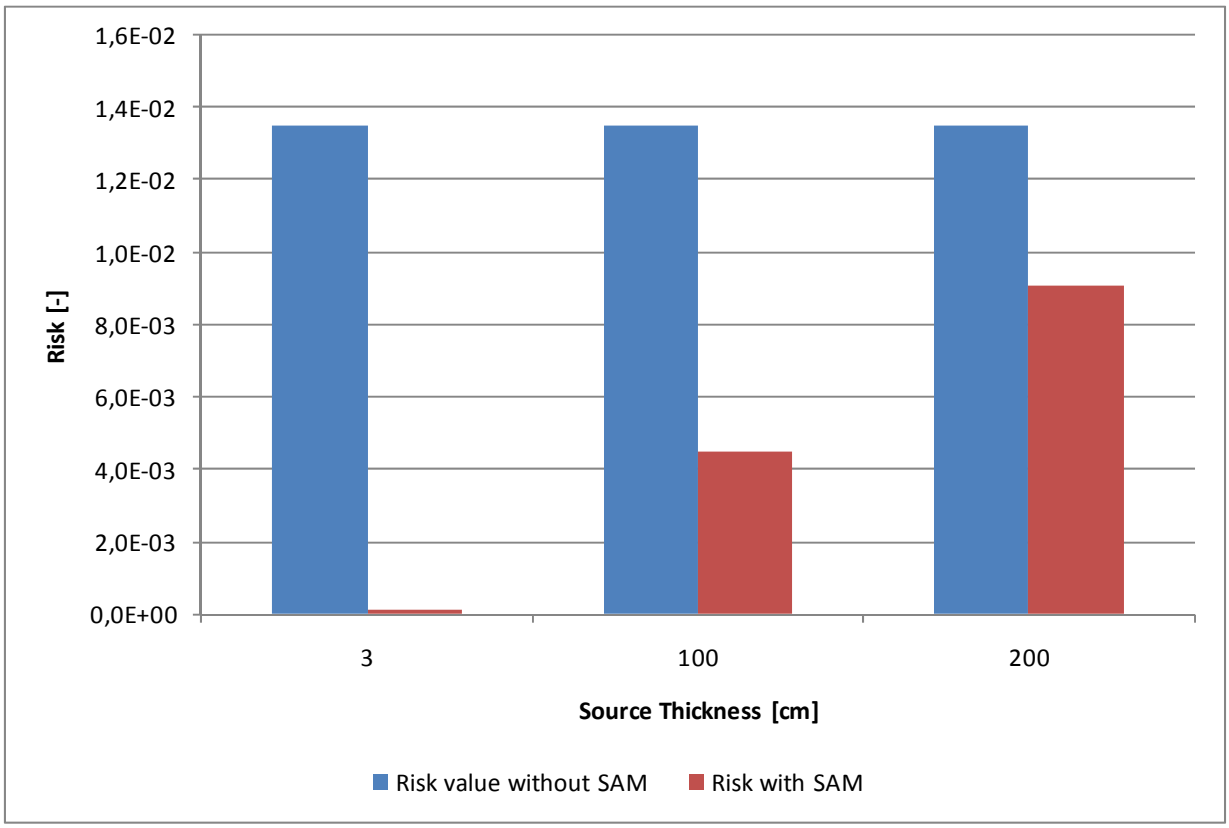

Figure 3.7: Carcinogenic Risk associated to ingestion of benzene-contaminated groundwater – analytical model

3.1.4.4 Numerical Models

As previously discussed the numerical model calculates the time evolution of the concentration at the water table and thus it could not be directly used to calculate the risk, as it can be done for the analytical model. This problem was overcome by dividing the simulation time in several time periods.

Applying this procedure it is possible to obtain the risk evaluation for each period.

$$R_{ij} = \left(C_{poe}\right)_i \cdot ED \cdot \frac{IR \cdot EF}{AT \cdot BW} \cdot SF$$

By adding each risk term, the risk evaluation for the whole time period is obtained.

$$R_{Tj} = \sum_{i=1}^{n} R_{ij}$$

Risk derived from benzene-contaminated groundwater obtained for the different soil textures are reported both in Table 3-15 and in Figure 3.8.

Table 3-15: Groundwater ingestion risk – analytical method

Soil Texture	Risk
SAND	4,12E-04
LOAMY SAND	4,17E-04
SANDY LOAM	4,26E-04
SANDY CLAY LOAM	4,28E-04
LOAM	4,28E-04
SILT LOAM	4,28E-04
CLAY LOAM	4,30E-04
SILTY CLAY LOAM	4,30E-04
SILT	4,27E-04
SANDY CLAY	4,34E-04
CLAY	4,37E-04

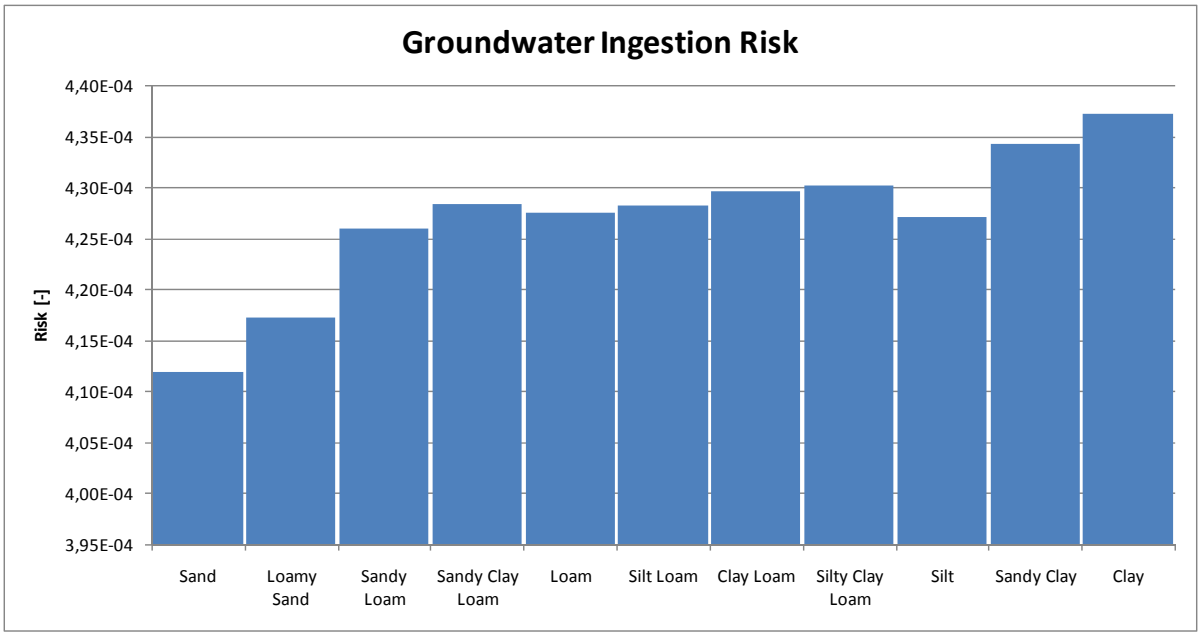

Figure 3.8: Groundwater ingestion risk – analytical method

3.1.4.5 Comparison between analytical and numerical methods

The greater difference between the analytical and the numerical models is the concentration value. In fact for the analytical model the concentration is constant for all the study period while in the numerical one it is possible to observe three step:

1. No chemical reach the water table in a initial period;
2. The chemical concentration at the water table increase until it reaches a maximum value;
3. The chemical concentration decreases, after all the contaminant has been washed out by the groundwater flow.

Considering that in a risk analysis there is an exposure duration of 25 years, in the analytical model the human receptor is exposed to a constant concentration for all the exposure duration. In the numerical one the human receptor is exposed to the contaminant only for a part of the exposure duration, so even if the receptor is exposed to higher chemical concentration compared to the analytical model for a short time probably the total risk is lower than the one evaluated with the analytical model.

By comparing the results of the analytical and numerical models (Figure 3.9 and Table 3-16) the following conclusion can be drawn:

- Risk evaluated with the numerical model is always lower or equal to the one evaluated with the analytical one. In particular:
    - For the Sand class (Sand, Loamy Sand and Sandy Loam) the risk evaluated by the analytical model with SAM is ten times higher than the one evaluated with the numerical model.
    - For the Silt class (Sandy Clay Loam, Loam, Silt Loam and Silt) the risk evaluated with SAM is five times higher than the one evaluated with the numerical model.
    - For the Clay class (Clay Loam, Silty Clay Loam, Sandy Clay and Clay) the risk evaluated without SAM is the same order of magnitude of the one evaluated with the numerical model.
- For the numerical model the difference in risk calculated for the different soil textures looks small. This is due to the fact that no degradation occurs and that within the exposure period the contaminant will, in any case, reach the point of exposure, whichever soil texture is considered.

Table 3-16: Comparison between analytical and numerical ingestion of groundwater risk for the different texture.

Texture	Numerical Risk(VS2DTI)	Analytical Risk (Without SAM)	Analytical Risk (With SAM)
Sand	4,118E-04	1,163E-02	3,839E-03
Loamy Sand	4,172E-04	1,144E-02	3,776E-03
Sandy Loam	4,259E-04	1,083E-02	3,575E-03
Sandy Clay Loam	4,284E-04	6,181E-03	2,040E-03
Loam	4,275E-04	5,985E-03	1,975E-03
Silt Loam	4,282E-04	5,808E-03	1,917E-03
Clay Loam	4,295E-04	1,342E-03	4,428E-04
Silty Clay Loam	4,302E-04	1,300E-03	4,290E-04
Silty Clay	---	1,290E-03	4,257E-04
Silt	4,271E-04	1,258E-03	4,151E-04
Sandy Clay	4,342E-04	1,328E-03	4,382E-04
Clay	4,372E-04	1,263E-03	4,169E-04

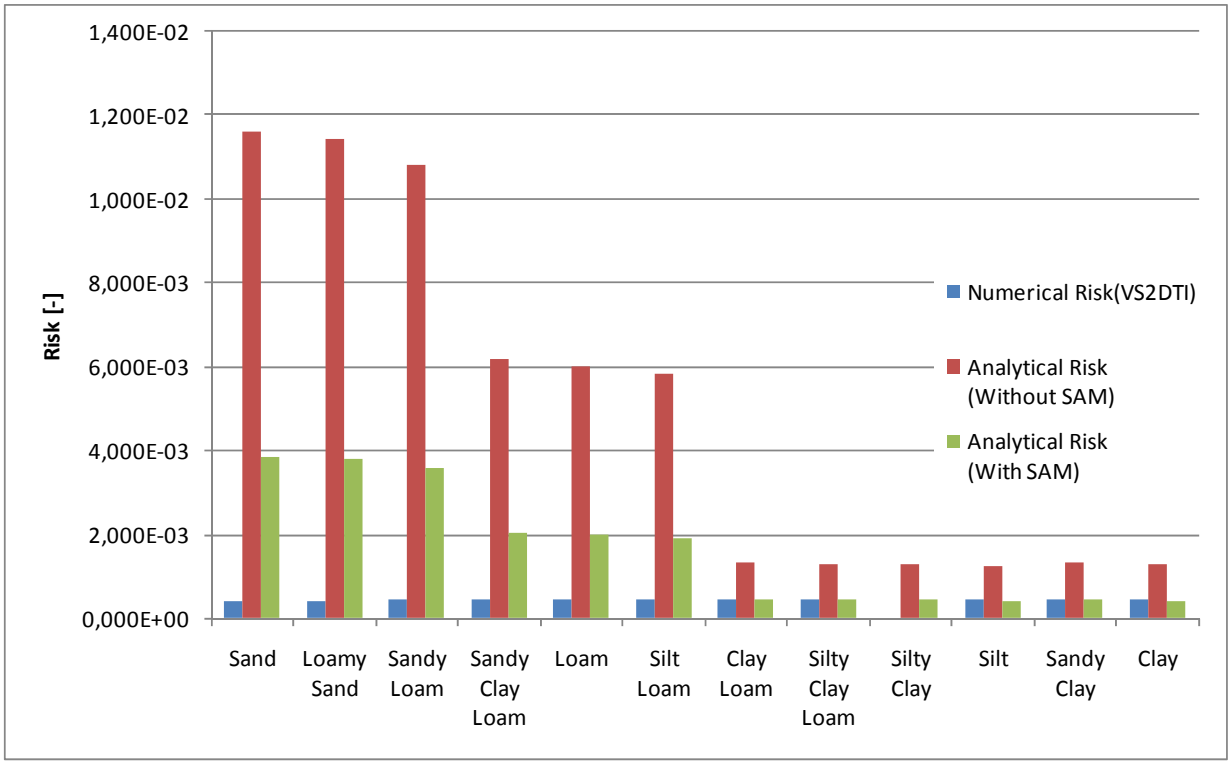

Figure 3.9: Comparison between analytical and numerical ingestion of groundwater risk for the different texture.

3.2 CHEMICAL TRANSPORT IN SATURATED ZONE

In a homogeneous and isotropic porous media, the groundwater flow can be described by the Darcy's law [1856], where the flux velocity v_{gw}, through the porous media, is proportional to the hydraulic gradient i through the hydraulic conductivity K:

$$v_{gw} = -K \cdot i = -K \cdot \frac{dh}{dL}$$

Eq. 3-27

The pore velocity (v_e) is related to flux velocity (v_{gw}) by the effective porosity (θ_e).

$$v_e = \frac{v_{gw}}{\theta_e}$$

Eq. 3-28

The flux is divided by porosity to account for the fact that only a fraction of the total formation volume is available for the fluid flow. The pore velocity would be the velocity a conservative tracer would experience if carried by the fluid through the formation.

The Darcy's law has to be coupled with the continuity equation (Eq. 3-29) in order to obtain the flow field in the saturated media:

$$\frac{\partial \rho}{\partial t} + \nabla(\rho \cdot v_e) = \frac{D\rho}{Dt} + \rho \nabla(v_e) = 0$$

Eq. 3-29

Where:

ρ = water density [kg/m^3]

If there is a homogeneous distribution of temperature, to null temperature gradients correspond null fluid density gradient, so:

$$\frac{D\rho}{Dt} = 0$$

Eq. 3-30

From Eq. 3-29 and Eq. 3-30:

$$\nabla(v_e) = 0$$

Eq. 3-31

The equation for chemical transport in saturated zone is:

$$R\frac{\partial C}{\partial t} = -\nabla(C \cdot v_e) + \nabla[(D_h + D_m) \cdot \nabla C] - k_d C$$

Eq. 3-32

Where:

$\boldsymbol{\nabla(C \cdot v_e)}$: Advection term. Advection is a transport mechanism of substance with a moving fluid along the fluid direction with the fluid velocity.

$\boldsymbol{\nabla[(D_h + D_m) \cdot \nabla C]}$ **:** Hydrodynamic dispersion and molecular diffusion term. The Hydrodynamic (or mechanical) dispersion results from variations in the movement of water which carries out pollutant. It can be split in longitudinal dispersion and transversal dispersion. The former one is caused by the viscosity term that slows down some contaminants' molecules, whereas the latter one is caused by the pore structure tortuosity.

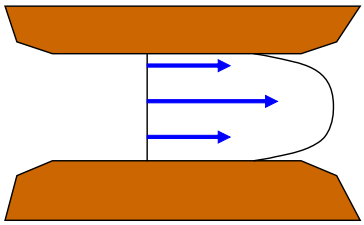

Dispersion longitudinal

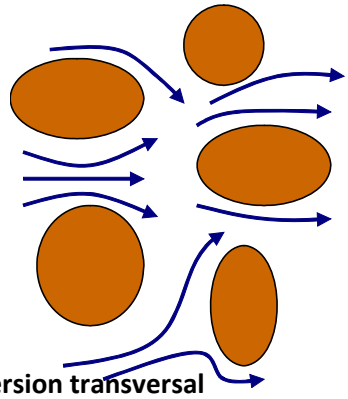

Dispersion transversal

Molecular diffusion is a net transport of molecules from a region of higher concentration to one of lower concentration by random molecular motion. The result of diffusion is a gradual mixing of material. In a phase with uniform temperature, absent external net forces acting on the particles, the diffusion process will eventually result in complete mixing or a state of equilibrium. Molecular diffusion is typically described mathematically using the Fick's law (Eq. 3-33):

$$q = -D_m \nabla C$$

Eq. 3-33

Where

q : is the contaminant mass flux, i.e. the amount of substance that will flow through a small area during a small time interval [kg/s];

D_m : is the diffusion coefficient [m^2/s];

$\boldsymbol{k_d}$ [Dimensionless] is a factor related to the partitioning of a contaminant between the solid and aqueous phases.

$\boldsymbol{R}$ [Dimensionless] is the retardation factor:

$$R = 1 + k_d \frac{\rho_b}{\theta_w}$$

Eq. 3-34

Retardation factor represents the reduction in the rate at which dissolved contaminants move through an aquifer due to sorption of contaminants to the solid aquifer matrix. The degree of retardation depends on both aquifer and constituent properties. The retardation factor is the ratio of the groundwater seepage velocity to the rate that organic chemicals migrate in the groundwater.

The equation for chemical transport in saturated zone is a differential equation whose solution can be determined analytically or numerically. These models will be described below.

3.3 OFF-SITE RECEPTORS

Tier 2 risk analysis uses simple analytical models to evaluate risk from contamination in saturated zone for off-site receptors. In this section a comparison between analytical and numerical model will be performed in order to evaluate the analytical model conservative assumption.

The following models have been compared:

- Domenico analytical model;
- FeFlow numerical model;

3.3.1 Domenico analytical model

The equation that describes the chemical transport in saturated zone is:

$$R\frac{\partial C}{\partial t} = -\nabla(C \cdot v_e) + \nabla[(D_h + D_m) \cdot \nabla C] - k_d C$$

Eq. 3-35

An analytical solution of Eq. 3-35 can be obtained for one of the following conditions; either with or without biodegradation:

- Instantaneous release (pulse)
- Continuous release (plume)

3.3.1.1 Derivation of the analytical solution

One of the most used analytical solution for the continuous release, with or without biodegradation, is the Domenico solution.

Domenico model is a three-dimensional analytical solute transport model that assumes a vertical plane source oriented perpendicular to groundwater flow to simulate the release of organics to moving groundwater. Related to Figure 3.10 the source dimension are $y = S_w$ on y direction and $z = S_d = \delta_{gw}$ on z adirection.

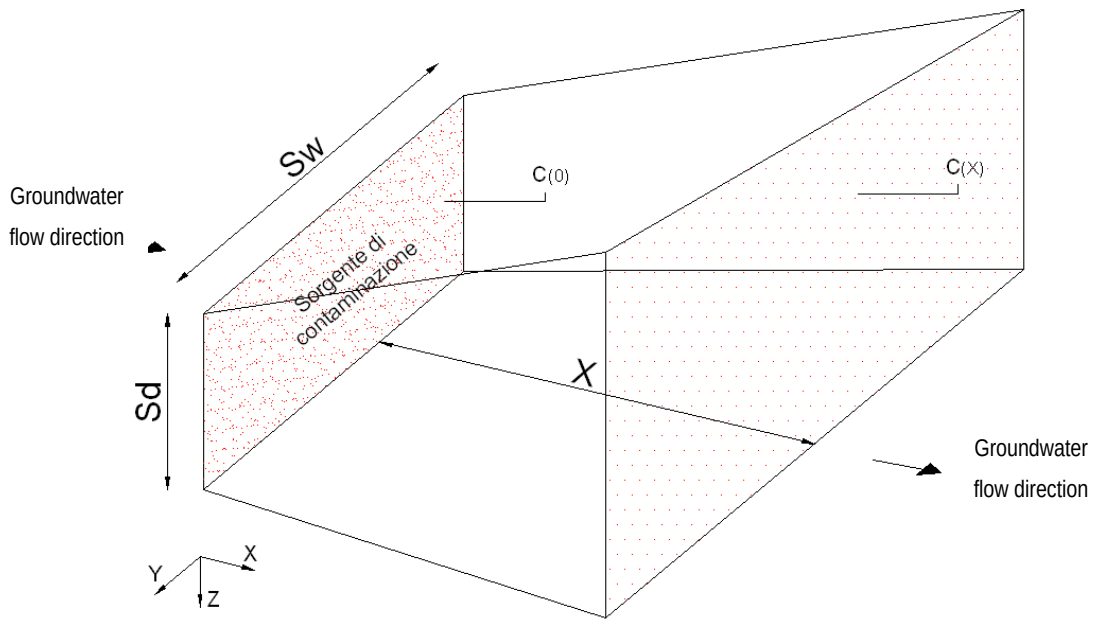

Figure 3.10: source geometry for Domenico solution

Considering the dispersion on x axis along the other direction (y,z) the chemical concentration distribution is given by:

$$C(x,y,z,t) = \frac{C_0}{8} \cdot exp\left[\frac{x \cdot v_e}{2 \cdot D_x} \cdot \left(1 - \sqrt{1 + 4 \cdot \lambda \cdot R \cdot \frac{D_x}{v_e^2}}\right)\right] \cdot erfc\left[\frac{x - v \cdot \frac{t}{R} \cdot \sqrt{1 + 4 \cdot \lambda \cdot R \cdot \frac{D_x}{v_e^2}}}{2 \cdot \sqrt{\frac{D_x}{v_e} \cdot t}}\right] \cdot$$
$$\cdot \left[erf\left(\frac{y + \frac{Y}{2}}{2 \cdot \sqrt{\frac{D_y}{R} \cdot \frac{x}{v_e}}}\right) - erf\left(\frac{y - \frac{Y}{2}}{2 \cdot \sqrt{\frac{D_y}{R} \cdot \frac{x}{v_e}}}\right)\right] \cdot \left[erf\left(\frac{z + \frac{Z}{2}}{2 \cdot \sqrt{\frac{D_z}{R} \cdot \frac{x}{v_e}}}\right) - erf\left(\frac{z - \frac{Z}{2}}{2 \cdot \sqrt{\frac{D_z}{R} \cdot \frac{x}{v_e}}}\right)\right]$$

Eq. 3-36

Assuming the diffusion as the product between dispersivity, in all three space direction (a_x, a_y, a_z), and the effective velocity:

$$D_x = a_x \cdot v_e$$
$$D_y = a_y \cdot v_e$$
$$D_z = a_z \cdot v_e$$

Eq. 3-36 yields:

$$C(x,y,z,t) = \frac{C_0}{8} \cdot exp\left[\frac{x}{2 \cdot a_x} \cdot \left(1 - \sqrt{1 + 4 \cdot \lambda \cdot R \cdot \frac{a_x}{v_e}}\right)\right] \cdot erfc\left[\frac{R \cdot x - v \cdot t \cdot \sqrt{1 + 4 \cdot \lambda \cdot R \cdot \frac{a_x}{v_e}}}{2 \cdot \sqrt{a_x \cdot v_e \cdot R \cdot t}}\right] \cdot$$
$$\cdot \left[erf\left(\frac{y + 0{,}5 \cdot S_w}{2 \cdot \sqrt{a_y \cdot x}}\right) - erf\left(\frac{y - 0{,}5 \cdot S_w}{2 \cdot \sqrt{a_y \cdot x}}\right)\right] \cdot \left[erf\left(\frac{z + 0{,}5 \cdot S_d}{2 \cdot \sqrt{a_z \cdot x}}\right) - erf\left(\frac{z - 0{,}5 \cdot S_d}{2 \cdot \sqrt{a_z \cdot x}}\right)\right]$$

Eq. 3-37

Where:

R is the retardation factor;

v_e is the effective velocity;

λ is the first order degradation rate.

$erfc(x)$ is the complementary error function defined as $erfc(x) = 1 - erf(x)$;

$erf(x)$ is the error function defined as:

$$\mathrm{erf}(x) = \frac{2}{\sqrt{\pi}} \int_0^x e^{-t^2} dt$$

The time variable appears only within function $erfc(x)$. When the argument of the function reaches the value of -2, the $erfc(x)$ function reaches the asymptotic value of 2 and the steady state solution, known as "Domenico equation", is obtained.

$$\frac{C(x,y,z)}{C_0} = \frac{1}{4} \cdot exp\left[\frac{x}{2 \cdot a_x} \cdot \left(1 - \sqrt{1 + \frac{4 \cdot \lambda \cdot R \cdot a_x}{v_e}}\right)\right] \cdot \left[erf\left(\frac{y + 0{,}5 \cdot S_w}{2 \cdot \sqrt{a_y \cdot x}}\right) - erf\left(\frac{y - 0{,}5 \cdot S_w}{2 \cdot \sqrt{a_y \cdot x}}\right)\right] \cdot \left[erf\left(\frac{z + 0{,}5 \cdot S_d}{2 \cdot \sqrt{a_z \cdot x}}\right) - erf\left(\frac{z - 0{,}5 \cdot S_d}{2 \cdot \sqrt{a_z \cdot x}}\right)\right]$$

Eq. 3-38

Where all the parameters are discussed above

The main assumptions underlying this equation are: steady state ($tt \to \infty$), continuous release, constant representative source concentration, finite dimension source, three dimensional dispersion and convection only along flow direction

The higher concentration value will naturally be along the x-axis, thus placing $y = z = 0$ in Eq. 3-38 and taking into account the fact that $\mathrm{erf}(-B) = -\mathrm{erf}(B)$, the simplified following term of the equation for evaluating the concentration along the flow direction, can be obtained:

Case 1 – DAF(1)

$$\frac{C(x)}{C_0} = \frac{1}{4} \cdot exp\left[\frac{x}{2 \cdot a_x} \cdot \left(1 - \sqrt{1 + \frac{4 \cdot \lambda \cdot R \cdot a_x}{v_e}}\right)\right] \cdot \left[erf\left(\frac{S_w}{4 \cdot \sqrt{a_y \cdot x}}\right)\right] \cdot \left[erf\left(\frac{S_d}{4 \cdot \sqrt{a_z \cdot x}}\right)\right]$$

Eq. 3-39

This equation takes in account the dispersive phenomena in all three space directions

Case 2 – DAF(2)

If vertical dispersion is considered only in the positive direction, Eq. 3-38 becomes:

$$\frac{C(x)}{C_0} = \frac{1}{4} \cdot exp\left[\frac{x}{2 \cdot a_x} \cdot \left(1 - \sqrt{1 + \frac{4 \cdot \lambda \cdot R \cdot a_x}{v_e}}\right)\right] \cdot \left[erf\left(\frac{S_w}{4 \cdot \sqrt{a_y \cdot x}}\right)\right] \cdot \left[erf\left(\frac{S_d}{2 \cdot \sqrt{a_z \cdot x}}\right)\right]$$

Eq. 3-40

This hypothesis is valid assuming that the groundwater level is acting as an upper limit in the z direction and that the top of the source is at the limit of the water table.

Case 3 – DAF(3)

If the whole aquifer thickness is interested by the contamination, there will be no vertical dispersion, so the Eq. 3-38 becomes

$$\frac{C(x)}{C_0} = exp\left[\frac{x}{2 \cdot a_x} \cdot \left(1 - \sqrt{1 + \frac{4 \cdot \lambda \cdot R \cdot a_x}{v_e}}\right)\right] \cdot \left[erf\left(\frac{S_w}{4 \cdot \sqrt{a_y \cdot x}}\right)\right]$$

Eq. 3-41

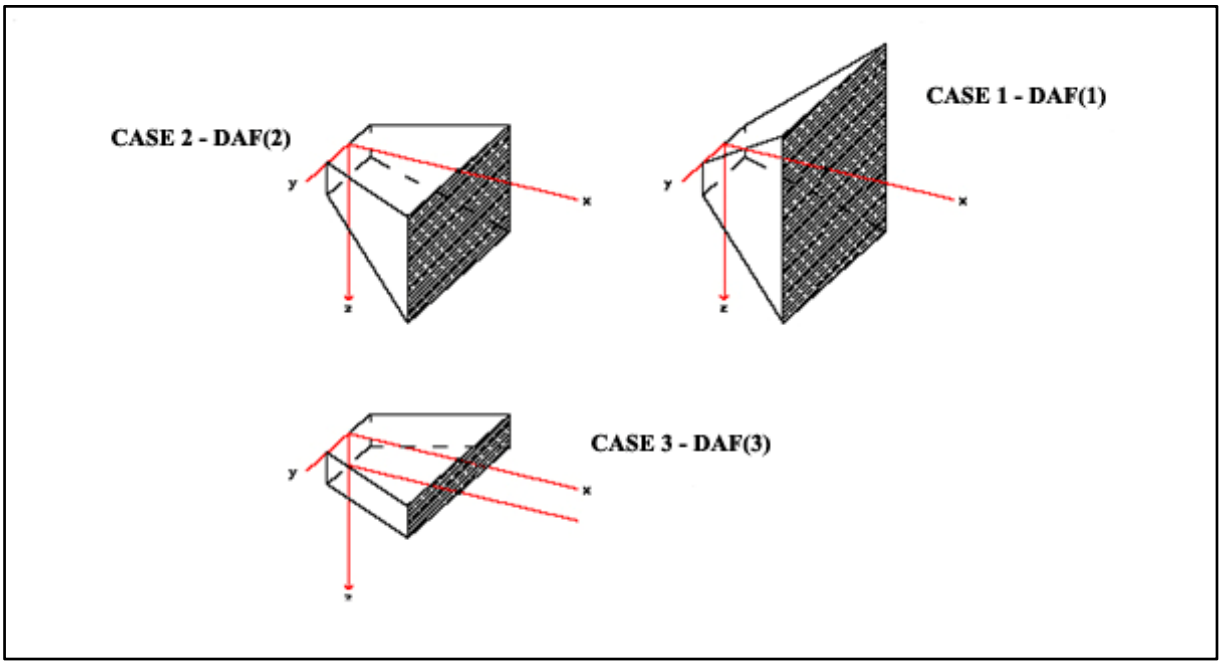

3.3.2 FeFlow numerical model

The FeFlow software (Finite Element subsurface FLOW system, WASY GmbH (Institute for Water Resources Planning and Systems Research, Berlin) version 5.3x was used in this work. This version allows to simulate 2D and 3D fluid flow, mass and heat transport problems in a saturated media (groundwater) in unsaturated media and also in variable saturation media. The following simulation options can be used:

- Fluid flow;
- Steady state
- Transient state

Fluid flow and mass transport:

- Steady state for both fluid flow and mass transport
- Steady state for fluid flow and transient state for mass transport.
- Transient state for both fluid flow and mass transport

Heat transport

- Steady state
- Transient state

In the following, no heat transport will be considered. And for the mass transport two kind of simulation are possible:

- Single species transport
- Multi species transport

For the 2D modeling three kind of projection are possible:

- Horizontal
- Vertical (transport in unsaturated zone or in confined aquifer)
- Asymmetric (transport in unsaturated zone or in confined aquifer)
-

3.3.2.1 Input data

Table 3-17 and Table 3-18 report the input parameter necessary for flow and mass transport, respectively.

Table 3-17: material condition for flow (extracted from FeFlow manual)

Parameter	Symbol	Description	Unit
Conductivity	K_{max}	Proportional to flow resistance in aquifer	m/s
Transmissivity	T_{max}	Proportional to flow resistance and aquifer thickness	
Anisotropy	Ξ_{aniso}	Ratio of maximum directional value to its original value	
Aquifer bottom elevation	x_l^{bottom}	Bottom geometry of aquifer	m
Aquifer top elevation	x_l^{top}	Top geometry of aquifer	m
storativity	ε_e	Drain/fillable void space in aquifer	
Density ratio	$\bar{\alpha}$	Mass buoyant expansion coefficient for density-coupled flow	
In/outflow on top/bottom	P_0	Spatially variable recharge/evaporation on top or bottom slice	m/d
Source/sink	Q_ρ	Spatially variable recharge/evaporation	d^{-1}
Transfer rate in/out		Value computed from conductivity and thickness of colmation layer	d^{-1}

Table 3-18: material condition for mass transport (confined and unconfined)

Parameter	Symbol	Description	Unit
Aquifer thickness	B	For confined aquifer	M
Porosity	ε	Void space	
Sorption coefficient	κ	Sorbed materials, described by Henry, Langmuir or Freunlich isoterm	
Molecular diffusion	D_d	Diffusion of a chemical in solution	m^2/s
Longitudinal dispersivity	β_L	Spreading of a chemical due to heterogeneity of the porous medium in flow direction	m
Transverse dispersivity	β_T	Spreading of a chemical due to heterogeneity of the porous medium in the direction orthogonal to the flow	m
Decay rate	ϑ	Rate of contaminant decay due to biodegradation or radioactivity	s^{-1}
Source/sink	$\bar{Q}_C$	Spatially varying in/outflow of contaminant mass	g/m^2s
Transfer rate		Transmission resistance for contaminated mass flow	

3.3.3 Application of transport model in saturated zone

This section reports the results obtained by the application of the analytical model (Domenico equations) and the numerical model (FeFlow) for a specific case study described below in detail.

3.3.3.1 Conceptual model

For the implementation of the different models a conceptual model of the site, the representative contaminants and the source representative concentration, were defined.

As conceptual model the one proposed by APAT document [5] for a tier 1 risk analysis was considered as far as the geometry of the site, the contamination source and the physical soil properties, are concerned. Benzene was considered as model contaminant in groundwater, with a source representative concentration of 0,1 mg/l, that is one hundred time higher than the screening level concentration set by the Italian legislation (D.M. 152/06).

Table 3-19: Benzene physical properties

Chemical	S [mg/L]	P_v [mmHg]	H [---]	K_{oc}/K_d [mL/g]	$logk_{oc}$ [---]	D_a [cm^2/sec]	D_w [cm^2/sec]
Benzene	1,75E+03	9,53E+01	2,28E-01	6,20E+01	2,13E+00	8,80E-02	9,80E-06

Table 3-20 reports the parameters value used for the simulation.

Table 3-20: parameter values for the simulation.

				FeFlow 5.3		Domenico		
	Symbol	Unit	Value	2D	3D	DAF1	DAF2	DAF3
Geometry								
Source extension in flow direction	W	m	45	X	X	-	-	-
Source extension orthogonal to flow direction	Sw	m	45	X	X	X	X	X
Aquifer thickness	Sd	m		X (*)	X (*)	=δgw	=δgw	-
Investigation area extension in flow direction	---	m	300	X	X	-	-	-
Investigation area extension orthogonal to flow direction	---	m	300	X	X	-	-	-
Flow								
Hydraulic head gradient	Δh	m	3	X (*)	X (*)	-	-	-
Bottom aquifer deep	Z_{bottom}	m	(**)	X	X	-	-	-
Top aquifer deep	Z_{top}	m	(**)	X	X	-	-	-
Effective Darcy velocity	v_e	cm/year	7082	X (*)	X (*)	X	X	X
Retardation factor	R	---		X (*)	X (*)	X	X	X
Max hydraulic conductivity (Kmax)	K_{SAT}	L/t	4,5E-03	X	-	-	-	-
Anisotropy factor (Kmax/Kmin)	---	---	1	X	-	-	-	-
Kmax on x angle	°	---	0	X	-	-	-	-
hydraulic conductivity along x	Kxx	L/t		-	X	-	-	-
hydraulic conductivity along y	Kyy	L/t		-	X	-	-	-
hydraulic conductivity along z	Kzz	L/t		-	X	-	-	-
Fluid density ratio	---	---		-	X	-	-	-
Storativity	---	---	0.2	X	X	-	-	-
Compressibility	---	L^{-1}	1E-04	X	X	-	-	-
Superficial flux In/out	---	L/t	0	-	X	-	-	-
Secondary source	---	L/t	0	X	X	-	-	-
Transfer factor(in/out)	---	t^{-1}	0	X	X	-	-	-
Mass								
Initial concentration	C_0	mg/l	0.1	X	X	X	X	X
Porosity	Θ_e	---	0.353	X	X	-	-	-
Henry adsorption coefficient	k	---	0.163	X	X	-	-	-
Water diffusion coefficient	D_w	cm^2/s	9,8E-06	X	X	-	-	-
Longitudinal dispersivity	ax	m	0,1xL	X	X	X	X	X
Transversal dispersivity	ay	m	ax/10	X	X	X	X	X
Vertical dispersivity	az	m	ax/10	-	-	X	X	-
First order decay constant	λ	t^{-1}	9,6E-04	X	X	X	X	X
Secondary source	---	$ML^{-3}t^{-1}$	0	X	X	-	-	-
Transfer rate (in/out)	---	L/t	0	X	X	-	-	-
Observation point								
Observation point along x axis	x_{obs}	m	100	X	X	X	X	X
Observation point along y axis	y_{obs}	m	0	X	X	-	-	-
Observation point along z axis	z_{obs}	m	0	-	X	-	-	-

(*) indirect calculation (**) different case by case

3.3.3.2 Dispersion

Dispersion is caused by the media porosity heterogeneity, which creates variations in the velocity and travel direction of contaminants. The mass transport due to dispersion, occurs in the direction of groundwater flow (longitudinal dispersion) and in the direction normal to the flow (transverse dispersion).

The dispersivity is an empirical factor which allows to quantify the contaminant dispersion in the porous media. Studies on column test show the dispersion as a function of average linear velocity and a factor called dispersivity (α). The dispersivity is "scale-dependent" which means that the values measured in a aquifer of 1 m³ are different from those measured in 10 m³. The values reported in literature, obtained from one-dimensional (1-D) column tests and field measurements, confirm this statement. The first ones are in the order of magnitude centimeters, while the dispersivity coefficients obtained in the field are in the range within 1 to 1000 m.

This case is designed to compare the analytical model 1-D (Domenico) with the numerical one (FEFLOW) and not to describe a real case. So the following dispersivity values was used for both models:

$$\alpha_x = \frac{L_{poe}}{10} = 10\text{m}$$

$$\alpha_y = \alpha_z = \frac{\alpha_x}{10} = 1\text{m}$$

It worth noting that the choice of considering both horizontal and vertical dispersivity equal to $^1/_{10}$ of longitudinal dispersivity, is due to a limit of FEFLOW software that makes it impossible to differentiate the two dispersivity values. The APAT document suggestion for these dispersivity value:

$$\alpha_y = \frac{\alpha_x}{3}$$

$$\alpha_z = \frac{\alpha_x}{20}$$

So the choice of considering both dispersivity values equal to 1 / 10 of the longitudinally dispersivity, compensates the two values proposed by the document APAT. The charts below (Figure 3.11, Figure 3.12 and Figure 3.13) shows the results obtained with the 1D model of Domenico using the two different approaches for dispersivity.

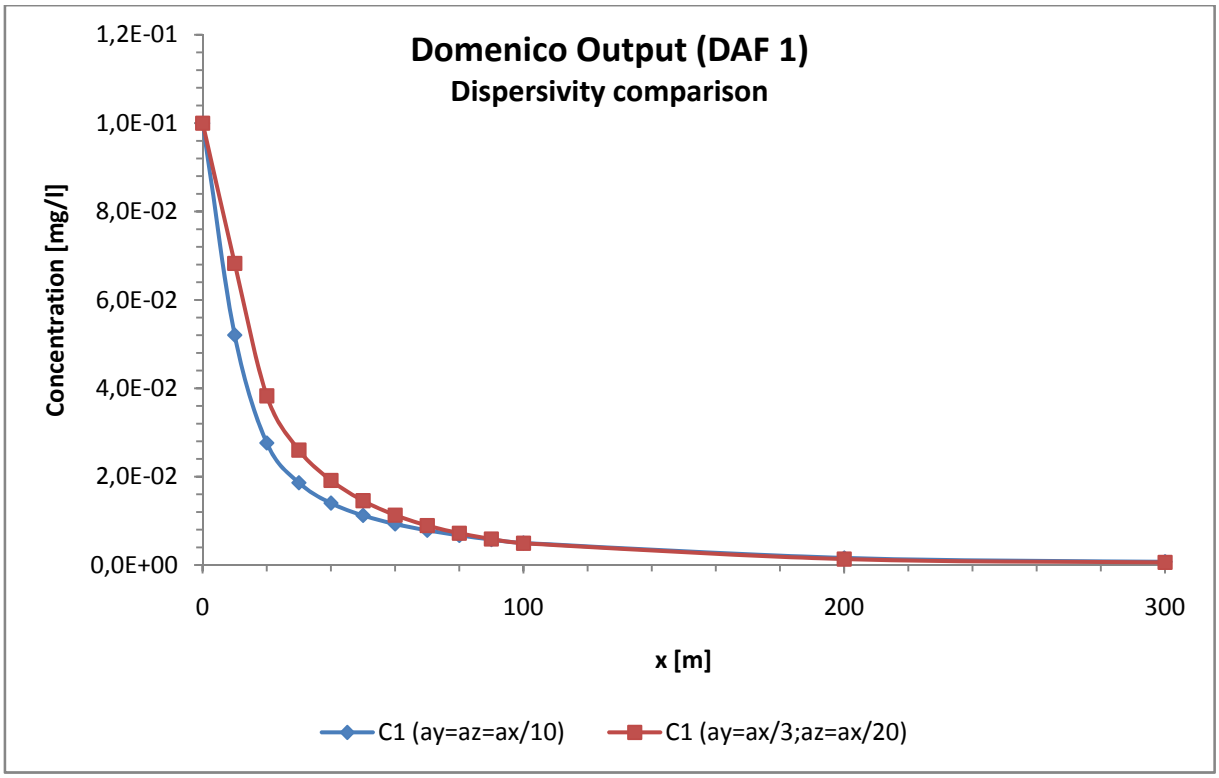

Figure 3.11: Domenico output comparison with different approaches for longitudinal and vertical dispersivity with dispersion in all directions (DAF1)

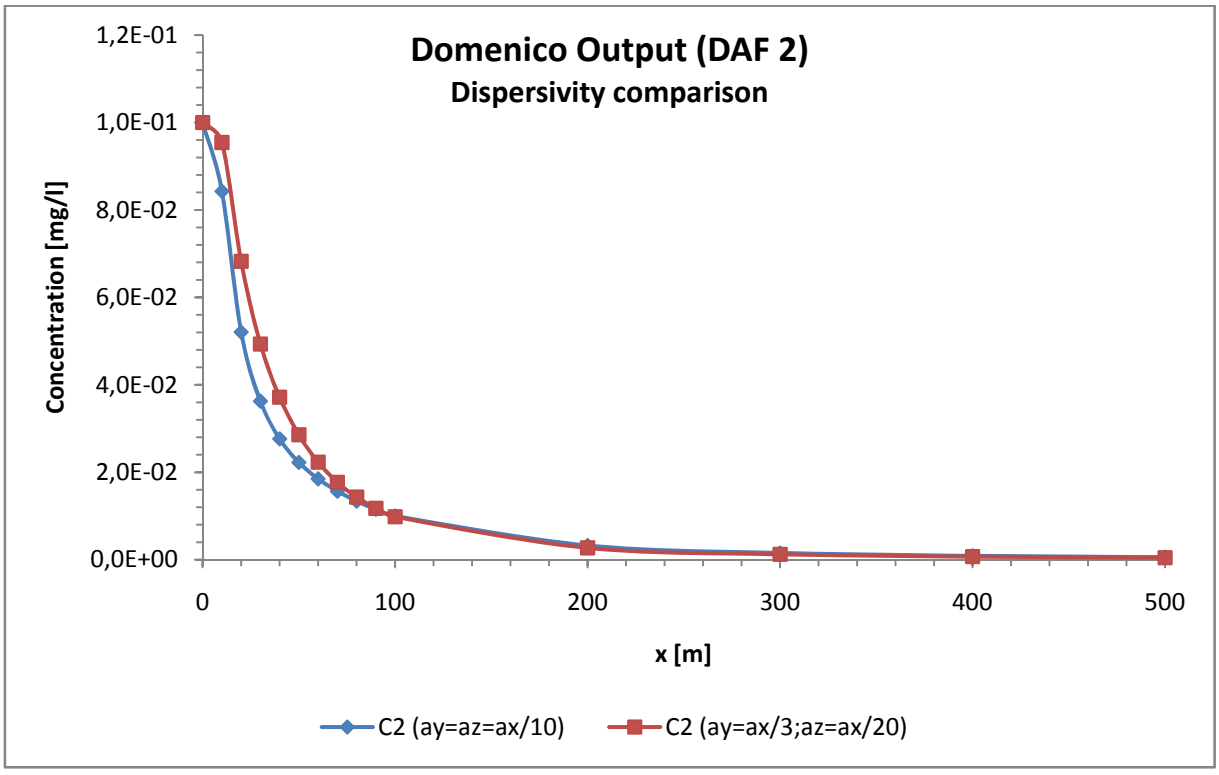

Figure 3.12: Domenico output comparison with different approaches for longitudinal and vertical dispersivity with vertical dispersion only in positive direction (DAF2)

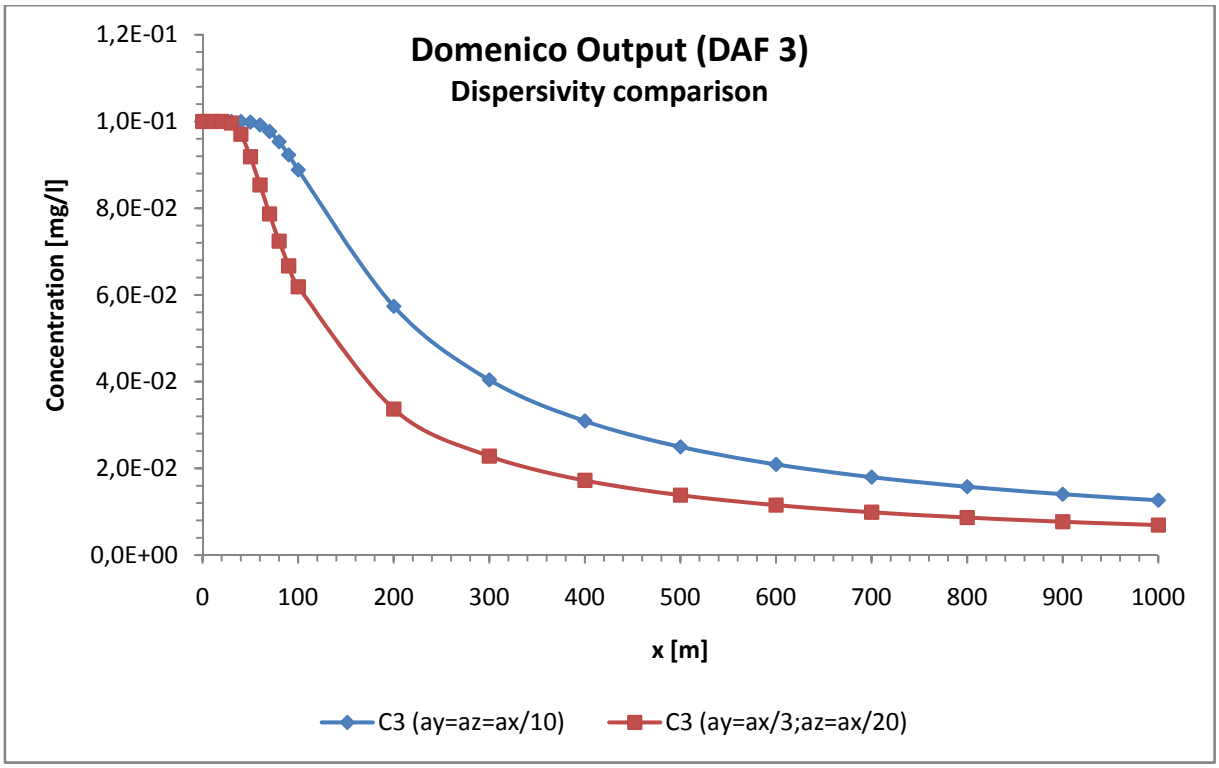

Figure 3.13: Domenico output comparison with different approaches for longitudinal and vertical dispersivity with no vertical dispersion (DAF3)

As it is possible to see from the graphs above, the approach proposed in the APAT document [5] is slightly more conservative for DAF1 and DAF2, whereas it is consistently less conservative for DAF3. Therefore, the assumption made in this work looks reasonable.

3.3.4 Benzene transport in unconfined aquifer

In this section the results of benzene transport in an unconfined aquifer obtained with numerical and analytical models are compared, where the conformity point was set at 100 m downstream the contaminant source.

The analytical model of Domenico simulates the transport of pollutants in the aquifer assuming a continuous release of contaminant. This situation differs from the real case, especially if transport in a span of 25 years shall be analyzed, since transport of the contaminant leads to a predictable run-off of the contaminant source. This effect have been accounted for in the FeFlow simulation. The simulation has been performed assuming the three diffusion scenarios specified above (DAF1, DAF2 and DAF3) and:

- Without biodegradation ($\lambda = 0$)
- With biodegradation ($\lambda = 0{,}00096\ d^{-1}$)

3.3.4.1 Case 1 - Dispersion in all direction (DAF 1)

This chapter shows the output obtained with the analytical and numerical models simulating the transport of benzene in the unconfined aquifer considering contaminant dispersion in all directions.

Domenico analytical model

The result obtained with Eq. 3-39 are:

Without biodegradation:

$$C(x = 100m) = C_0 \cdot \exp\left[\frac{x}{2 \cdot a_x} \cdot \left(1 - \sqrt{1 + \frac{4 \cdot \lambda \cdot R \cdot a_x}{v_e}}\right)\right] \cdot \left[\operatorname{erf}\left(\frac{S_w}{4 \cdot \sqrt{a_y \cdot x}}\right)\right] \cdot \left[\operatorname{erf}\left(\frac{S_d}{4 \cdot \sqrt{a_z \cdot x}}\right)\right] = 0{,}005 \frac{mg}{l}$$

With biodegradation:

$$C(x = 100m) = C_0 \cdot \exp\left[\frac{x}{2 \cdot a_x} \cdot \left(1 - \sqrt{1 + \frac{4 \cdot \lambda \cdot R \cdot a_x}{v_e}}\right)\right] \cdot \left[\operatorname{erf}\left(\frac{S_w}{4 \cdot \sqrt{a_y \cdot x}}\right)\right] \cdot \left[\operatorname{erf}\left(\frac{S_d}{4 \cdot \sqrt{a_z \cdot x}}\right)\right] = 0{,}0026 \frac{mg}{l}$$

These values are obtained by assuming a groundwater velocity equal to 2500 cm/year which is the default value provided by the APAT document [5].

For a more meaningful comparison the actual value that corresponds to Loamy Sand soil was calculated:

$$v_{gw} = K \cdot i = 1277{,}2\, {}^{cm}/_{year}$$

Whit the following resulting effective velocity:

$$v_e = \frac{v_{gw}}{\theta_e} = 3618{,}1\, {}^{cm}/_{year}$$

Using this value, the concentration at the point of exposure, considering the attenuation due to biodegradation, is:

$$C(x = 100m) = C_0 \cdot \exp\left[\frac{x}{2 \cdot a_x} \cdot \left(1 - \sqrt{1 + \frac{4 \cdot \lambda \cdot R \cdot a_x}{v_e}}\right)\right] \cdot \left[\operatorname{erf}\left(\frac{S_w}{4 \cdot \sqrt{a_y \cdot x}}\right)\right] \cdot \left[\operatorname{erf}\left(\frac{S_d}{4 \cdot \sqrt{a_z \cdot x}}\right)\right] = 0{,}0015 \frac{mg}{l}$$

FeFlow Analytical model

For the contaminants transport with dispersion and diffusion in all directions, necessary to the comparison with the Domenico analytical model (DAF1) a 3D scenario has been modeled with the FEFLOW software with the features listed in Table 3-21

Table 3-21: Case 1: FeFlow 3D scenario

Parameter	Unit	Value
Source extension in flow direction	m	45
Source extension orthogonal to flow direction	m	45
Aquifer thickness	m	300
Bottom aquifer deep	m	150 (*)
Top aquifer deep	m	148 (*)
Mixing height	m	2

(*) z-axis origin on water table

Values obtained with Domenico analytical model and FeFlow software are reported in Figure 3.14

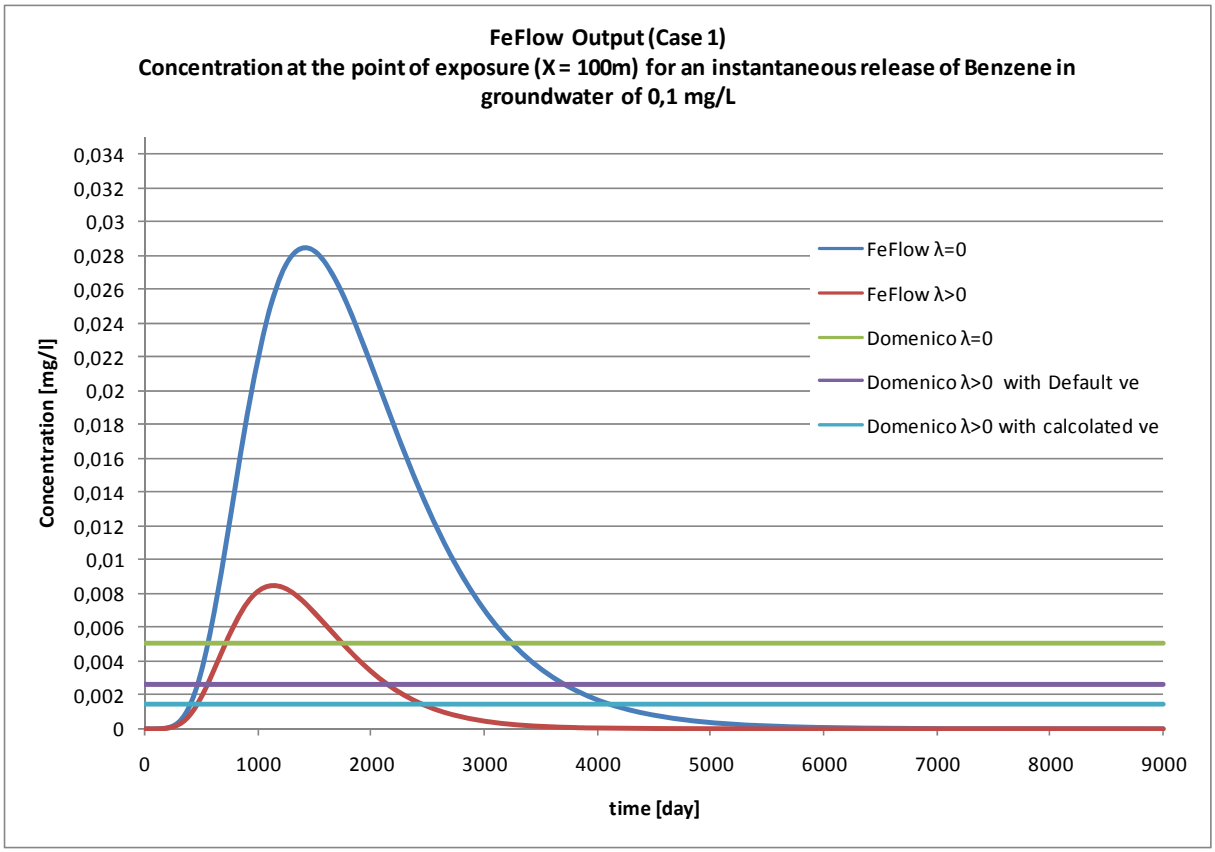

Figure 3.14: Domenico and FeFlow comparison with dispersion in all direction

3.3.4.2 Case 2 - Longitudinal and horizontal dispersion in all directions and vertical dispersion in the direction of positive z (DAF 2)

This section reports the output obtained with the analytical and numerical model simulating the transport of benzene in unconfined aquifer with a longitudinal and horizontal dispersion in all directions and vertical dispersion only in the direction of positive z.

Domenico analytical model

The result obtained with Eq. 3-40 are:

Without biodegradation:

$$C(x = 100m) = C_0 \cdot exp\left[\frac{x}{2 \cdot a_x} \cdot \left(1 - \sqrt{1 + \frac{4 \cdot \lambda \cdot R \cdot a_x}{v_e}}\right)\right] \cdot \left[erf\left(\frac{S_w}{4 \cdot \sqrt{a_y \cdot x}}\right)\right] \cdot \left[erf\left(\frac{S_d}{4 \cdot \sqrt{a_z \cdot x}}\right)\right]$$
$$= 0{,}010 \frac{mg}{l}$$

With biodegradation:

$$C(x = 100m) = C_0 \cdot exp\left[\frac{x}{2 \cdot a_x} \cdot \left(1 - \sqrt{1 + \frac{4 \cdot \lambda \cdot R \cdot a_x}{v_e}}\right)\right] \cdot \left[erf\left(\frac{S_w}{4 \cdot \sqrt{a_y \cdot x}}\right)\right] \cdot \left[erf\left(\frac{S_d}{4 \cdot \sqrt{a_z \cdot x}}\right)\right]$$
$$= 0{,}0052 \frac{mg}{l}$$

These values are obtained by assuming a groundwater velocity equal to 2500 cm/year which is the default value provided in the APAT document [5].

For a more meaningful comparison the actual value that corresponds to Loamy Sand soil was calculated:

$$v_{gw} = K \cdot i = 1277{,}2 \, {}^{cm}/_{year}$$

Whit the following resulting effective velocity:

$$v_e = \frac{v_{gw}}{\theta_e} = 3618{,}1 \, {}^{cm}/_{year}$$

Using this value, the concentration at the point of exposure, considering the attenuation due to biodegradation, is:

$$C(x = 100m) = C_0 \cdot exp\left[\frac{x}{2 \cdot a_x} \cdot \left(1 - \sqrt{1 + \frac{4 \cdot \lambda \cdot R \cdot a_x}{v_e}}\right)\right] \cdot \left[erf\left(\frac{S_w}{4 \cdot \sqrt{a_y \cdot x}}\right)\right] \cdot \left[erf\left(\frac{S_d}{4 \cdot \sqrt{a_z \cdot x}}\right)\right]$$
$$= 0{,}0029 \frac{mg}{l}$$

FeFlow Analytical model

For the contaminants transport with longitudinal and horizontal dispersion in all directions and vertical dispersion in the direction of positive z, necessary to the comparison with the Domenico analytical model (DAF2) a 3D scenario has been modeled with FEFLOW software with the features listed in Table 3-22.

Table 3-22: Case 2: FeFlow 3D scenario

Parameter	Unit	Value
Source extension in flow direction	m	45
Source extension orthogonal to flow direction	m	45
Aquifer thickness	m	300
Bottom aquifer deep	m	0 (*)
Top aquifer deep	m	2 (*)
Mixing height	m	2

(*) z-axis origin on water table

Values obtained with Domenico analytical model and FeFlow software are reported in Figure 3.15.

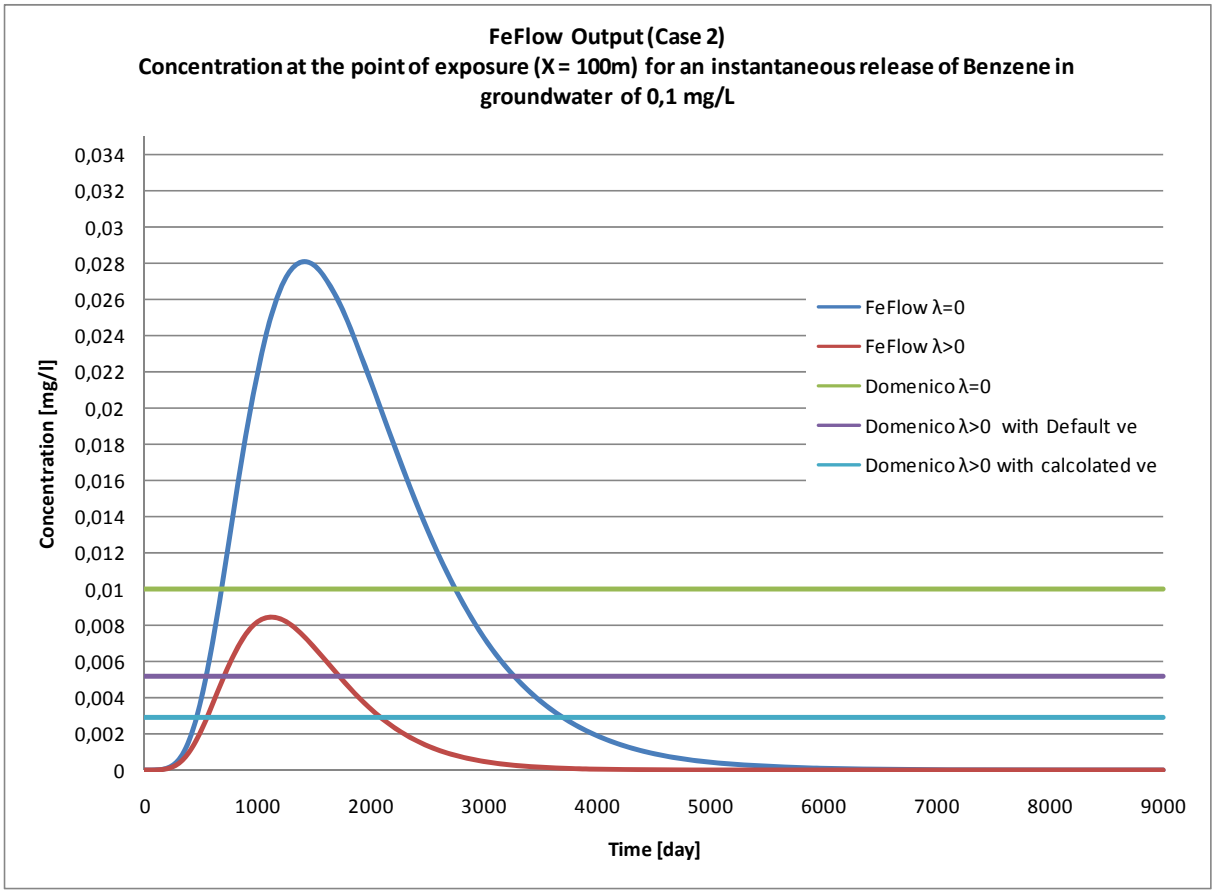

Figure 3.15: Domenico and FeFlow comparison with longitudinal and horizontal dispersion in all directions and vertical dispersion in the direction of positive z

3.3.4.3 Case 3 - Longitudinal and horizontal dispersion (DAF 3)

This section reports the output obtained with the analytical and numerical model simulating the transport of benzene in unconfined aquifer with a longitudinal and horizontal dispersion.

Domenico analytical model

The result obtained with Eq. 3-41 are:

Without biodegradation:

$$C(x = 100m) = C_0 \cdot exp\left[\frac{x}{2 \cdot a_x} \cdot \left(1 - \sqrt{1 + \frac{4 \cdot \lambda \cdot R \cdot a_x}{v_e}}\right)\right] \cdot \left[erf\left(\frac{S_w}{4 \cdot \sqrt{a_y \cdot x}}\right)\right] \cdot \left[erf\left(\frac{S_d}{4 \cdot \sqrt{a_z \cdot x}}\right)\right]$$

$$= 0{,}0888 \frac{mg}{l}$$

With biodegradation:

$$C(x = 100m) = C_0 \cdot exp\left[\frac{x}{2 \cdot a_x} \cdot \left(1 - \sqrt{1 + \frac{4 \cdot \lambda \cdot R \cdot a_x}{v_e}}\right)\right] \cdot \left[erf\left(\frac{S_w}{4 \cdot \sqrt{a_y \cdot x}}\right)\right] \cdot \left[erf\left(\frac{S_d}{4 \cdot \sqrt{a_z \cdot x}}\right)\right]$$

$$= 0{,}046 \frac{mg}{l}$$

These value are obtained by assuming a groundwater speed equal to 2500 cm/year which is the default value provided in the APAT document [5].

For a more meaningful comparison the actual value that corresponds to Loamy Sand soil has been calculated:

$$v_{gw} = K \cdot i = 1277{,}2\,{}^{cm}/_{year}$$

Whit the following resulting effective velocity:

$$v_e = \frac{v_{gw}}{\theta_e} = 3618{,}1\,{}^{cm}/_{year}$$

Using this value, the concentration at the point of exposure, considering the attenuation due to biodegradation, is:

$$C(x = 100m) = C_0 \cdot exp\left[\frac{x}{2 \cdot a_x} \cdot \left(1 - \sqrt{1 + \frac{4 \cdot \lambda \cdot R \cdot a_x}{v_e}}\right)\right] \cdot \left[erf\left(\frac{S_w}{4 \cdot \sqrt{a_y \cdot x}}\right)\right] \cdot \left[erf\left(\frac{S_d}{4 \cdot \sqrt{a_z \cdot x}}\right)\right]$$

$$= 0{,}0261\,\frac{mg}{l}$$

FeFlow Analytical model

For the contaminants transport with longitudinal and horizontal, necessary to the comparison with the Domenico analytical model (DAF3) a 3D scenario has been modeled by FEFLOW software with features listed in Table 3-23.

Table 3-23: Case 2: FeFlow 3D scenario

Parameter	Unit	Value
Source extension in flow direction	m	45
Source extension orthogonal to flow direction	m	45
Aquifer thickness	m	2
Bottom aquifer deep	m	0 (*)
Top aquifer deep	m	2 (*)
Mixing height	m	2

(*) z-axis origin on water table

Values obtained with Domenico analytical model and FeFlow software are reported in Figure 3.16.

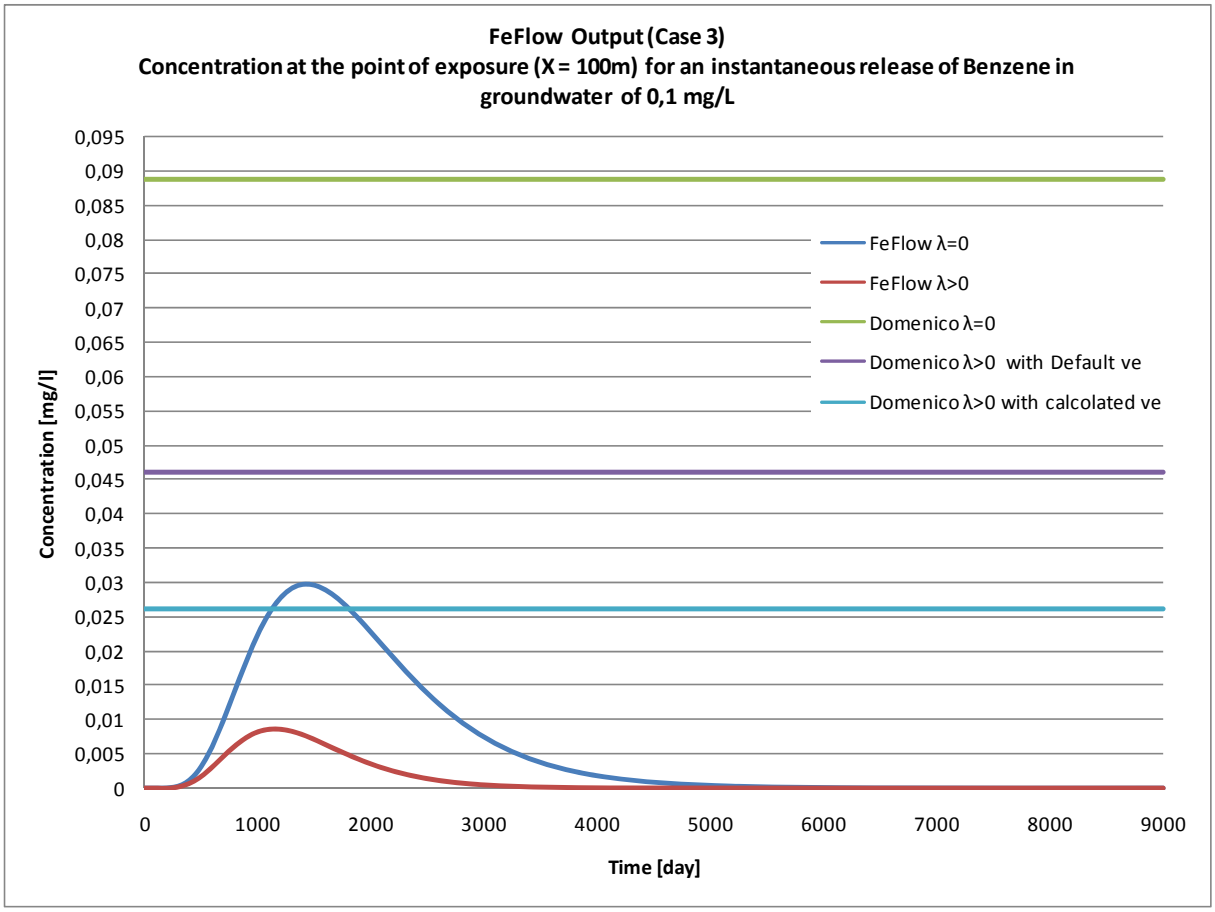

Figure 3.16: Domenico and FeFlow comparison with longitudinal and horizontal dispersion in all directions and vertical dispersion in the direction of positive z

3.3.5 Risk evaluation for transport in the unsaturated zone

In this section the risk analysis results obtained for water ingestion for a site contaminated by benzene and applying analytical and numerical model, are presented and discussed.

3.3.5.1 Equation analysis

The basic equation for the risk analysis has been provided in chapter 1.

3.3.5.2 Input parameters

In this section the parameter values used in the risk analysis for water ingestion, are reported.

Table 3-24 reports the saturated soil characteristic

Table 3-24: saturated zone physical parameters

Symbol	Value	Unit
W	4500	Cm
v_{gw}	2500	cm/year
δ_{gw}	200	cm

Table 3-25 reports the parameters used to estimate the exposure rate.

Table 3-25: default value for exposure parameters

Symbol	Value	Unit
IR_w	1	l/day
EF	250	day/year
ED	25	year
BW	70	Kg
AT	70	year

Table 3-26 reports the parameters required for risk evaluation.

Table 3-26: parameter for risk evaluation

Symbol	Value	Unit
SF	5,50E-02	$(mg/Kg\ day)^{-1}$
EM	3,50E-03	l/ Kg day

3.3.5.3 Analytical model

For the risk calculation, using the analytical model, the following cases were considered:

- Risk of ingestion of water at the point of compliance (x = 100m) after a transport in groundwater with dispersion in all directions (DAF1).
- Risk of ingestion of water at the point of compliance (x = 100m) after a transport in groundwater with longitudinal and horizontal dispersion in all directions and vertical dispersion in the direction of positive z (DAF2).
- Risk of ingestion of water at the point of compliance (x = 100m) after a transport in groundwater only with horizontal and longitudinal dispersion (DAF3).

The above three cases were analyzed:

- Without biodegradation ($\lambda = 0$)
- With biodegradation ($\lambda = 0{,}00096\ d^{-1}$)

Table 3-27, and Figure 3.17 report the risk for ingestion of water calculated for the cases described above:

Table 3-27: Risk of ingestion of water at the point of compliance (x = 100m) with Domenico analytical model with an exposure duration of 25 years

Case	Risk (λ=0)	Risk (λ>0)
Risk (DAF1)	9,76E-07	2,88E-07
Risk (DAF2)	1,92E-06	5,57E-07
Risk (DAF3)	1,71E-05	5,02E-06

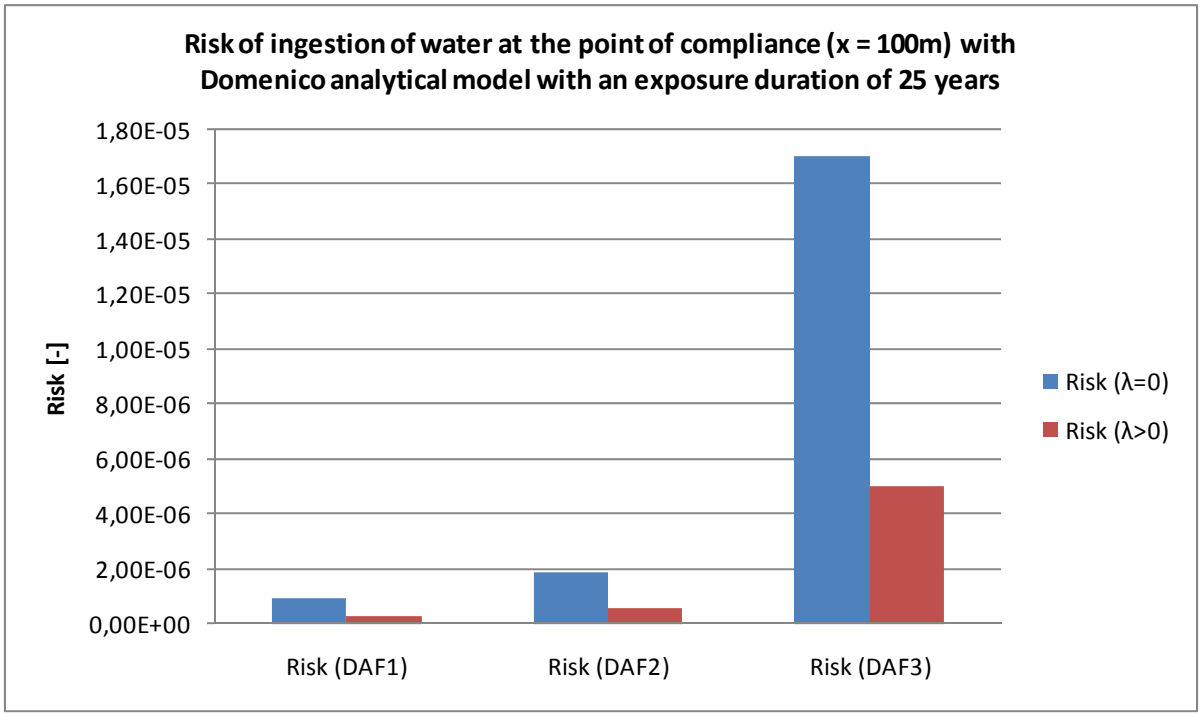

Figure 3.17: Risk of ingestion of water at the point of compliance (x = 100m) with Domenico analytical model with an exposure duration of 25 years

Comparison of the obtained results shows that:

- The risk evaluated with the analytical model considering attenuation due to biodegradation (λ> 0) leads to less conservative results. Actually, the health risk obtained is an order of magnitude below the one obtained without biodegradation.
- The risk evaluated considering benzene transport only with horizontal and longitudinal dispersion (DAF3) is extremely conservative. The risk obtained is an order of magnitude greater than the other two cases.
- The risk evaluated considering benzene transport with dispersion in all direction (DAF1) leads to less conservative results

3.3.5.4 Numerical Models

Applying the same procedure described in section 3.1.4.4, it is possible to obtain the risk for water ingestion from concentration vs. time data calculated through the numerical model. Results are shown in Table 3-28, and in Figure 3.18.

Table 3-28: Risk of ingestion of water at the point of compliance (x = 100m) with numerical model with an exposure duration of 25 years

Case	Risk (λ=0)	Risk (λ>0)
Risk (DAF1)	1,08E-06	2,28E-07
Risk (DAF2)	1,09E-06	2,31E-07
Risk (DAF3)	1,12E-06	2,33E-07

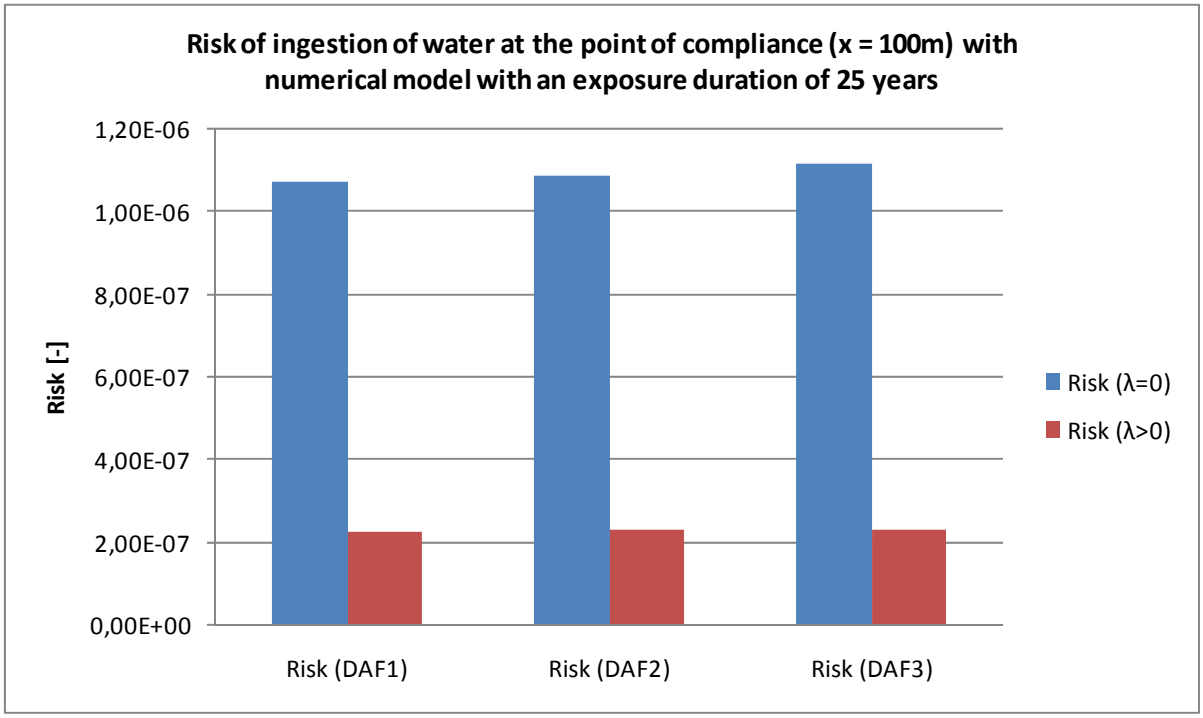

Figure 3.18: Risk of ingestion of water at the point of compliance (x = 100m) with numerical model with an exposure duration of 25 years

Comparison of the obtained results shows that:

- The risk evaluated with the numerical model considering attenuation due to biodegradation (λ> 0) leads to less conservative results. Actually the health risk obtained is an order of magnitude below the one obtained without biodegradation.
- Unlike analytical models, the risk calculated with the numerical one considering benzene transport with different types of dispersion (DAF1, DAF2 and DAF3) leads to almost identical results. This can be attributed to a modest range of dispersivity values, particularly for the transverse dispersion (horizontal and vertical) which was assumed to be 1m, resulting in a very small attenuation due to this phenomenon. This parameter should be estimated in the field for a more accurate phenomenon description.

3.3.6 Comparison between analytical and numerical models

In this section the results obtained in terms of health risk for water ingestion applying the analytical and numerical models are compared.

The main difference between the analytical and the numerical models is that the first one provides a constant chemical concentration for all the exposure time, while the second one provides a transient solution, with a concentration front moving to and travelling through the point of compliance, until complete run-off. Risk has been calculated considering an exposure duration of 25 years; when the analytical model is used, the receptor is exposed to a constant concentration for all the period, while using the numerical one the receptor is exposed to a contaminant concentration, although higher than the ones provided by the analytical model, for a shorter time.

The result provided by the analytical and numerical model have been compared for two conditions:

1. Exposure duration of 25 years without biodegradation;
2. Exposure duration of 25 years with biodegradation

The corresponding results are reported below.

1. **Exposure duration of 25 years without biodegradation;**

Table 3-29, and Figure 3.19 report the comparison between analytical and numerical models in terms of risk for water ingestion

Table 3-29: Risk for water Ingestion at the point of compliance (X = 100m) obtained by applying the numerical model (FEFLOW) and the analytical model (Domenico) for an exposure period of 25 years with λ = 0

Case λ=0 ED = 25 years	DOMENICO	FEFLOW
Risk (DAF 1)	9,76E-07	1,08E-06
Risk (DAF 2)	1,92E-06	1,09E-06
Risk (DAF 3)	1,71E-05	1,12E-06

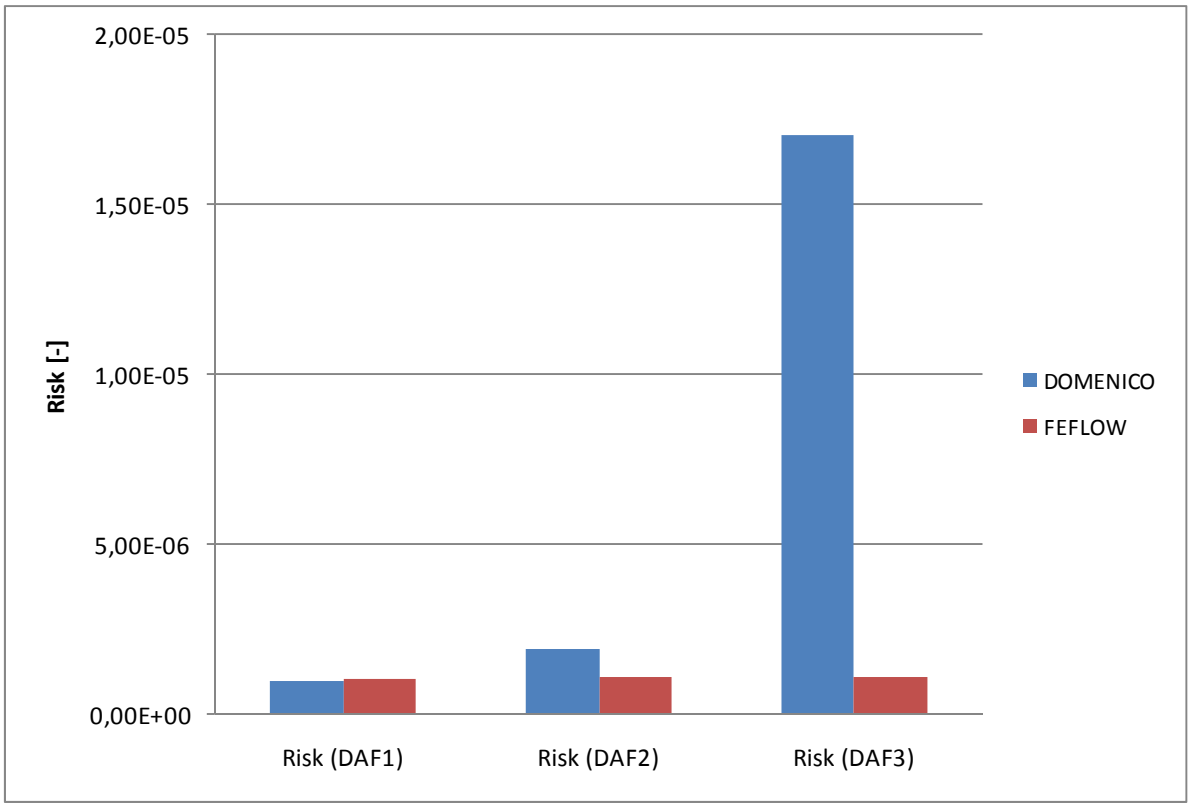

Figure 3.19: Risk for water Ingestion at the point of compliance (X = 100m) obtained by applying the numerical model (FEFLOW) and the analytical model (Domenico) for an exposure period of 25 years with λ = 0

2. Exposure duration of 25 years with biodegradation

Table 3-30 and Figure 3.20 report the comparison between analytical and numerical models in terms of risk for water ingestion

Table 3-30: Risk for water Ingestion at the point of compliance (X = 100m) obtained by applying the numerical model (FEFLOW) and the analytical model (Domenico) for an exposure period of 25 years with λ > 0

Case λ>0 ED = 25 years	DOMENICO	FEFLOW
Risk (DAF 1)	2,88E-07	2,35E-07
Risk (DAF 2)	5,57E-07	2,39E-07
Risk (DAF 3)	5,02E-06	2,41E-07

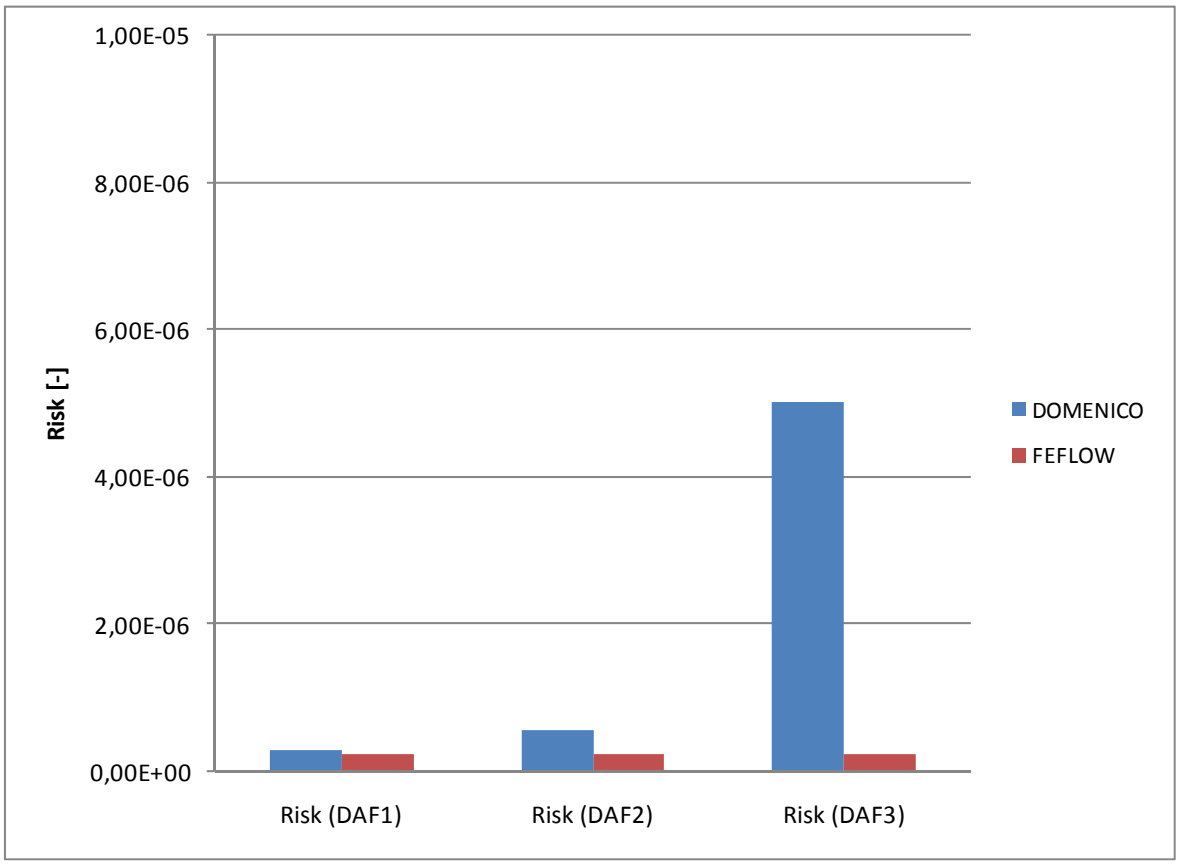

Figure 3.20: Risk for water Ingestion at the point of compliance (X = 100m) obtained by applying the numerical model (FEFLOW) and the analytical model (Domenico) for an exposure period of 25 years with λ > 0

An analysis of these two case compared shows that:

- Risk evaluated with the Domenico analytical model considering the attenuation due the dispersion in all directions (Case 1) gives results close to the numerical model in the presence of biodegradation, while in the absence of biodegradation little underestimates risk.

- Risk evaluated considering longitudinal and horizontal dispersion in all directions and vertical dispersion in the direction of positive z (DAF2), appears to be more conservative with the application of analytical model compared to that numerical one.
- Risk evaluated considering longitudinal and horizontal dispersion in all directions (DAF3), appears to be extremely conservative with the application of analytical model compared to that numerical one.
- The risk evaluated considering the attenuation due to biodegradation ($\lambda > 0$) leads to less conservative results. In fact the health risk obtained is an order of magnitude below the one obtained without biodegradation.

Considering the results shown above the proposal of APAT document [5] to use the analytical model for dispersion of pollutants in the aquifer DAF2, is better supported. Indeed, this equation leads to the slightly more conservative results compared to the numerical model, but not overestimated as in the case of horizontal and longitudinal dispersion (DAF3).

It was considered appropriate to analyze and compare the risk obtained from the analytical and numerical model whereas periods longer exposures. In particular:

3. Exposure duration of 30 years without biodegradation
4. Exposure duration of 30 years with biodegradation
5. Exposure duration of 35 years without biodegradation
6. Exposure duration of 35 years with biodegradation
7. Exposure duration of 25 years without biodegradation for two soil type

3) Exposure duration of 30 years without biodegradation

Table 3-31 and Figure 3.21 report the comparison between analytical and numerical models in terms of risk for water ingestion.

Table 3-31: Risk for water Ingestion at the point of compliance (X = 100m) obtained by applying the numerical model (FEFLOW) and the analytical model (Domenico) for an exposure period of 30 years with λ = 0

Case λ=0 ED = 30 years	DOMENICO	FEFLOW
Risk (DAF 1)	1,17E-06	1,08E-06
Risk (DAF 2)	2,31E-06	1,09E-06
Risk (DAF 3)	2,05E-05	1,12E-06

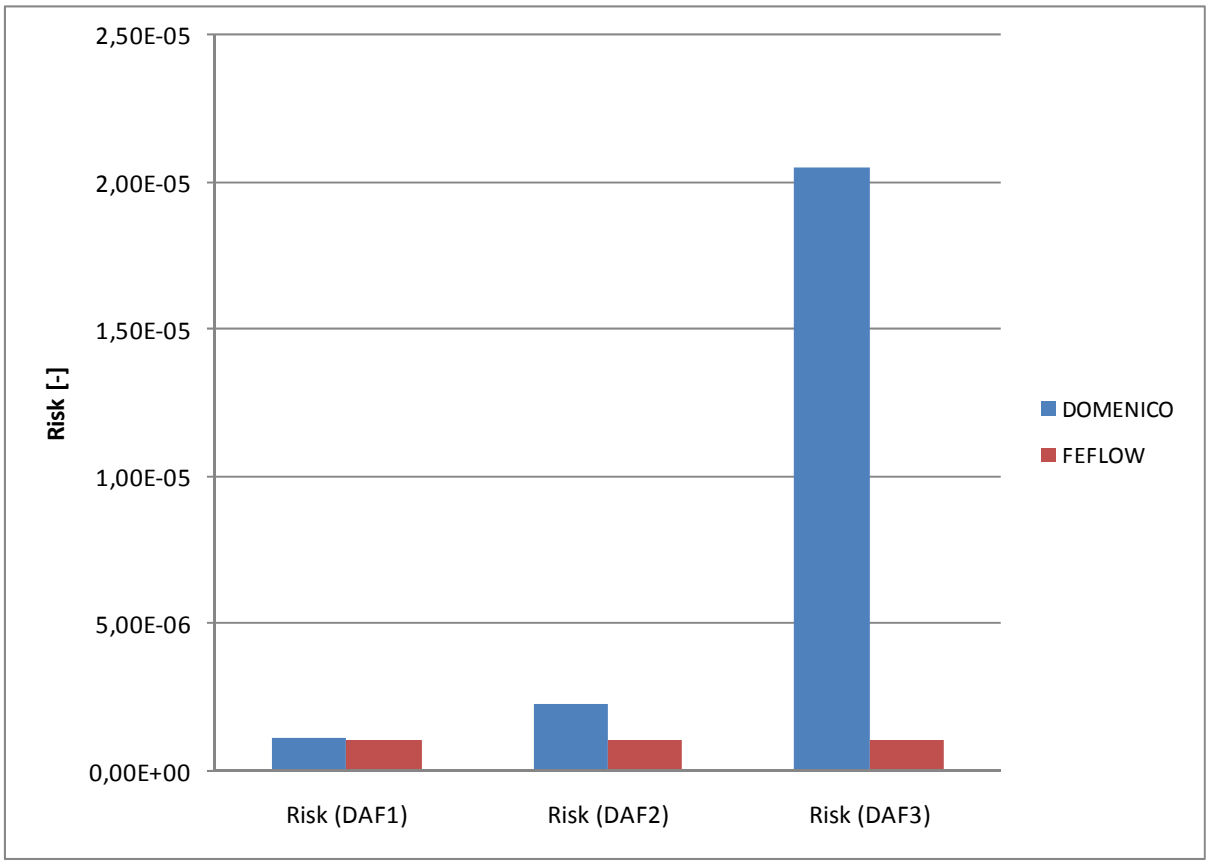

Figure 3.21: Risk for water Ingestion at the point of compliance (X = 100m) obtained by applying the numerical model (FEFLOW) and the analytical model (Domenico) for an exposure period of 30 years with λ = 0

4) Exposure duration of 30 years with biodegradation

Table 3-32 and Figure 3.22 report the comparison between analytical and numerical models in terms of risk for water ingestion

Table 3-32: Risk for water Ingestion at the point of compliance (X = 100m) obtained by applying the numerical model (FEFLOW) and the analytical model (Domenico) for an exposure period of 30 years with λ > 0

Case λ>0 ED = 30 years	DOMENICO	FEFLOW
Risk (DAF 1)	3,46E-07	2,35E-07
RisK (DAF 2)	6,69E-07	2,39E-07
Risk (DAF 3)	6,02E-06	2,41E-07

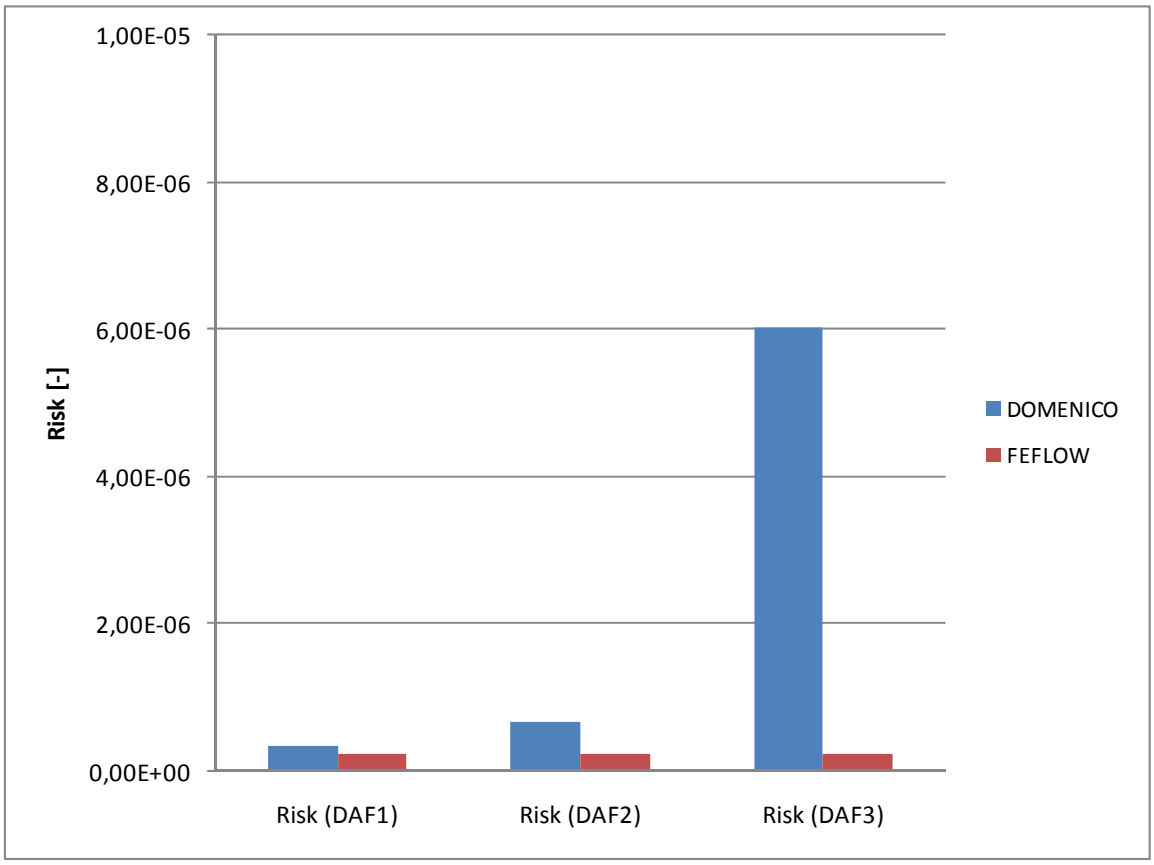

Figure 3.22: Risk for water Ingestion at the point of compliance (X = 100m) obtained by applying the numerical model (FEFLOW) and the analytical model (Domenico) for an exposure period of 30 years with λ > 0

5) Exposure duration of 35 years without biodegradation

Table 3-32 and Figure 3.23 report the comparison between analytical and numerical models in terms of risk for water ingestion

Table 3-33: Risk for water Ingestion at the point of compliance (X = 100m) obtained by applying the numerical model (FEFLOW) and the analytical model (Domenico) for an exposure period of 35 years with λ = 0

Case λ=0 ED = 35 years	DOMENICO	FEFLOW
Risk (DAF 1)	1,37E-06	1,08E-06
Risk (DAF 2)	2,69E-06	1,09E-06
Risk (DAF 3)	2,39E-05	1,12E-06

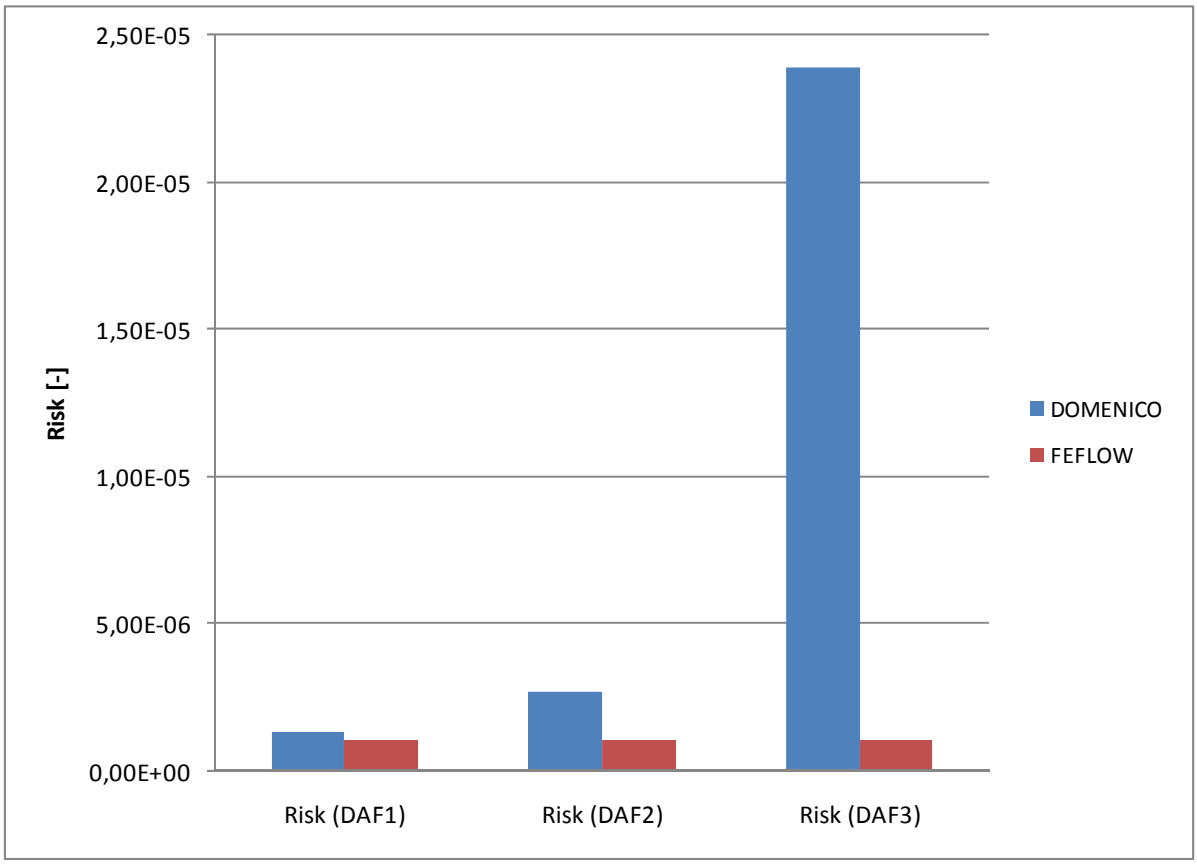

Figure 3.23: Risk for water Ingestion at the point of compliance (X = 100m) obtained by applying the numerical model (FEFLOW) and the analytical model (Domenico) for an exposure period of 35 years with λ = 0

6) Exposure duration of 35 years with biodegradation

Table 3-32 and Figure 3.24 report the comparison between analytical and numerical models in terms of risk for water ingestion

Table 3-34: Risk for water Ingestion at the point of compliance (X = 100m) obtained by applying the numerical model (FEFLOW) and the analytical model (Domenico) for an exposure period of 35 years with λ > 0

Case λ>0 ED = 35 years	DOMENICO	FEFLOW
Risk (DAF 1)	4,04E-07	2,35E-07
Risk (DAF 2)	7,80E-07	2,39E-07
Risk (DAF 3)	7,02E-06	2,41E-07

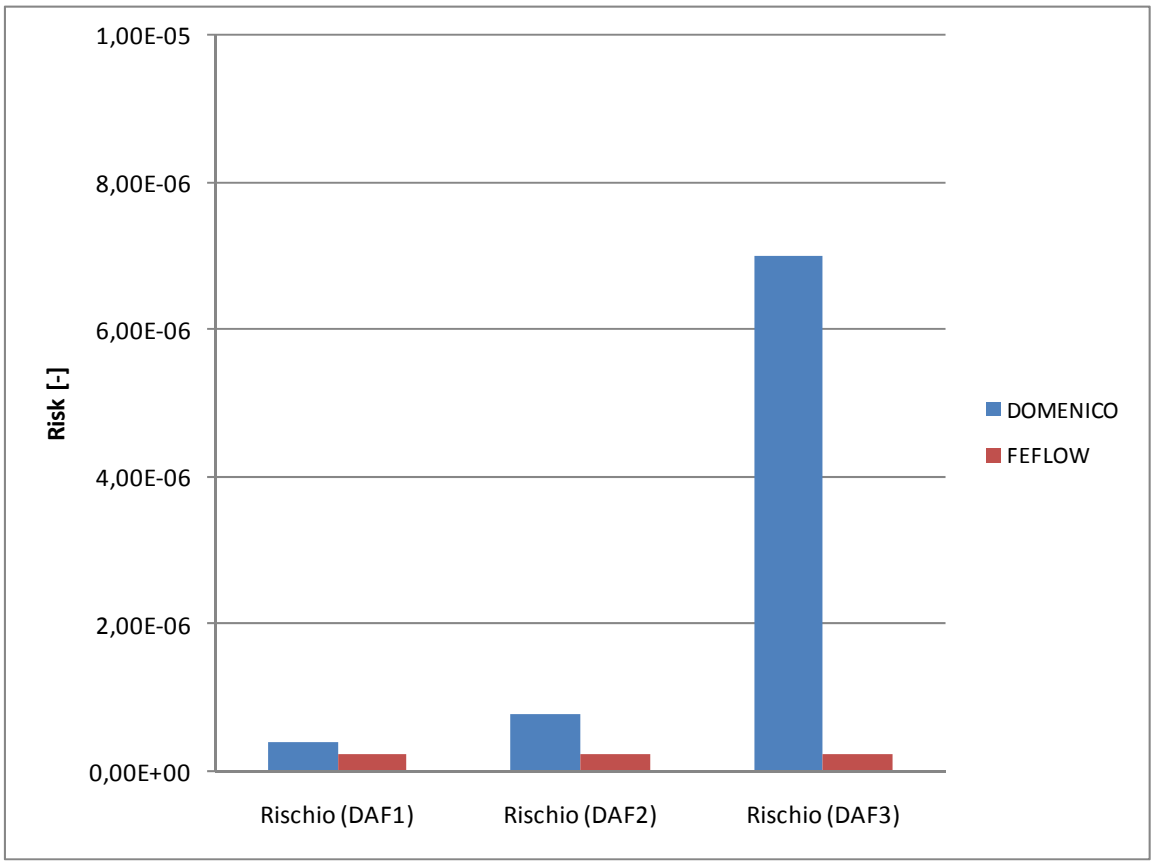

Figure 3.24: Risk for water Ingestion at the point of compliance (X = 100m) obtained by applying the numerical model (FEFLOW) and the analytical model (Domenico) for an exposure period of 35 years with λ > 0

7) Exposure duration of 25 years without biodegradation for two soil type

Not consider the biodegradation phenomenon involves some limitations to the Domenico model. Indeed assume the biodegradation constant equal to zero, means cancels the first term in Eq. 3-38 that takes into account, in addition to degradation processes, the nature of the contaminant (retardation factor R) and the soil type (effective velocity, longitudinal dispersivity).

Considering the biodegradation factor equal to zero the equation for dispersion in all direction (DAF1) become:

$$C(x) = C_0 \cdot \left[erf\left(\frac{S_w}{4 \cdot \sqrt{a_y \cdot x}}\right)\right] \cdot \left[erf\left(\frac{S_d}{4 \cdot \sqrt{a_z \cdot x}}\right)\right]$$

Eq. 3-42

In order to evaluate this approximation a comparison, in term of health risk for water ingestion, has been performed between Domenico analytical model DAF 1 and FeFlow for two soil type:

- Loamy Sand
- Loam

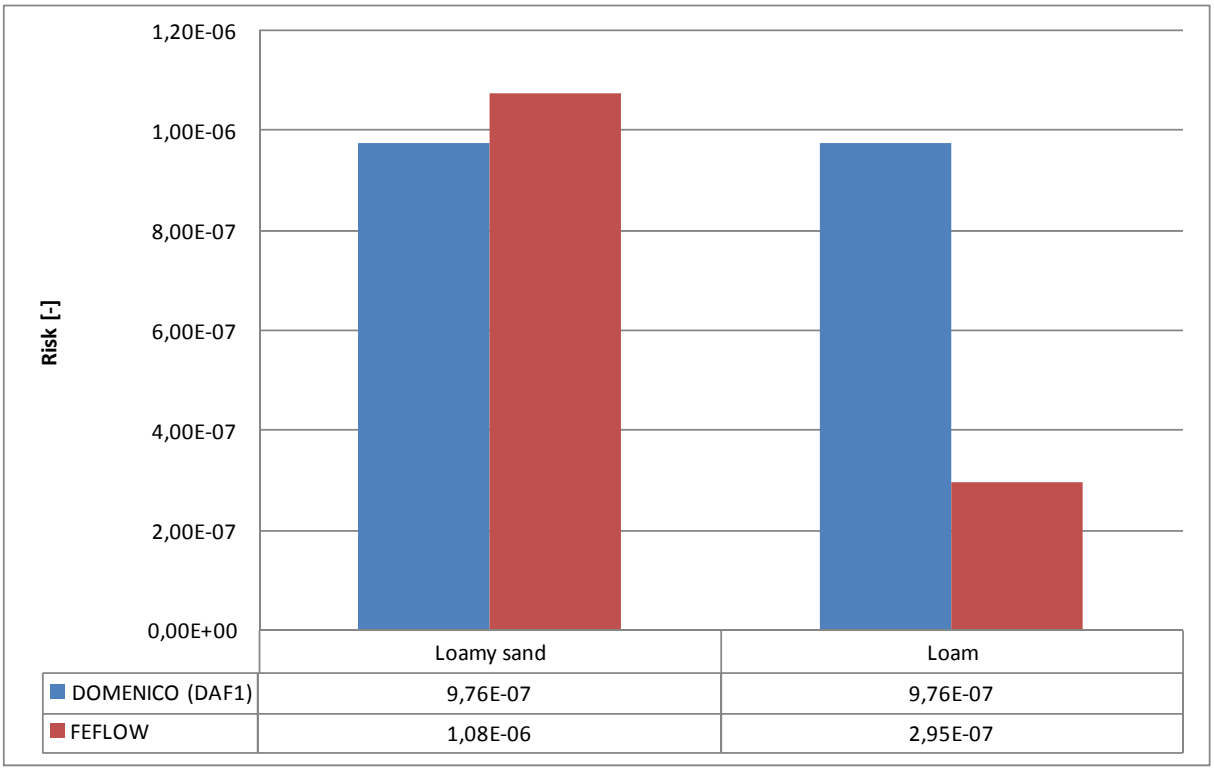

Figure 3.25: Comparing Risk for water Ingestion at the point of compliance (X = 100m) obtained by applying the numerical model and the analytical model for two kind of soil textures years with λ > 0

An analysis of the comparison shows that:

- Using the DAF1 analytical model with a Loamy Sand soil in the absence of biodegradation implies a risk slightly less conservative than the one obtained with the numerical model.
- Using the DAF1 analytical model with a Loam soil in the absence of biodegradation implies a risk more conservative than the one obtained with the numerical model.

- The same results are obtained with the application of DAF2 and DAF3 analytical models. These results justify the results previously obtained by comparison with the numerical model, which in the absence of biodegradation. The DAF1 analytical model is slightly less conservative than the numerical model.
- Risk for sandy soil type, estimated by the analytical models in the absence of biodegradation, it may be slightly underestimated compared to the one obtained with the numerical one whereas for clayey soils the risk is too conservative

After the comparison performed between the analytical and numerical models any results could be summarized:

- The analytical risk is highly dependent on the dispersion assumptions, while it does not happen in the case of numerical models.
- The DAF1 analytical model provides results close to the numerical model in the presence of biodegradation, while in the absence of biodegradation slightly underestimates the risk.
- The DAF2 analytical model provides results more conservative than the one furnished by the numerical model.
- The DAF3 analytical model overestimate risk of about an order of magnitude compared to the numerical model.
- When the exposure time increase (30 and 35 years) the analytical models seem to be more conservative than the numerical model indeed the first one assumed a constant concentration for the exposure duration.
- Put equal to zero the biodegradation constant, implies restrictions on the Domenico model. Indeed don not consider the biodegradation constant, means cancels the first term in Eq. 3-38 that takes into account, in addition to degradation processes, the nature of the contaminant (retardation factor R) and the soil type (effective velocity, longitudinal dispersivity). So for sandy soils, risk may be slightly underestimated compared to the numerical model and for clayey soils the risk is too conservative.

In view of these results for Tier 2 risk analysis is considered appropriate to use a dispersion model of type 2 (DAF2), because this condition leads to the slightly more conservative results of the numerical model, but not overestimated as in the case of horizontal and longitudinal dispersion (DAF3). It is noted that this choice coincides with that suggested by the APAT document [5].

4 INDOOR VAPOR INTRUSION AND VADOSE ZONE BIODEGRADATION

4.1 INTRODUCTION

When soils are impacted by leaks or spills, or wastes are placed in impoundments, there is the potential for contaminant vapor migration to enclosed spaces (buildings, conduits, etc.) and leachate migration to groundwater. Historically, leachates from contaminated soil and wastes have been considered the main pathway of contamination; however, the issue of vapor migration has recently begun to be formally and quantitatively studied.

This has been brought about in large part by the move toward more structured risk-based corrective action (RBCA) approaches (e.g., ASTM 1995) and an increased awareness of this pathway.

The significance of the vapor intrusion pathway and natural attenuation of vapors in the vadose zone are currently the subject of intense debate. When common screening-level algorithms (e.g., Johnson and Ettinger, 1991) are combined with conservative soil properties, geometries, and exposure assumptions, then the resulting target risk-based screening levels (RBSLs) are very low. In fact, they are often one to three orders-of-magnitude lower than existing cleanup guidelines in many states.

Many people intuitively feel that the current generation of screening-level predictive models are too conservative and lead to unnecessarily low cleanup targets. Some point to the fact that the algorithms generally do not account for biodegradation and other possible vadose zone attenuation mechanisms. Based on the biodegradation literature, it is reasonable to expect that some chemicals of interest degrade as they migrate.

4.2 VADOSE ZONE

The part of the subsurface which lays above the groundwater table is called unsaturated zone or vadose zone. The term unsaturated indicates that pore spaces in soil (void) are not entirely filled with water, but also contain a certain amount of air. A common way to quantify the degree of saturation is the moisture content, which is defined as the volume of water divided by the total volume. In addition to the soil and water phase which are present in the saturated zone, air is present as a third phase in the unsaturated zone. This additional phase strongly influences the partitioning, transport and biodegradation of contaminants.

The unsaturated zone has three major subdivisions:

- Soil zone. This zone lies between the ground surface and the maximum depth to which roots penetrate. It is characterized by large fluctuations in the quantity and quality of moisture in response to transpiration and evaporation.

- Intermediate (vadose) zone. This zone consists of parent material which is not affected by soil-forming factors.
- Capillary fringe. This zone marks the final transition between the unsaturated zone and the saturated zone and is characterized by large capillarity.

4.3 INDOOR VAPOR INTRUSION WITHOUT BIODEGRADATION

The Johnson and Ettinger model is commonly used to predict vapor intrusion rates in case without biodegradation. This model is a steady-state, one-dimensional analytical model that describes the chemical transport of volatile compounds from soil, or groundwater, to enclosed space (e.g. houses). Figure 4.1 presents a simplified sketch of the problem under consideration, in which a contaminant vapor source of concentration C_{source} is located some distance L_T below the floor of a basement or building slab. In order to predict the intrusion rate of vapours into the building, the following assumptions are made:

(i) Contaminant vapors penetrate structures primarily through cracks and openings in the walls and foundation (electrical outlets, wall-floor seams, sump drains, etc.).

(ii) Convective transport is likely to be most significant in the region very close to a basement, or foundation, and vapor velocities decrease rapidly with increasing distance from a structure.

(iii) Vapor-phase diffusion is the dominant mechanism for the transport of contaminant vapors from contaminant sources (located away from the foundation) to the soil region near the foundation.

(iv) All contaminant vapors originating from directly below the basement will penetrate it, unless the floor and walls are perfect vapor barriers.

This model is based on experiment on Radon transport. By Radon indoor concentration data, Johnson observed that there is a gap between indoor and outdoor pressures due to the wind action and temperature difference.

This contribution could be calculated by:

- Wind action (Bernoulli Equation): $$\Delta P_w = \frac{1}{2}\rho v^2$$ Eq. 4-1

- Temperature difference: $$\Delta P_w = \alpha(z - z_0)\Delta T$$ Eq. 4-2

Following the Nazarof experiment he also found that:

- When the building is depressurized compared to external air then there is a pressure difference between soil air and indoor air too;

- Pressure field influences air soil movement near the basement;
- Far from the basement the diffusion phenomena is prevalent compared to convection whereas near the basement both phenomena are important

Figure 4.1 summarizes these conditions.

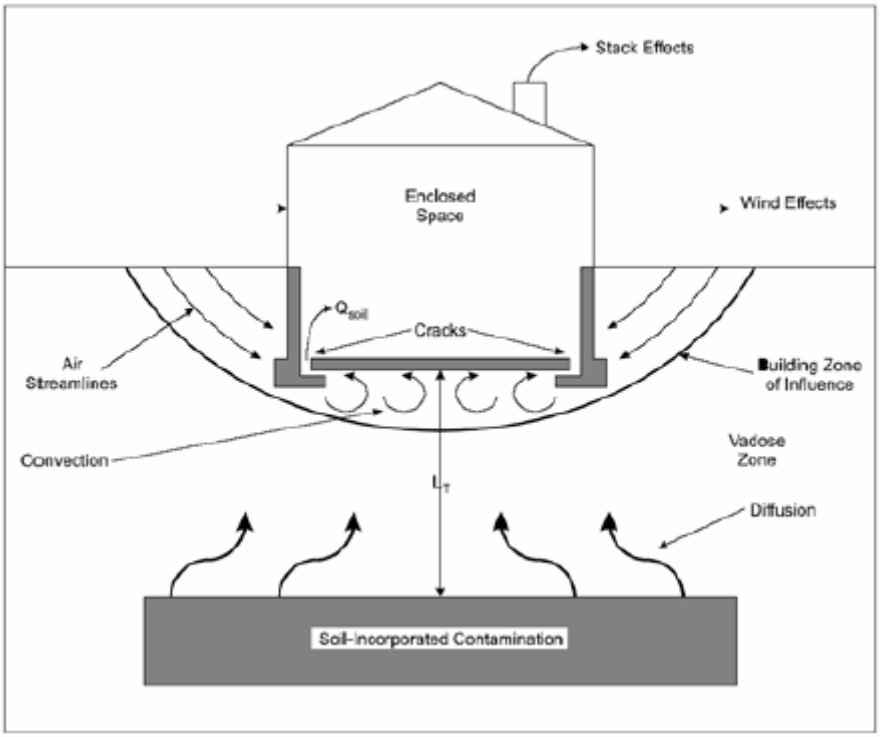

Figure 4.1 - Chemicals migration pathways

The resulting algorithms then depend on parameters related to soil, chemical, and building characteristics, so the "attenuation coefficient" $\alpha_{J\&E}$ is:

$$\alpha_{J\&E} = \frac{C_{indoor}}{C_{source}} = \frac{\left[\frac{D_T^{eff} A_B}{Q_B L_T}\right] exp\left(\frac{Q_{soil} L_{crack}}{D_{crack}^{eff} \eta A_B}\right)}{exp\left(\frac{Q_{soil} L_{crack}}{D_{crack}^{eff} \eta A_B}\right) + \left[\frac{D_T^{eff} A_B}{Q_B L_T}\right] + \left[\frac{D_T^{eff} A_B}{Q_{soil} L_T}\right]\left[exp\left(\frac{Q_{soil} L_{crack}}{D_{crack}^{eff} \eta A_B}\right) - 1\right]}$$

Eq. 4-3

Where

A_B = surface area of enclosed space in contact with soil [m^2];

D_{crack}^{eff} = effective overall vapor-phase diffusion coefficient through the walls and foundation cracks [m^2/d];

D_T^{eff} = effective overall vapor-phase diffusion coefficient between the source and foundation [m^2/d];

L_{crack} = thickness of enclosed space walls and foundation [m];

L_T = source-foundation separation [m];

Q_B = enclosed space air exchange rate [m^3/d];

Q_{soil} = soil gas flow rate into enclosed space due to underpressurization [m^3/d];

η = fraction of enclosed space surface area open for vapor intrusion [m^2/m^2].

The effective porous media overall vapor-phase diffusion coefficients are generally determined from the Millington-Quirk formulation (Millington, 1959; Millington and Quirk, 1961; Millington and Shearer, 1971):

$$D^{eff} = D_a \frac{\theta_a^{3.33}}{\theta_T^2} + \left(\frac{D_w}{H_i}\right)\frac{\theta_w^{3.33}}{\theta_T^2}$$

Eq. 4-4

where:

H_i = Henry's Law constant [(mg/m^3-vapor)/(mg/m^3-H_20)];

θ_w= volumetric moisture content [m^3-H_20/m^3-soil];

θ_T = total porosity [m^3-voids/m^3-soil];

θ_a = volumetric vapor content [m^3-vapor/m^3-soil];

D_a = molecular diffusion coefficient in air [m^2/d];

D_w = molecular diffusion coefficient in water [m^2/d].

In typical RBSL calculations, the source zone vapor concentration C_{source} [mg/m^3] is often assumed to be related to the source zone total soil concentration C_T [mg/ kg-soil], assuming a single-component, linear-partitioning relationships, and three-phase equilibrium (vapor, sorbed, dissolved phases):

$$C_T = C_{source}\theta_v = \frac{\left[1 + \frac{\theta_m}{\theta_v H_i} + \frac{\rho_s K_s}{\theta_v H_i}\right]}{\rho_s} = C_{source}\theta_v \frac{R_v}{\rho_s}$$

Eq. 4-5

where:

K_s = soil sorption coefficient [(mg/kg-soil)/(mg/m^3-H_20)];

R_v = soil vapor retardation factor [unitless];

ρ_s = soil bulk density [kg-soil/m^3-soil].

The time required for vapors to reach near-steady concentrations at any point increases with the square of the distance from the source and is also affected by the chemical properties of the compound of interest. An estimate of the time τ_{ss} [d] required to reach near-steady vapor concentrations and fluxes at any distance L [m] from a source is:

$$\tau_{ss} \approx > \frac{R_v \theta_v L^2}{D_v^{eff}}$$

Eq. 4-6

where all quantities are as defined above with R_v, the vapor-phase retardation factor, given by Eq. 4-5. Eq. 4-6 derives from solutions to transient diffusion problems (Crank, 1956) with step-change boundary conditions imposed at zero time.

4.4 BIODEGRADATION MODELS

Degradation is the only mechanism accounting for a true loss of compounds from the environmental system. Other processes like sorption or volatilization only lead to a transfer of compound from one compartment to the other. Two types of degradation processes are possible: chemical degradation and biological degradation (Biodegradation). Chemical degradation in natural condition is extremely slow and therefore considered not relevant as degradation mechanism.

Biodegradation processes require bacteria to degrade contaminants. Bacteria are known to be exclusively in the aqueous phase and in its interfaces with the unsaturated zone, and are therefore only capable to biodegrade compounds which are in the liquid phase. Since contaminants in the unsaturated zone are partitioned between the aqueous, solid, non aqueous phase liquids (NAPL), and gaseous phase, these contaminants are not always bioavailable. Sorption to organic matter and entrapment in micropores provoke an efficient protection from microbial attack, and this one will occur only if chemicals can diffuse outside soil particle or if natural organic matter itself is attacked by micro-organism.

To assess if significant vapor migration attenuation due to biodegradation is occurring, it is necessary to characterize the vertical soil gas distribution and vapor transport properties of the unsaturated zone. Information needed includes:

- Total hydrocarbon soil gas concentration vs. depth.
- Specific chemicals soil gas concentrations of interest vs. depth (e.g., benzene)
- Oxygen soil gas concentrations vs. depth
- Site conceptual model (layers, soil types, depth to source, etc.)

When selecting specific analytes, it is useful to include at least one compound that is known to be recalcitrant to degradation and is relatively unretarded, even though it does not pose concern within a health risk perspective. These data can be used to ensure that estimates of the diffusive properties of the soil are reasonable and that near-steady conditions exist.

If it is assumed that biodegradation is playing an important role, then it is important to look for multiple lines of supporting evidence, including:

- Decreasing oxygen concentration with depth, consistent with the contaminant vapor concentration profile;
- Carbon dioxide concentration profile consistent with oxygen profile;
- Relatively stable soil gas concentration with time.

These are traditional indicators of aerobic biodegradation. To demonstrate that natural attenuation is occurring in the vadose zone, the data listed above are sufficient for this purpose at most sites. If, however, one wishes to be more quantitative and to incorporate bio-attenuation into the development of site-specific vapor intrusion pathway screening levels, additional analysis is necessary.

A simple algorithm could be used in case of shallow soil with relatively homogeneous setting. Generally in these settings the oxygen concentration in the soil gas remains high (>5% v/v), except perhaps in the vicinity of the source zone. The contaminant vapor concentrations appear to decrease exponentially with distance away from the source, and at any point are less than those that would be predicted by the one-dimensional steady-state model presented above, assuming uniform properties and no degradation.

Here a screening model that assumes a first-order reaction in a homogeneous medium is used. In this case the equation describing the steady-state vapor concentration profile $C(Z)$ [mg/m^3] is:

$$C(Z) = \frac{C(z=1)\left[e^{-\delta z} - e^{\delta z}\right] + C(z=0)\left[e^{-\delta(1-z)} - e^{\delta(1-z)}\right]}{\left[e^{-\delta z} - e^{\delta z}\right]}$$

Eq. 4-7

where L [m] is the depth interval of interest, $Z = {}^{z}/_{L}$ is the normalized height above the source zone, δ is given by:

$$\delta = \sqrt{\frac{\lambda_i \theta_m L^2}{H_i D^{eff}}}$$

Eq. 4-8

Where λ_i [d^{-1}] is a first-order decay coefficient for degradation that is assumed to occur in the soil moisture. The parameter δ represents a ratio of degradation rate to diffusion rate; therefore, it is expected that attenuation will increase with increasing δ.

Incorporating Eq. 4-7 into the development of Johnson and Ettinger (1991) yields the following refined equation for the attenuation factor:

$$\alpha = \frac{C_{indoor}}{C_{source}} = \left\{ \frac{1-\beta}{(1-\beta)\left(\frac{Q_B L}{D^{eff} A_B}\right)\left(\frac{e^{\delta}-e^{-\delta}}{2\delta}\right) + \beta\left(\frac{Q_B}{Q_{soil}}\right)\left(\frac{e^{-\delta}+e^{\delta}}{2}\right) + \left(\frac{e^{-\delta}+e^{\delta}}{2}\right)} \right\}$$

Eq. 4-9

Where:

$$\beta = 1 - exp\left(\frac{Q_{soil} L_{crack}}{D_{crack} A_B}\right)$$

Eq. 4-10

and all other parameters are as defined above for Eq. 4-3

4.4.1 Oxygen –limited biodegradation model [4]

This chapter describes a model which includes biodegradation, but which neglects the attenuating effects of a building and foundation on chemical vapor transport. A shallow aerobic layer, L_a, with biodegradation, and a deeper anaerobic layer, L_b, without biodegradation are included, as in Figure 4.2. Chemical vapor concentrations are indicated in the source zone, c_s, at the anaerobic-aerobic interface, c_t, and within indoor building enclosure air, c_e. Diffusive chemical flux, J (mg/cm^2 s), in a vertical direction, z (cm), is:

$$J = -D_{eff} \frac{\partial c_v}{\partial z}$$

Eq. 4-11

Chemical vapor concentration is indicated at the source, c_s, and in indoor air, c_e, and is assumed to be constant along an horizontal direction. Assuming no other chemical sources or sinks and a well mixed building, chemical vapor flux is related to an indoor air concentration using a building air exchange rate, ER (s^{-1}), as volume exchanges per unit time, and to an indoor air mixing height (or building volume to foundation area ratio), L_{mix} (cm).

$$J = L_{mix} \cdot ER \cdot c_e$$

Eq. 4-12

For chemicals, an algebraic solution is first shown for a soil layer of depth, L, then applied for the layers L_a and L_b as in Figure 4.2. Aerobic chemical biodegradation is assumed to occur in the water-phase soil matrix as a source (+) or sink (-) per unit mass of soil, Λ (mg/g-soil·s), specified by a first-order biodegradation rate, k_w (1/s) and with a vapor concentration c_v.

$$\Lambda = -\frac{\theta_w}{\rho_s H} \cdot k_w c_v$$

Eq. 4-13

The value ρ_s (g-soil /cm^3-soil) is the soil bulk density. The biodegradation term is included in chemical transport as

$$\frac{\partial J}{\partial z} = \rho_s \Lambda$$

Eq. 4-14

From Eq. 4-13 and Eq. 4-14:

$$D_{eff} \cdot \frac{\partial^2 c_v}{\partial z^2} = -\rho_s \Lambda$$

Eq. 4-15

Using a reference chemical vapor concentration (at $z = 0$) of c_o, boundary conditions are specified as:

$$\left(\frac{c(z/L=1)}{c_0}\right) = \beta \qquad \left(\frac{c(z/L=0)}{c_0}\right) = 1$$

Eq. 4-16

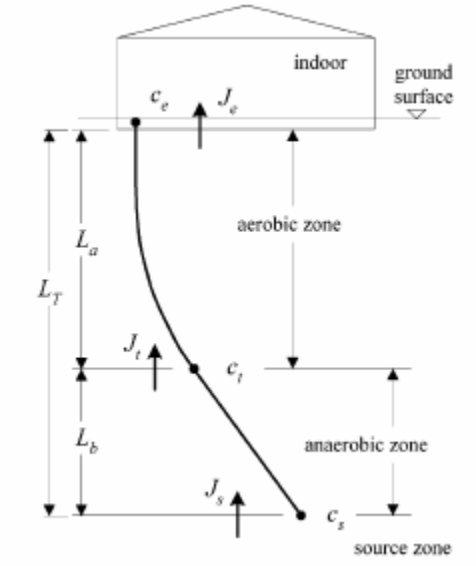

Figure 4.2 - Conceptual model for the oxygen-limited model

A steady state solution to Eq. 4-15 is given by:

$$\left(\frac{c(z)}{c_0}\right) = \frac{\left(e^{-\delta} - \beta\right)e^{\delta\frac{z}{L}} + \left(\beta - e^{\delta}\right)e^{-\delta\frac{z}{L}}}{e^{-\delta} - e^{\delta}}; \quad \delta > 0$$

Eq. 4-17a

$$\left(\frac{c(z)}{c_0}\right) = 1 - \left(\frac{z}{L}\right) \cdot (1 - \beta); \quad \delta = 0$$

Eq. 4-17b

Differentiating Eq. 4-17a/b and replacing them in Eq. 4-11, the following equations for flux are obtained:

$$\frac{LJ(z)}{D_{eff}c_0} = \delta \frac{\left(e^{-\delta} - \beta\right)e^{\delta\frac{z}{L}} + \left(\beta - e^{\delta}\right)e^{-\delta\frac{z}{L}}}{e^{\delta} - e^{-\delta}}; \quad \delta > 0$$

Eq. 4-18a

$$\frac{LJ(z)}{D_{eff}c_0} = (1-\beta); \quad \delta = 0$$

Eq. 4-18b

The chemical flux solutions of Eq. 4-18 are applied with subscripts to designate aerobic (a) and anaerobic (b) soil layers. In the aerobic zone with chemical degradation ($\delta_a > 0$), a conservative overestimate of chemical flux from subsurface soil to indoor air at $z_a = L_a$ is made assuming $c_t >> c_e$, or approximately, $\beta_a = 0$ in Eq. 4-18a.

$$\frac{LJ(z)}{D_{eff}c_0} = \delta_a \frac{\left(e^{-\delta_a}\right)e^{\delta_a\frac{z_a}{L_a}} + e^{\delta_a}e^{-\delta_a\frac{z_a}{L_a}}}{e^{\delta_a} - e^{-\delta_a}}$$

Eq. 4-19

At the aerobic-anaerobic interface, at $z_a = 0$, Eq. 4-19 is

$$\frac{LJ(z)}{D_{eff}c_0} = \delta_a \frac{e^{-\delta_a} + e^{\delta_a}}{e^{\delta_a} - e^{-\delta_a}}$$

Eq. 4-20

In the anaerobic zone with no degradation, flux is constant ($J_s = J_t$). At the aerobic-anaerobic interface, from Eq. 4-18b:

$$\frac{LJ_t}{D_{eff}c_s} = (1-\beta_b)$$

Eq. 4-21

With:

$$\beta_b = \frac{c_t}{c_s}$$

Eq. 4-22

Setting Eq. 4-20 and Eq. 4-21 as equal and solving for $1/\beta_b$ yields:

$$\left(\frac{1}{\beta_b}\right) = 1 - \left(\frac{L_b}{L_a}\right)\cdot\delta_a \cdot \frac{e^{-\delta_a} + e^{\delta_a}}{e^{\delta_a} - e^{-\delta_a}}$$

Eq. 4-23

For $z_a = L_a$ in the aerobic zone, from Eq. 4-19:

$$\frac{LJ(z)}{D_{eff}c_0} = \frac{2\delta_a}{e^{\delta_a} - e^{-\delta_a}}$$

Eq. 4-24

With Eq. 4-12, Eq. 4-23 yields:

$$\frac{c_e}{c_t} = \frac{D_{eff}}{L_a L_{mix} ER} \cdot \frac{2\delta_a}{e^{\delta_a} - e^{-\delta_a}}$$

Eq. 4-25

The equation for the attenuation factor from source to indoor is obtained combining Eq. 4-22, Eq. 4-23 and Eq. 4-25:

$$\alpha_{OM} = \frac{c_e}{c_s} = \left(\frac{D_{eff}}{L_{mix} ER}\right) \cdot \frac{2\delta_a}{L_b \delta_a (e^{-\delta_a} + e^{\delta_a}) - L_a (e^{-\delta_a} - e^{\delta_a})}$$

Eq. 4-26

4.4.2 Layer method biodegradation

The following analysis is appropriate only for sites that have reached near-steady conditions, because time factor is not considered in this analytical analysis. Time required for vapor to reach near-steady state concentration at any point increase with the square of the distance from the source and also is affected by the chemical properties of compound of interest.

The basic concept of the layer approach is to divide the subsoil in layers as shown in Figure 4.3. A central layer where the biodegradation reaction takes place is constricted by two layers where mass transport occurs without reaction. At steady state condition the concentrations profile for this scenario is given by:

$$c(z) = c_{source} - (c_{source} - c_2)\left(\frac{z}{L_1}\right); \qquad Layer\ 1\ (0 < z < L_1)$$

Eq. 4-27

$$c(z) = \frac{c_3 e^{\delta_D \frac{(L_1 - z)}{(L_2 - L_1)}} - c_2 e^{\delta_D \frac{(L_2 - z)}{(L_2 - L_1)}}}{e^{-\delta_D} - e^{\delta_D}} + \frac{c_2 e^{-\delta_D \frac{(L_1 - z)}{(L_2 - L_1)}} - c_3 e^{-\delta_D \frac{(L_1 - z)}{(L_2 - L_1)}}}{e^{-\delta_D} - e^{\delta_D}}; \ Layer\ 2\ (L_1 < z < L_2)$$

Eq. 4-28

$$c(z) = c_3 - (c_3 - c_4)\left(\frac{z - L_2}{L_3 - L_2}\right); \qquad Layer\ 3\ (L_2 < z < L_3)$$

Eq. 4-29

Where:

$$\delta_D = \sqrt{\frac{k_w \theta_w (L_2 - L_1)^2}{D_{eff} H}}$$

Eq. 4-30

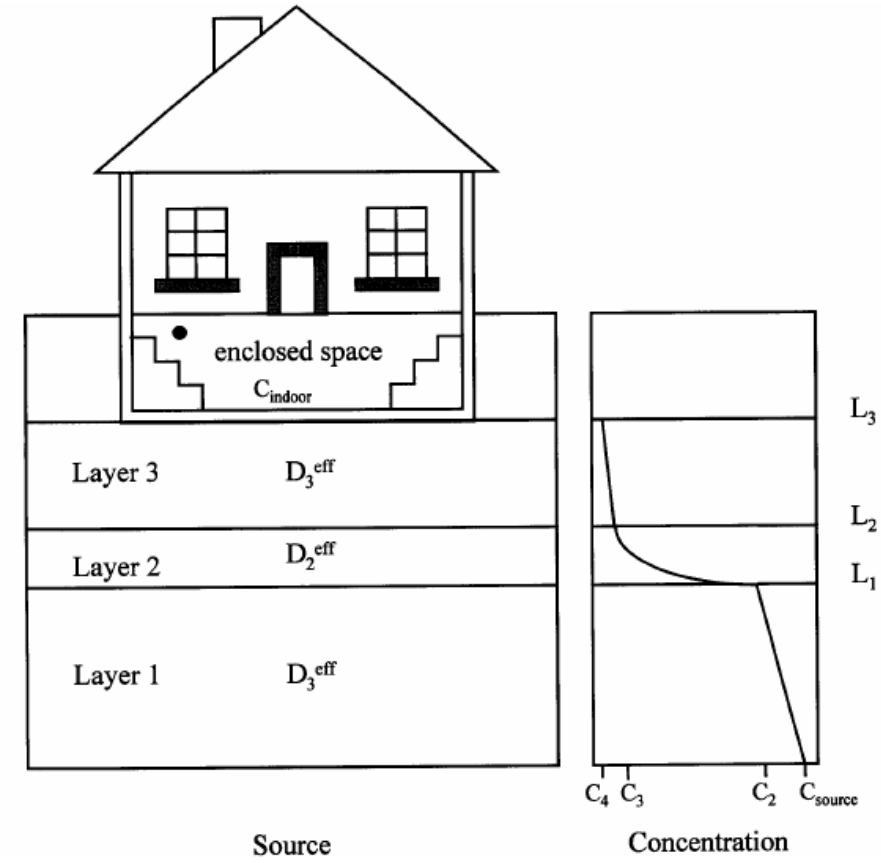

Figure 4.3 - Dominant layer model bio-attenuation scenario

Using the general development of Johnson and Ettinger model, the attenuation factor AF for this approach becomes:

$$\alpha_{DL} = \frac{c_i}{c_s} = \frac{1-\beta}{(1-\beta)\left(\frac{Q_B}{2\phi\gamma\psi}\right) + \left(\beta\left(\frac{Q_B}{Q_{soil}}\right) - 1\right)\left(\frac{1+\gamma\psi-4\psi^2}{2\gamma\psi^2}\right)}$$

Eq. 4-31

Where:

$$\beta = 1 - exp\left(\frac{Q_{soil}L_{crack}}{D_{crack}A_B}\right)$$

Eq. 4-32

$$\gamma = \left(\frac{D_1^{eff}}{D_2^{eff}}\right)\frac{e^{\delta_D} - e^{-\delta_D}}{\delta_D}\frac{(L_2 - L_1)}{L_1}$$

Eq. 4-33

$$\sigma = \left(\frac{D_3^{eff}}{D_2^{eff}}\right)\frac{e^{\delta_D} - e^{-\delta_D}}{\delta_D}\frac{(L_2 - L_1)}{(L_3 - L_2)}$$

Eq. 4-34

$$\psi = \frac{1}{e^{-\delta_D} + e^{\delta_D} - \gamma}$$

Eq. 4-35

$$\phi = \left(\frac{A_B D_3^{eff}}{L_3 - L_2}\right) \frac{1}{\left[\sigma - \frac{1}{\psi} - \gamma + 4\psi\right]}$$

Eq. 4-36

To solve for the concentration profile, Eq. 4-31 is first solved to get α_{DL}. Then each of the following equations is solved sequentially for c_4, c_3 and c_2 in terms of c_1:

$$\frac{c_4}{c_1} = \frac{2\beta\gamma\psi\phi - \alpha_{DL}Q_{soil}}{(\beta - 1)Q_{soil} - \frac{\beta\phi}{\psi} - \beta\gamma\phi + 4\beta\psi\phi}$$

Eq. 4-37

$$\frac{c_3}{c_1} = \frac{2\gamma\psi + \sigma\left(\frac{c_4}{c_1}\right)}{\sigma - \frac{1}{\psi} - \gamma + 4\psi}$$

Eq. 4-38

$$\frac{c_2}{c_1} = 2\psi\left(\frac{c_3}{c_1}\right) - \gamma\psi$$

Eq. 4-39

4.5 RESULTS

The results obtained by the two biodegradation models discussed above are shown in this chapter.

The data used in the models are:

A_b = 50 m^2

Q_b = 1200 m^3/d (12 air changes per days in 100 m^3 enclosed space)

Q_{soil} = 1.5 m^3/d (= 1 L/min)

L_{crack} = 0.15 m

η = 0.01 m^2/m^2

$L_T = L_b + L_a + L_{crack} = 3m$, L_a and L_b values were obtained by an iteration process based on O_2 and contaminant mass balance in soil.

The models have been run considering the BTEX fraction as test compounds (Table 4-1), since this type of chemical should be degraded in aerobical conditions.

Table 4-1: Chemicals used as test compounds

Chemical	Henry constant [dimensionless]	Solubility [mg/l]
Benzene	2,28E-01	1,75E+03
Toluene	2,72E-01	5,26E+02
Etylbenzene	3,23E-01	1,69E+02
Xylene	3,14E-01	1,85E+02

The soil profile has been simulated as homogenous in the entire unsaturated zone and in both models. Table 4-2 summarizes the soil parameters.

Table 4-2: Soil parameters

Symbol	parameter	Unit	Value
θ_T	Unsaturated zone total porosity	dimensionless	0,41
θ_e	Unsaturated zone effective porosity	dimensionless	0,353
θ_w	Soil water content	dimensionless	0,103
θ_a	Soil air content	dimensionless	0,25
θ_{wcrack}	Crack water content	dimensionless	0,12
θ_{acrack}	Crack air content	dimensionless	0,26

The biodegradation rates have been checked in the literature [11], and it was decided to vary them as shown in Table 4-3.

Table 4-3: Biodegradation Rates

Chemical	First Order Biodegradation rate [h^{-1}]
Benzene	0,5 – 2,0
Toluene	0,3 – 1,5
Etylbenzene	0,2 – 2,0
Xylene	0,2 – 0,8

4.5.1 Oxygen-limited method

Figure 4.4 shows the Attenuation Factor calculated with the Oxygen-limited model at increasing biodegradation rates, in comparison with a no biodegradation model (Johnson and Ettinger model). As expected, the attenuation factor decreases when the biodegradation rate increases.

The comparison between the two sets of calculation (no biodegradation/oxygen limited model) shows that including biodegradation in modeling vapor intrusion has a deep influence on the results. However, it was expected that at low biodegradation rates the attenuation factor would be the same as in the model not including biodegradation, whereas a difference of at least two orders of magnitude between the no-Biodegradation case (purple lines) and the oxygen model predictions (full lines), was observed.

BTEX showed similar behaviours varying biodegradation rate with a maximum difference of one order of magnitude. Further, some differences can be noticed between the three modeled compounds.

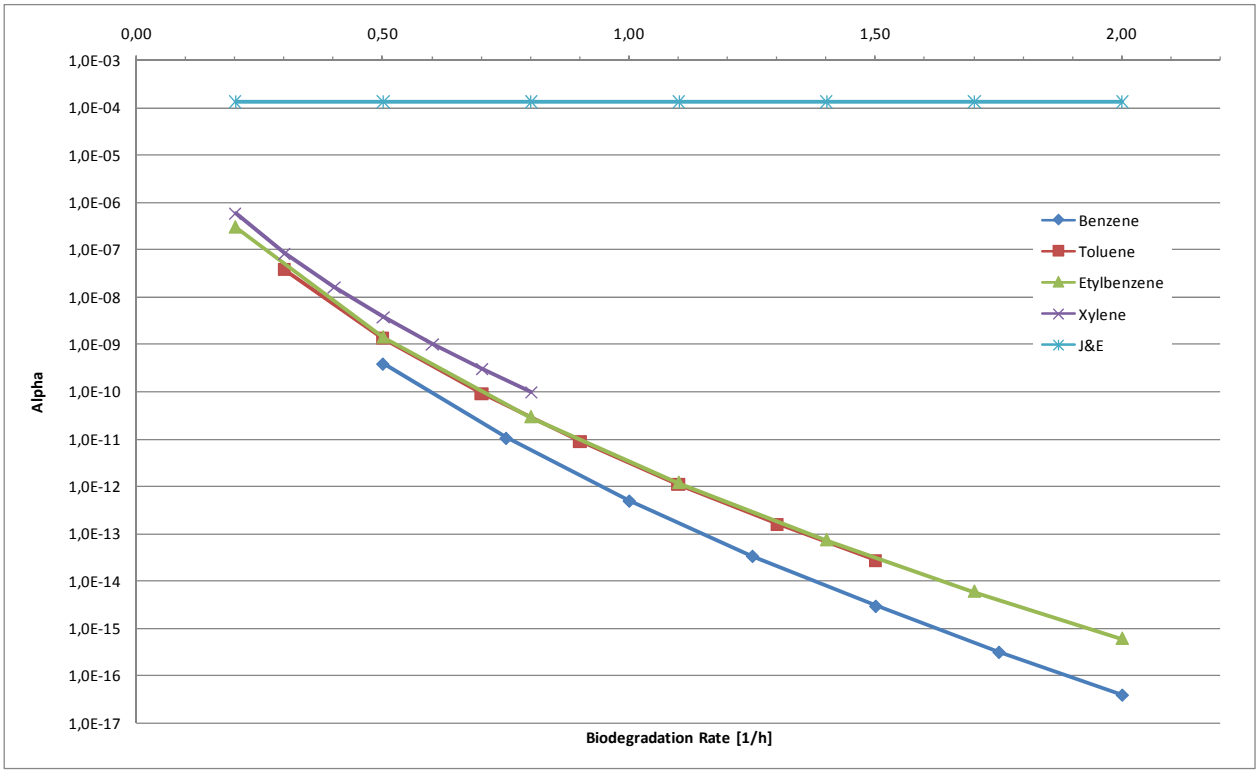

Figure 4.4: Attenuation Factor vs Biodegradation rate (Oxygen limited method)

A new calculation was performed in order to understand the attenuation factor behaviour when biodegradation rate approaches zero value. The model was run with the same input parameters as above and varying the biodegradation rates from $5 \cdot 10^{-2}$ to $1 \cdot 10^{-3}$.

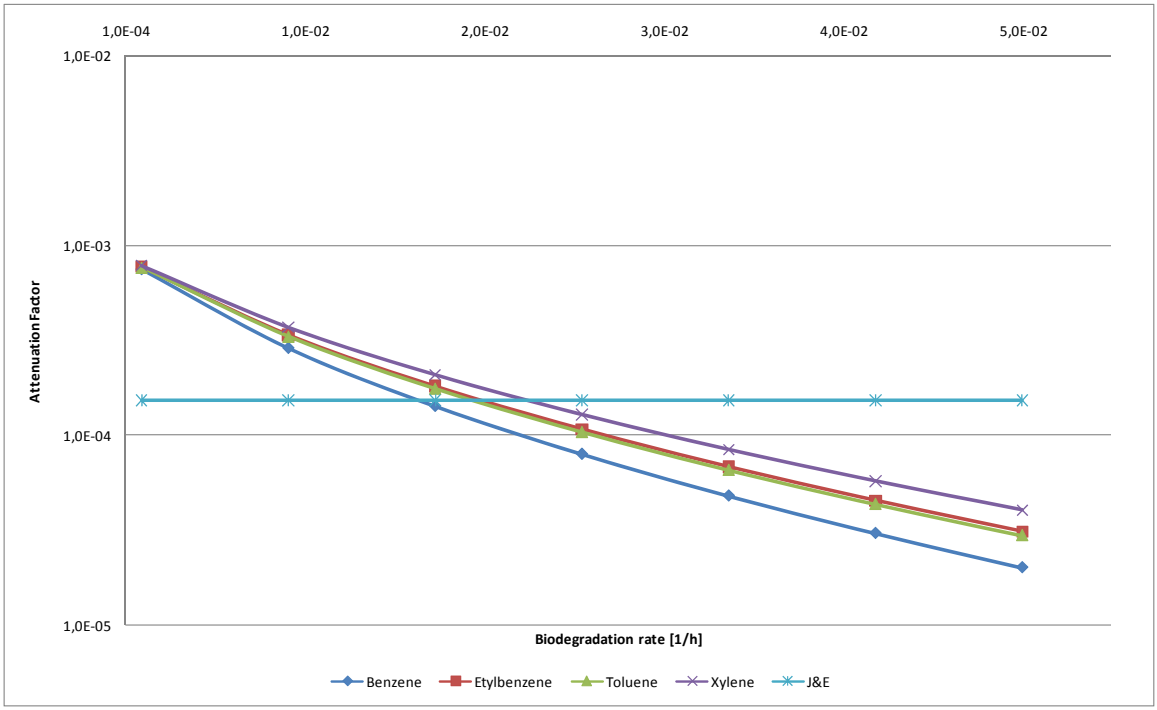

Figure 4.5: Attenuation factor for low biodegradation rates (Oxygen limited method)

Figure 4.5 shows that for small values of the biodegradation rate, the attenuation factor of each compound for the layer method have similar value, but these are different from the attenuation factor only with diffusion.

In order to explain this phenomenon it is possible to analyze Eq. 4-26.

Analyzing the limit for the Attenuation Factor we have:

$$\text{if } k_w \to 0 \text{ then } \delta = \sqrt{\frac{k_w \theta_w L^2}{D_{eff} H}} \to 0$$

so:

$$\lim_{\delta_a \to 0} \left(\frac{D_{eff}}{L_{mix} ER}\right) \cdot \frac{2\delta_a}{L_b \delta_a (e^{-\delta_a} + e^{\delta_a}) - L_a (e^{-\delta_a} - e^{\delta_a})}$$

$$\left(\frac{D_{eff}}{L_{mix} ER}\right) \cdot \lim_{\delta_a \to 0} \frac{2\delta_a}{L_b \delta_a (e^{-\delta_a} + e^{\delta_a}) - L_a (e^{-\delta_a} - e^{\delta_a})}$$

$$\left(\frac{D_{eff}}{L_{mix} ER}\right) \cdot \lim_{\delta_a \to 0} \frac{2\delta_a}{L_b \delta_a (2) - L_a (-2\delta_a)}$$

$$\left(\frac{D_{eff}}{L_{mix} ER}\right) \cdot \frac{1}{L_b + L_a} = \frac{D_{eff}}{L_{mix} \cdot ER \cdot L_T}$$

This result shows how the oxygen model neglects the attenuation effects of a building and foundation on chemical vapor transport, differently from the J&E attenuation factor, which includes a term for soil, foundation and building transport resistance:

$$\alpha_{J\&E} = \frac{\frac{1}{L_{mix} \cdot ER}}{\frac{1}{L_{mix} \cdot ER} + \frac{L_{crack}}{D_{crack} \eta} + \frac{L_T}{D_{eff}}}$$

Eq. 4-40

4.5.1.1 Oxygen demand and transport

Biodegradation within the aerobic soil layer, L_a, requires oxygen supplied from the surface. Using a flux balance it is possible to obtain the L_a value with the sufficient oxygen for the aerobic biodegradation. Depending of the site-specific data available, one of the two equation reported below (Eq. 4-41 and Eq. 4-42) can be used:

$$J_{e,O_2} = \frac{D_{eff} c_t}{\varphi} \sqrt{\frac{k_w \theta_w}{D_{eff} H}} \frac{2 - e^{-\delta_a} - e^{\delta_a}}{e^{\delta_a} - e^{-\delta_a}} + \rho_s L_a \Lambda_{\text{base},O_2}$$

Eq. 4-41

$$c_{e,O_2} = \frac{D_{eff}}{D_{eff,O_2}} \frac{1}{\varphi} c_r - \left(\frac{\rho_s \Lambda_{\text{base},O_2} L_a^2}{2 D_{eff,O_2}} \right)$$

Eq. 4-42

Where:

φ = The mass ratio of oxygen to chemical consumption, assuming complete aerobic reaction of hydrocarbon constituents to carbon dioxide and water on a mass basis;

$$\varphi_i = \frac{MW_i}{MW_{O_2} \cdot \left(n + \frac{m}{4}\right)}$$

Eq. 4-43

With MW_i the contaminant's molecular weight (g/g mole) and hydrocarbon chemical formula defined by:

$$C_n H_m + \left(n + \frac{m}{4}\right) \cdot O_2 \rightarrow \frac{m}{2} \cdot H_2O + n \cdot CO_2$$

$\Lambda_{\text{base},O_2}$ = Baseline soil respiration;

D_{eff,O_2} = Oxygen effective diffusion coefficient;

and all other parameters are as defined above.

This equation is solved by specifying a maximum downward oxygen flux or a maximum oxygen concentration at the upper soil boundary. Iteration within the range 0 <L_a < L_T yields an aerobic depth. Ambient oxygen concentration in air, $c_{amb,O2}$ (0,279 mg/cm^3-air), is an upper limit for $c_{e,O2}$ in Eq. 4-42.

This concentration ($c_{amb,O2}$ = 279 mg/l) has been used with different soil type contaminated by Benzene to evaluate the corresponding thickness of the aerobic layer, L_a. Table 4-4 and Table 4-5 show the soil properties.

Table 4-4: Soil properties part 1

Parameter	Unit	Sand	Loamy Sand	Sandy Loam	Sandy Clay Loam
θ_T	---	0,43	0,41	0,41	0,39
θ_e	---	0,385	0,353	0,345	0,29
θ_w	---	0,068	0,103	0,194	0,178
θ_a	---	0,317	0,25	0,151	0,112

Table 4-5: Soil properties part 2

Parameter	U.M.	Loam	Silt Loam	Clay Loam	Silty Clay Loam	Silt	Sandy Clay
θ_T	---	0,43	0,45	0,41	0,43	0,46	0,38
θ_e	---	0,352	0,383	0,315	0,341	0,426	0,28
θ_w	---	0,213	0,255	0,2	0,246	0,278	0,228
θ_a	---	0,139	0,128	0,115	0,095	0,148	0,052

Whereas Figure 4.6 shows the different L_a values obtained from the simulation. As shown in Figure 4.7 the aerobic layer thickness is related with the effective porous media diffusion of chemicals and oxygen. Namely L_a will, decrease by decreasing one of this parameter.

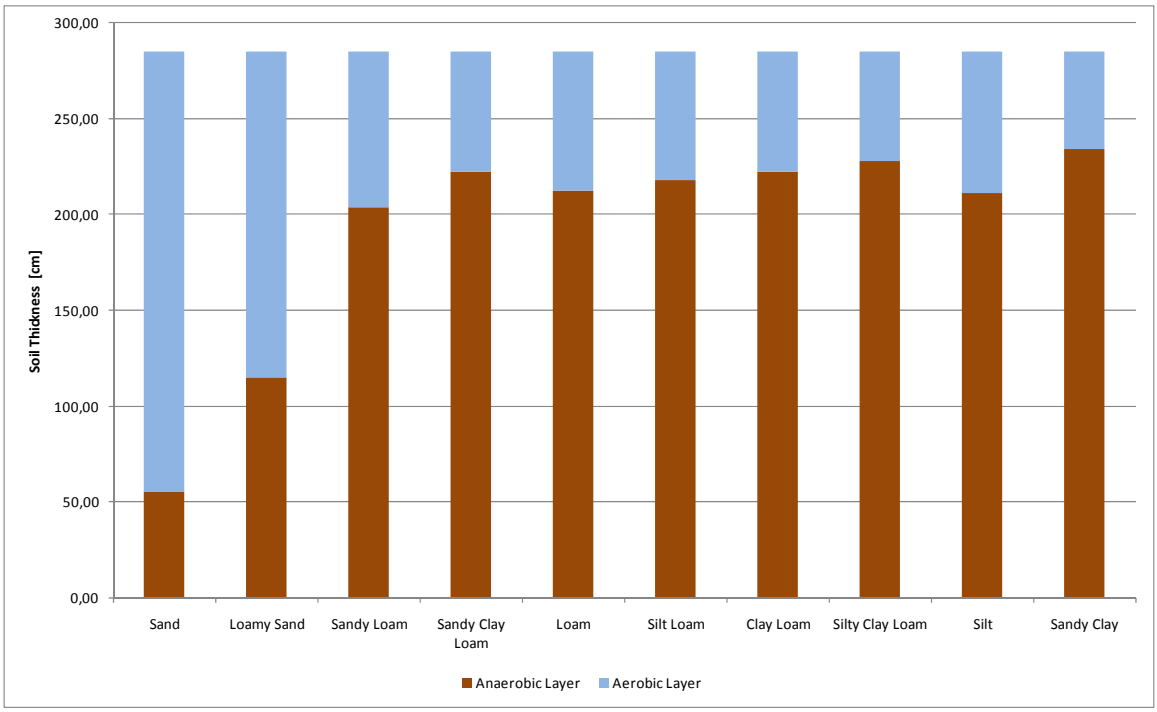

Figure 4.6: Aerobic layer thickness vs soil type

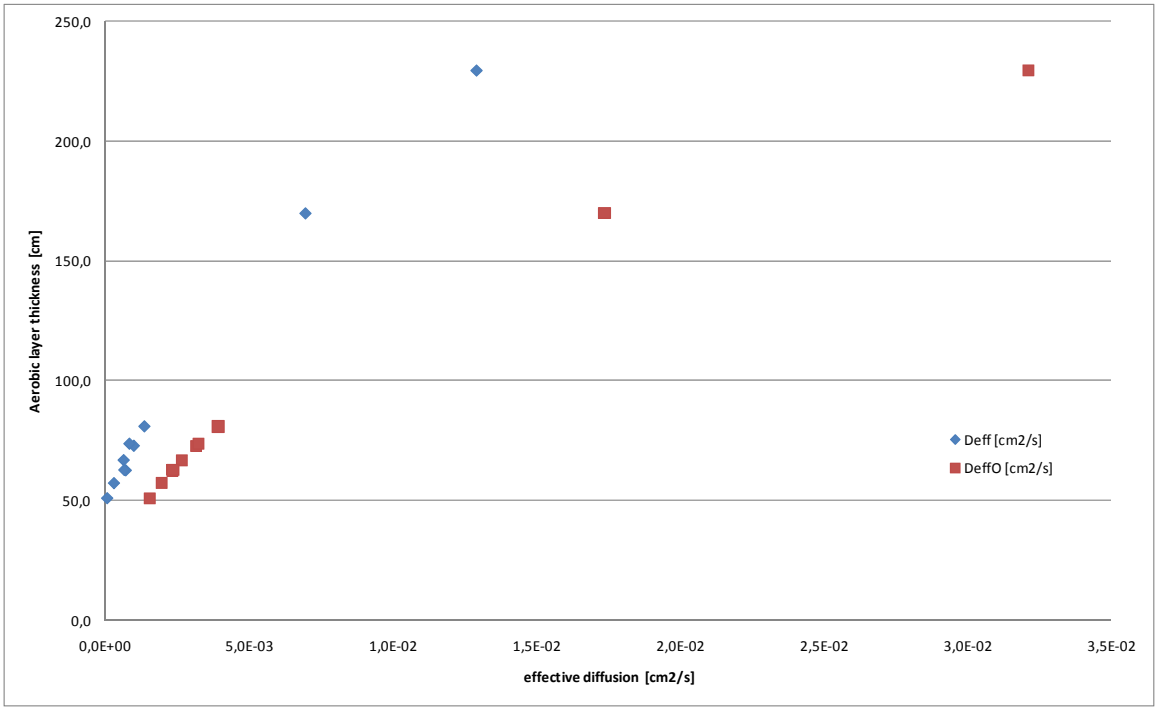

Figure 4.7: aerobic layer thickness Vs effective diffusion.

4.5.2 Layer method

Figure 4.8 shows the results obtained with the layer model, by varying the biodegradation rate between 0,2 and 1,8 h^{-1}. The attenuation factor decreases when the biodegradation rate increases, as observed for the Oxygen limited method. Also with this method, the figure shows that biodegradation has a great influence on the attenuation factor, considering that in the no-biodegradation case, it is at least two orders of magnitude higher than when biodegradation is accounted for.

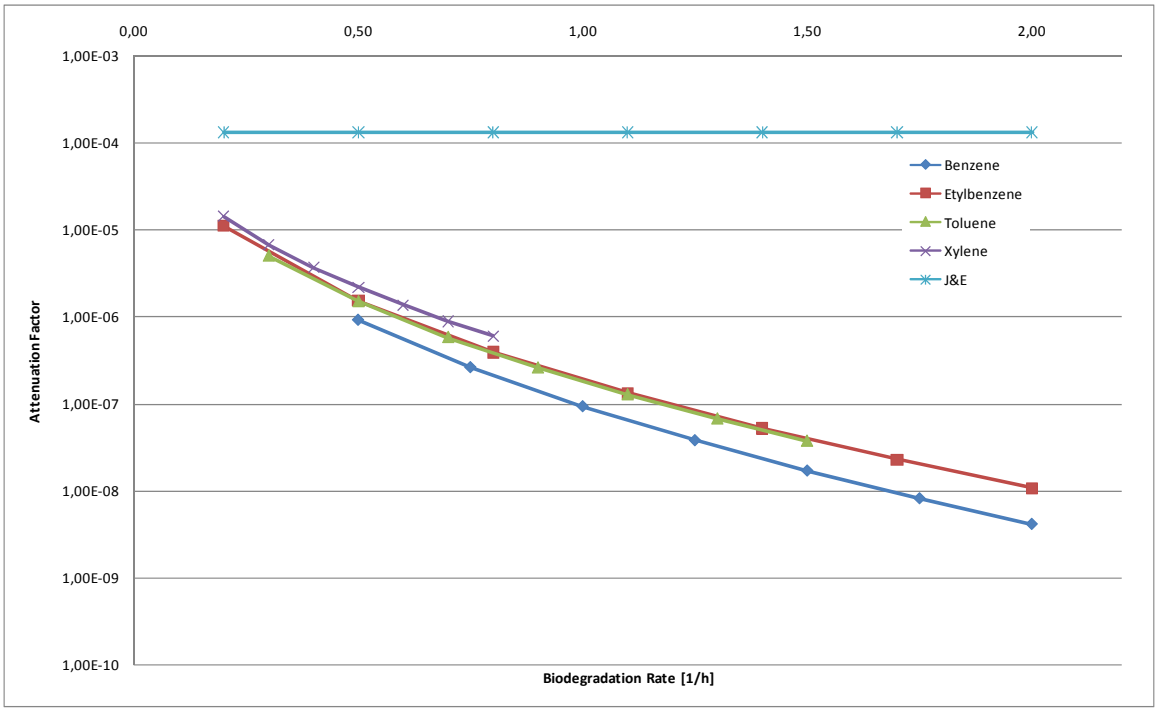

Figure 4.8: Attenuation Factor vs Biodegradation rate (Layer method)

4.5.3 Johnson & Ettinger with Biodegradation

The results obtained by including biodegradation in the J&E model, reported in Figure 4.9, show a similar behavior to the one obtained for the two models shown above, although in this case the aerobic process takes place through the whole soil layer (2,85 m).

This situation could be considered like an extreme case of the aerobic degradation, since with these settings the maximum value of the attenuation factor, is achieved.

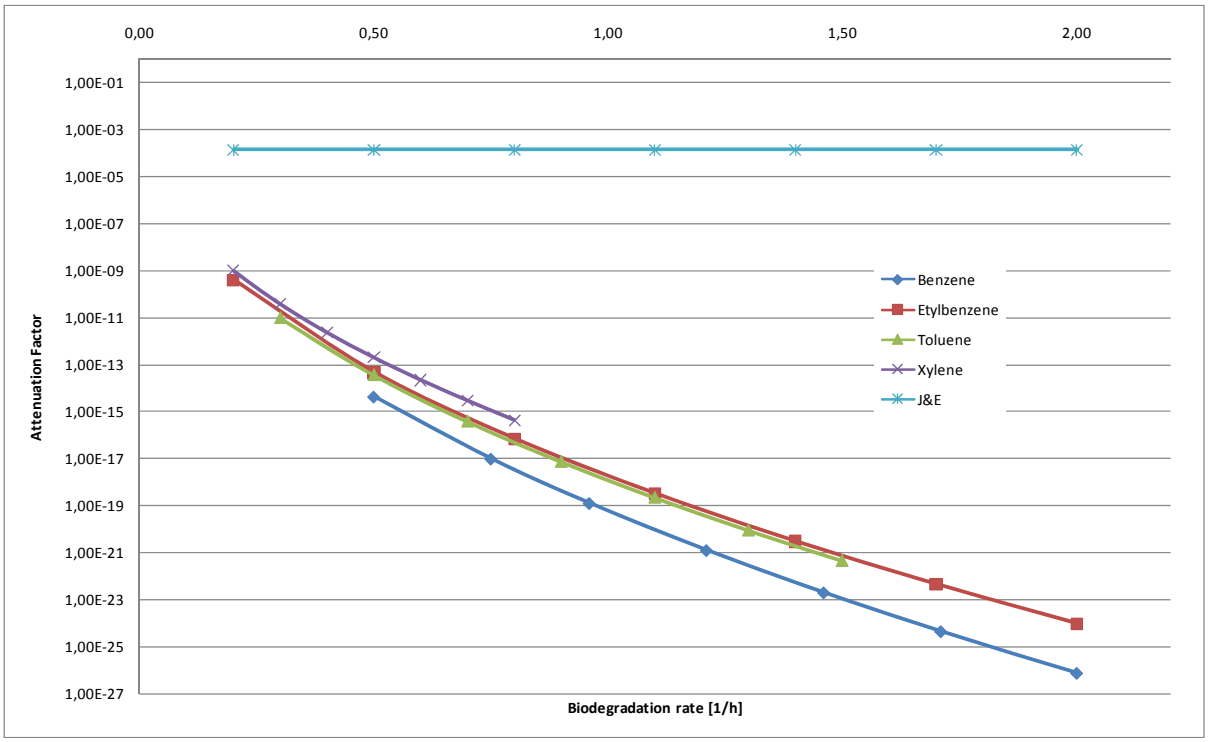

Figure 4.9: Attenuation Factor vs Biodegradation rate (Johnson and Ettinger with biodegradation).

4.5.4 Method Comparison

A comparison between the oxygen limited method and the layer method was performed for each compound of the BTEX mixture in order to highlight differences and similarities. Looking at Figure 4.10 to Figure 4.13, it can be observed that the results provided by the different models are very similar, although the oxygen-limited model seems to provide more conservative results, with lower values of the attenuation factors.

The Dominant Layer model leads to a higher attenuation factor value because, differentiating from the oxygen-limited one, it accounts for three different contribution to the attenuation:

1. Soil;
2. Foundation;
3. Building;

Therefore the dominant layer model should provide the more realistic picture of the actual physical phenomena and looks more suitable to simulate the biodegradation in vadose zone coupled with indoor vapor intrusion. To support this conclusion, a comparison with field data is reported below.

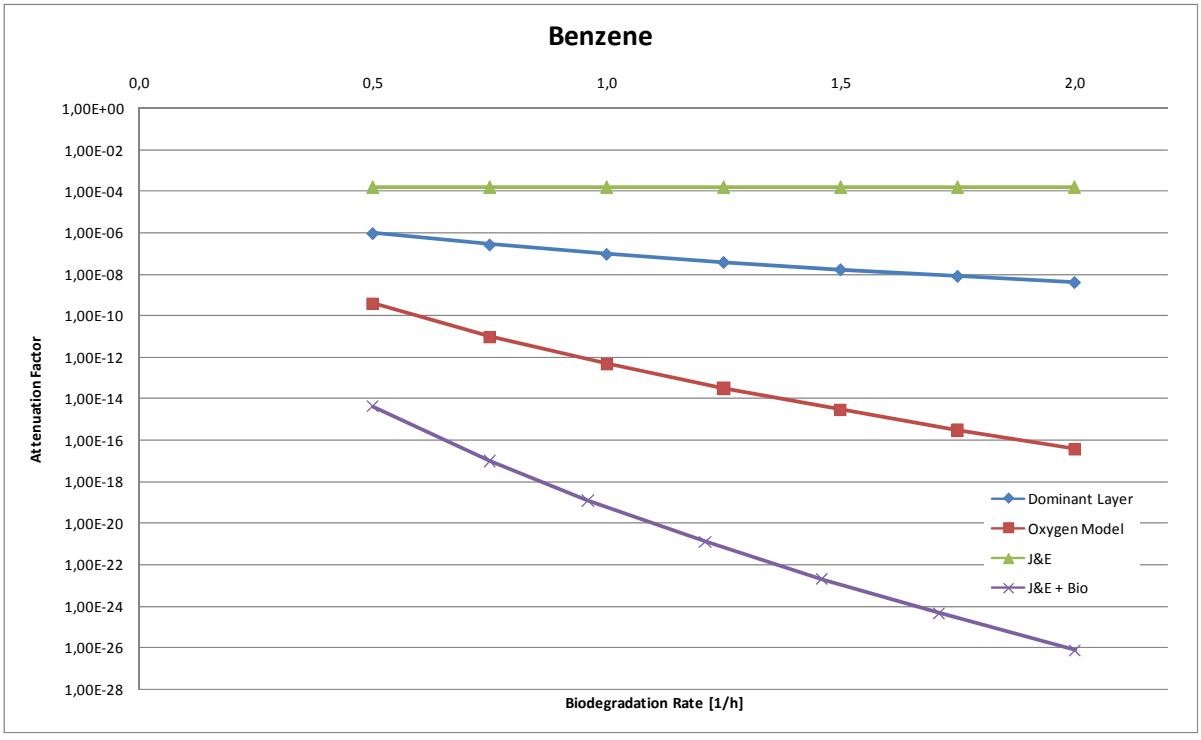

Figure 4.10: Comparison between different methods (benzene)

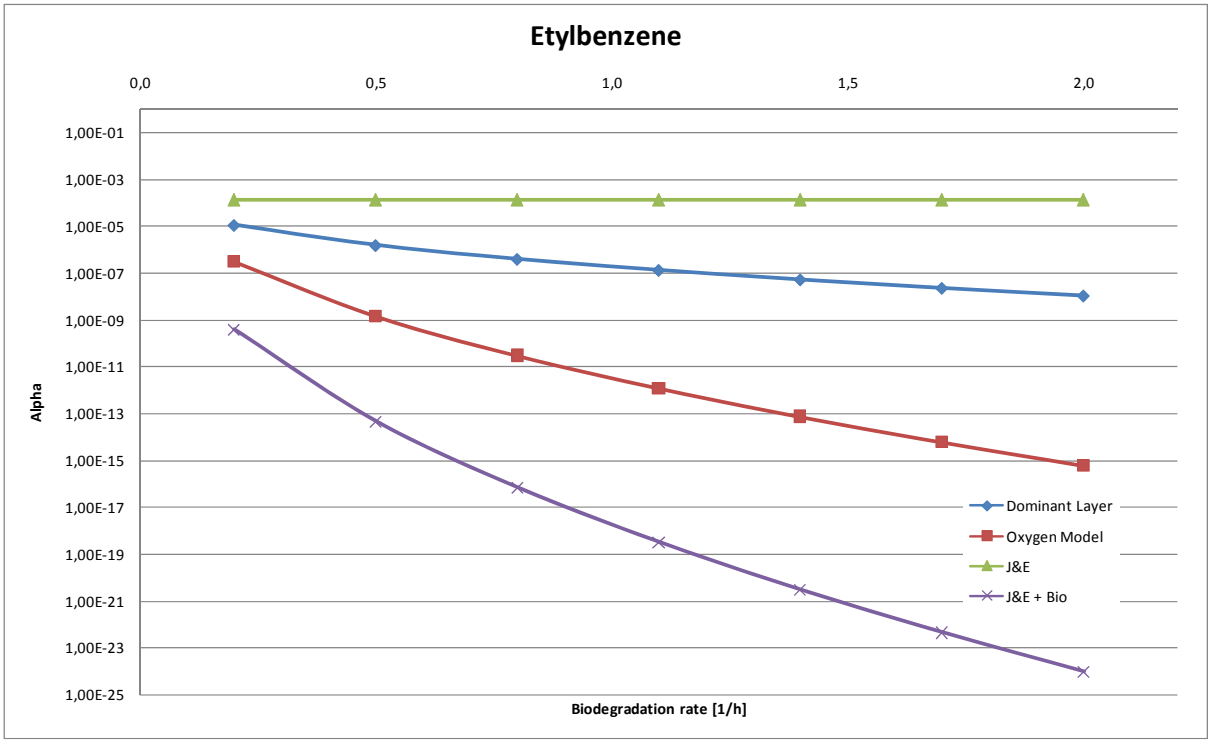

Figure 4.11: Comparison between different methods (Ethylbenzene)

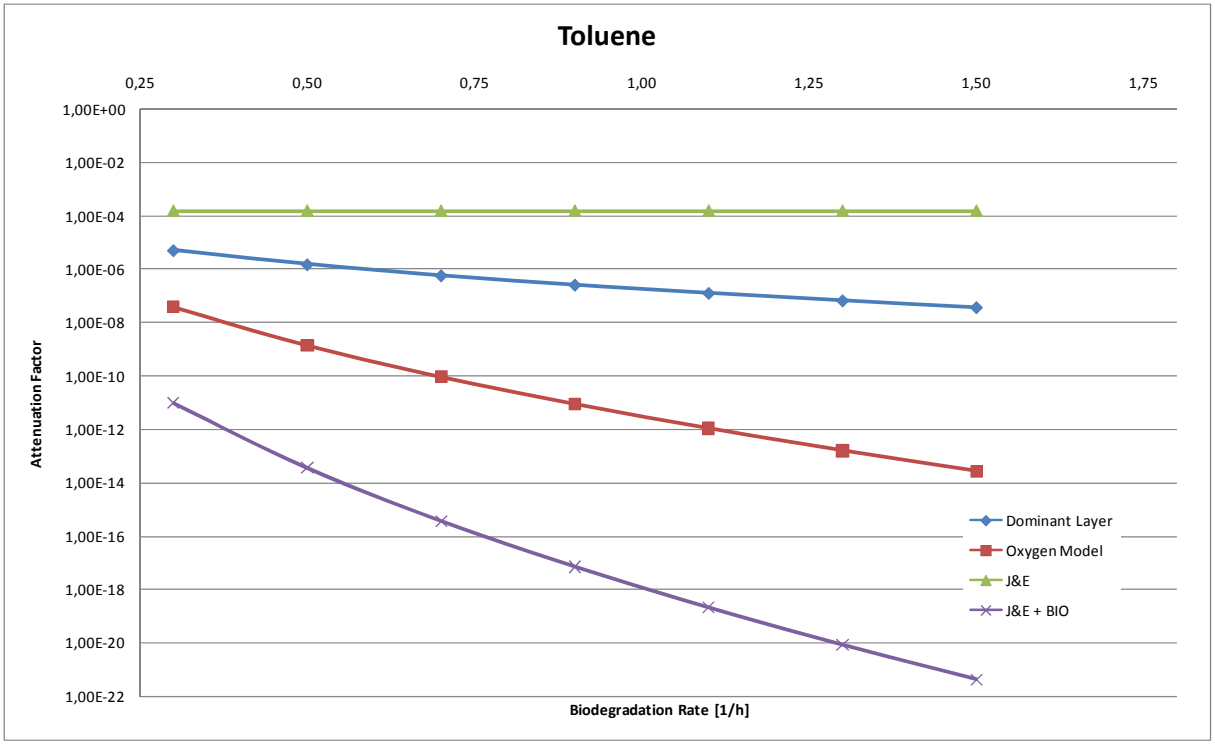

Figure 4.12: Comparison between different methods (Toluene)

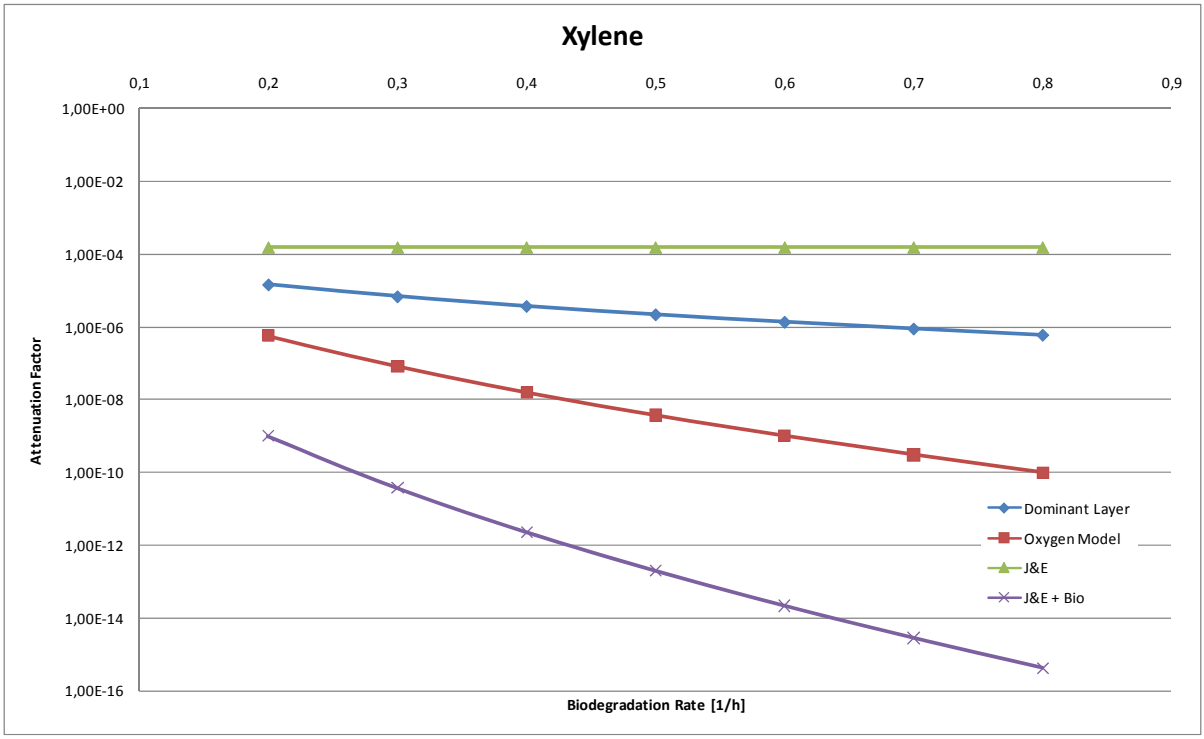

Figure 4.13: Comparison between different methods (Xylene)

4.5.5 Soil Gas Profile

Figure 4.14 reports the profile of soil gas concentration for the BTEX calculated using the dominant layer method. In the deeper layer the three compounds have the same behavior, characterized by a drop from the source concentration to the concentration at the aerobic/anaerobic interface.

In the aerobic layer the biodegradation takes place, so the chemical concentrations by the BTEX decreases more sharply depending on the chemical and the site specific characteristics, indeed, the parameter that has the main influence on the contaminant degradation is the attenuation factor, α_{DL} (values for BTEX are reported in Table 4-6). This parameter has not a linear dependence from the other ones as shown in Eq. 4-31.

Table 4-6: Attenuation Factor values for BTEX

BTEX	α_{DL}
Benzene	1,64E-08
Toluene	3,35E-08
Ethylbenzene	3,51E-08
Xilene	6,00E-08

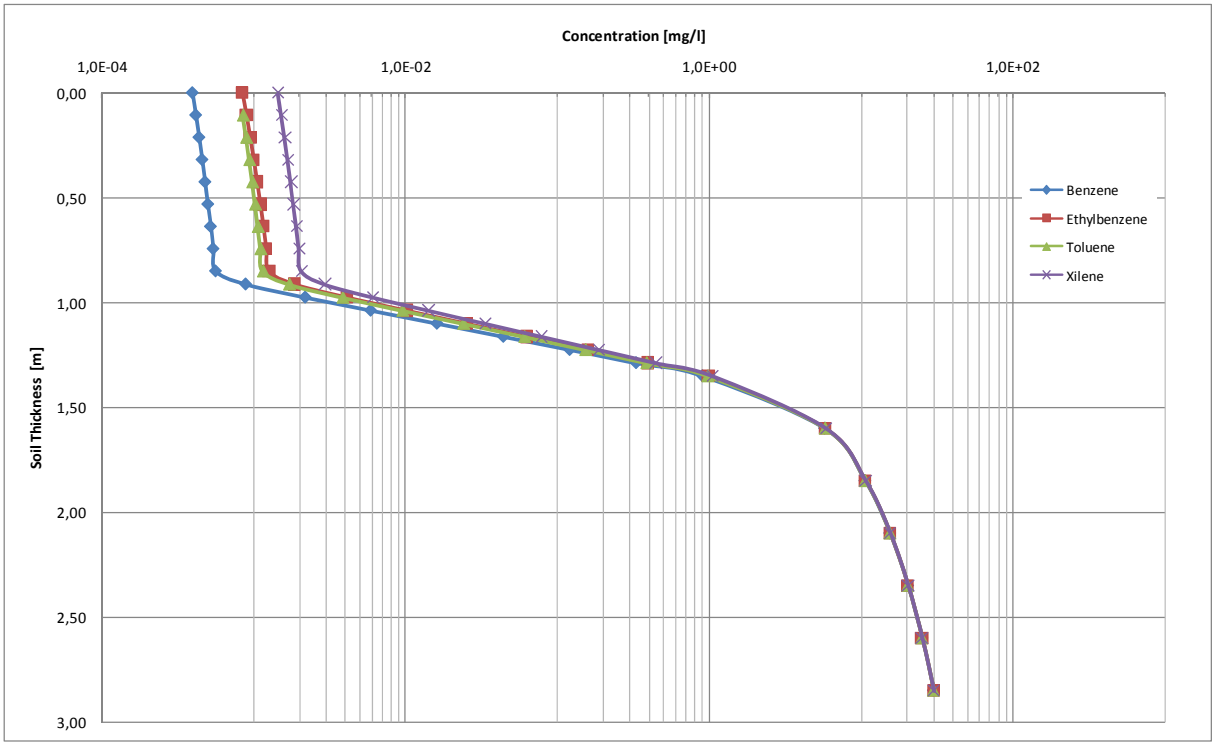

Figure 4.14: Concentration Profile (Layer method).

Finally, in order to understand the model behavior for different soil types, a simulation has been performed on several soil textures: Sand, Loamy Sand, Sandy Loam, Loam and Sandy Clay Loam. These soils types are characterized by different grain size and different water content as shown in Table 4-7. This simulation has been performed using benzene as model compound.

Table 4-7: effective porosity and soil water content ratio for different soil type

symbol	Sand	Loamy Sand	Sandy Loam	Loam	Sandy Clay Loam
θ_T	0,43	0,41	0,41	0,43	0,39
θ_e	0,385	0,353	0,345	0,352	0,29
θ_w	0,068	0,103	0,194	0,213	0,178
θ_a	0,317	0,25	0,151	0,139	0,112
θ_w/θ_e	17,66%	29,18%	56,23%	60,51%	61,38%

Figure 4.15 shows that the contaminant concentration value, in the layer where the biodegradation is accounted for, decreases when the ratio between the effective porosity and the soil water content grows.

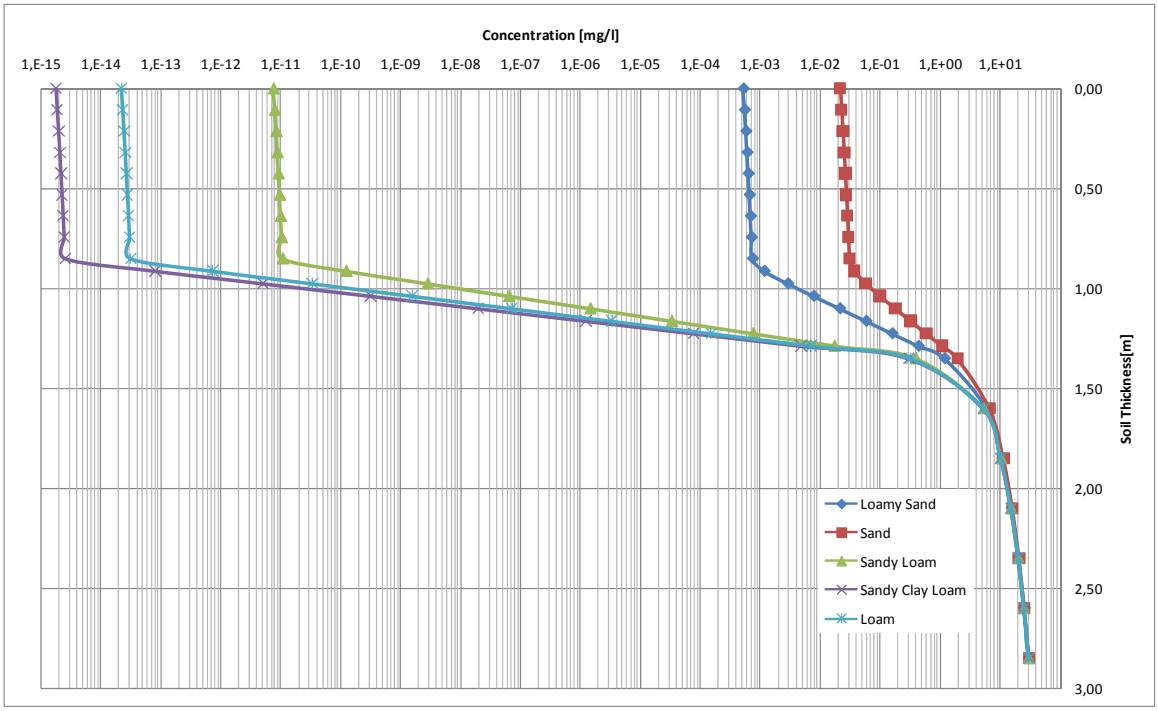

Figure 4.15: Concentration Profile for different soil types

4.5.6 Comparison with field data

In this section the dominant layer model, the oxygen limited model and the J&E models have been used to simulate field data. Table 4-8 and Table 4-9 show field contamination data and soil field data.

Table 4-8: Soil Contamination vs. depth

Benzene	
z [m]	C [mg/l]
1,5	30
1,2	25
0,85	26
0,75	7
0,6	0,1
0,45	0,003
0,3	0,005
0,15	0,004

Table 4-9: Soil Field Data

Parameter	Value	Unit
L_T	1,5	m
θ_e	0,36	---
θ_w	0,18	---
D_{eff}	0,044	cm^2/s

The models run have been obtained with the data provided in section 4.5 and using a biodegradation rate of 0,5 h^{-1} chosen in the range shown above in Table 4-3

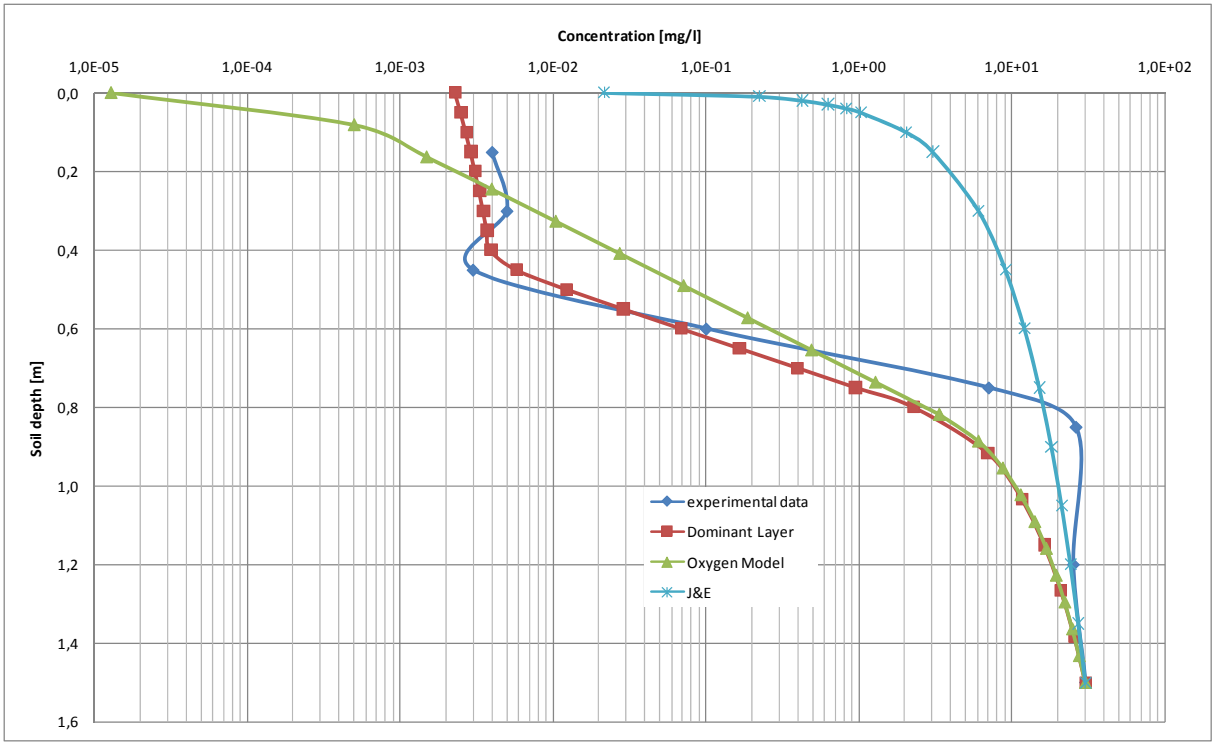

Figure 4.16: Comparison of model with field data.

It is worth noting that a comparison only with a case study does not allow to reach robust conclusion. Figure 4.16 reports the results obtained by the application of the three models. The following consideration can be done:

- The Johnson & Ettinger model gives a contaminant vapor concentration one order of magnitude higher than the experimental one, but this model does not take in account the biodegradation rate. In this case study the J&E model leads to conservative value of risk for human health due to indoor inhalation.
- The Oxygen limited model gives a contaminant vapor concentration two order of magnitude lower than the experimental one, but this model takes in account the biodegradation rate. In this case study the Oxygen limited model leads to an underestimation of the risk for human health due to indoor inhalation.
- The Dominant Layer Model gives the best approximation to the case study. Indeed the contaminated site was well characterized and all the layer dimension were given [11]. Moreover this model has specific equations to predict the soil gas profile (see Eq. 4-27, Eq. 4-28 and Eq. 4-29).

4.6 CONCLUSIONS

In this chapter two models including biodegradation for vapor intrusion into buildings, available from the literature, have been presented: the oxygen limited model and the Dominant layer model.

After the comparison performed between these two models the following conclusions can be drawn:

- The biodegradation term has a remarkable effect in the prediction of the contaminant concentration in indoor environment;
- it is very important to well characterize the soil parameters because they have an high influence on the biodegradation models.
- The Oxygen limited model neglects the attenuation effects of a building and foundation on chemical vapor transport, given a simplified picture of the actual condition.
- The Dominant Layer model provides the more realistic response, but it can not be used as predictive model, since the different layers thickness must be provided as input data.
- The Oxygen limited model is a predictive model and it could be used in a Tier 2 risk analysis approach. Using this model leads to a less conservative risk for human health but more similar to an actual situation, with respect to the J&E model.

5 CONCLUSIONS

Risk analysis for the assessment of a contaminated site is one of the most advanced procedures for assessing the degree of contamination of an area and to define the priorities and the ways of intervention on the site itself. The risk analysis procedure has been used for several years and has received a strong boost in the U.S. in the framework of the Superfund Program and in Italy has gained wider relevance after the introduction of new environmental legislation.

The Italian Agency for Environmental Protection (APAT) has recently issued a guideline document that provides a standard procedure for application of risk analysis to contaminated site. This guideline document is based on a Tier 2 risk analysis approach, which is based on a series of simplified assumptions.

During the work performed within this PhD thesis the procedure for application of risk analysis to contaminated sites has been upgraded.

In chapter 1 the procedure to obtain risk threshold value was described. This procedure uses the same equations applied for the forward mode and it can be summarized in following steps:

- Calculation of an acceptable exposure;
- Definition of a criteria for cumulating exposure of contaminants from different routes
- Calculation of the concentration at the point of exposure;
- Calculation of the risk threshold value.

In chapter 2 human exposure to the contaminant through the vegetable chain has been analyzed. An analytical method to evaluate the vegetables contaminant level starting from source concentration in soil has been obtained by comparing the following technical documents and software:

- Soil Screening Guidance: Technical Background Documents [1996];
- Food Chain Models for Risk Assessment [RAIS 2005];
- Risc 4.0 [2001].

The default values for the specific exposure and bioconcentration parameters have then been selected. Finally the risk deriving from exposure to contaminated soil with or without including the vegetable chain has been calculated, showing that neglecting the vegetable chain leads to a remarkable underestimation of risk for human health. Thus, the proposed procedure could help in filling the gaps of the Italian legislation remediation on agricultural areas.

In chapter 3 the following numerical models were used for the validation of the analytical equations:

- Chemflo 2000 and VS2DTI were used to simulate the leaching process in the vadose zone;
- FEFLOW was used for modelling fluid flow and transport of dissolved constituents in groundwater.

In order to compare the numerical and analytical models, calculated concentration in groundwater could not be used, since numerical models assume a finite source and provide variable concentration output with time, whereas analytical models assume infinite source and steady state conditions. Therefore the comparison was based in terms of cumulative health risk. The results obtained suggest that the use of the SAM (Soil Attenuation Model) within tier II risk analysis provides results which are still conservative with respect to those provided by the numerical model. Thus, neglecting the SAM parameter, as actually suggested in the ASTM-RBCA approach, could really lead to an excessive risk overestimate.

In chapter 4 two models including biodegradation for vapor intrusion into buildings, available from the literature, have been presented:

- the Oxygen limited model;
- the Dominant layer model.

After the comparison performed between these models, it can be concluded that the biodegradation term has a remarkable effect on the prediction of the contaminant concentration in indoor environment, and the Oxygen-Limited model can be used as a predictive model in a Tier 2 risk analysis approach.

6 BIBLIOGRAPHY

[1] Hartman et al (1998) Plant Science, Growth, Development and Utilization of Cultivated Plants

[2] Hinton, T.G. , 1992, Contamination of Plants by Resuspension: a Review, with Critique of Measurement Methods, Sci. Total Environ. , 121:177-193

[3] The fate of BTEX and chloroethenes in the unsaturated zone: a literature review on processes and effects on human risks, TNO report, TNO-MEP- R 99/090;

[4] Heuristic Model for Prediction the Intrusion Rate of Contaminant Vapors into Building, Johnson and Ettinger, Environ. Sci. Technol., 1991, 25, 1445-1452

[5] APAT [2005], Criteri metodologici per l'applicazione dell'analisi assoluta di rischio ai siti contaminati rev.0.

[6] APAT [2006] Criteri metodologici per l'applicazione dell'analisi assoluta di rischio ai siti contaminati rev. 1,

[7] Indoor Vapor Intrusion with Oxygen-Limited Biodegradation for a Subsurface Gasoline Source, Devaull, Environ. Sci. Technol., 2007, 41, 3241-3248

[8] Assessing the Significance of Subsurface Contaminant Vapor Migration to Enclosed Spaces; Site Specific Alternatives to Generic Estimates, American Petroleum Institute, publication number 4674, Johnson and Kewblosky, 1998

[9] Simulating the effect of Aerobic Biodegradation on Soil Vapor Intrusion in to Building: Influence of Degradation Rate, Source Concentration, and Depth Abreu and Johnson, Environ. Sci. Technol., 2006, 40, 2304-2315

[10] Assessing the significance of subsurface contaminant Vapor Migration to Enclosed Space: Site-Specific Alternatives to Generic Estimates, Johnson, P.C. et al, Journal of Soil Contamination, 1999, 8, 3, 389-421.

[11] Evaluation of vadose zone biodegradation of BTX vapours, Hers et al., Journal of Contaminant Hydrology, 2000, 46, 233-264.

[12] ASTM (1995), Standard Guide for Risk-Based Corrective Action Applied at Petroleum Release Sites.

[13] BP-RISC 4.0 (2001), Risk-Integrated Software for Clean-up –User's manual, BP-Amoco Oil, Sunbury UK.

[14] CONCAWE (1997), European Oil Industry Guideline for Risk-Based Assessment of Contaminated Sites, Report No 2/97.

[15] DM 471/99 (1999) Regolamento recante criteri, procedure e modalità per la messa in sicurezza, la bonifica e il ripristino ambientale dei siti inquinati, ai sensi dell'art.17 del D.Lgs. 5 febbraio 1997 n.22 e successive modificazioni e integrazioni.

[16] GIUDITTA 3.0 (2003), Manuale d'uso / Allegati.

[17] RBCA Tool Kit 1.2, RBCA toolkit for Chemical Releases.

[18] ROME 2.1 (2002), ReasOnable Maximum Exposure, User Manual;

[19] Bowles, D.S. , 1987, A Comparision of Methods for Integrated Risk Assessment of Dams, in Engineering Reliability and Risk in Water Resources, L. Duckstein and E. Plate (eds.), Dordrecht: M.Nijhoff

[20] Baes, C.F. , Sharp, R.D. , Sjoreen, A.L. , Shor, R.W. , September 1984, A Review and Analysis of Parameters for Assessing Transport of Environmentally Released Radionuclides Through Agriculture, Oak Ridge National Lab Report ORNL - 5786

[21] RAIS (Risk Assessment Infrmation System), Agosto 2005, Food Chain Models for Risk Assessment, Appendix F;

[22] Rowe, W.D. , 1977, An Anatomy of Risk, Wiley, New York

[23] Travis, C.C. , e A.D. Arms, 1988, Bioconcentration of Organics in beef, milk and vegetation, Environmental Science and Technology, 22(3): 271 – 274

[24] U.S.EPA [1977], Proposed Guidance on Dose Limits for Persons Exposed to Transuranium Elements in the General Environment

[25] U.S.EPA, [1989], Risk Assessment Guidance for Superfund: volume 1; Human Health Evaluation Manual (part A), EPA/540/1-89/002;

[26] U.S.EPA, [May 1996] Soil Screening Guidance: Tecnical Background Document 2nd Edition, Office of Solid Waste and Emergency Response, Washington, DC

[27] U.S.EPA, [August 1997] Exposure Factors Handbook, Office of Health and Environmental Assessment, Exposure Assessment Group, Wahington, DC;

[28] U.S. EPA / REGION 9 (2004), Users' guide and background technical document for U.S.EPA Region 9's Preliminary Remediation Goals (PRG) table;

[29] US.EPA Exposure Factors Handbook, 2005

[30] WASY GmbH, FEFLOW 5.3: Reference Manual, 2005.

[31] WASY GmbH, FEFLOW 5.3: User's Manual, 2006.

[32] WASY GmbH, FEFLOW 5.3: White Papers Vol.1, 2005.

[33] WASY GmbH, FEFLOW 5.3: White Papers Vol.2, 2005.

[34] WASY GmbH, FEFLOW 5.3: White Papers Vol.3, 2005.

[35] WASY GmbH, FEFLOW 5.3: White Papers Vol.4, 2005.

[36] L. D'Aprile, E. Scozza "Application of environmental risk analysis at contaminated sites" Ann Ist Super Sanità 2008, vol44, No. 3: 244-251;

[37] E. Beccaloni,S.Berardi, E.Scozza "La Banca Dati Ambientale e Tossicologica: Criteri di Selezione dei Parametri e dei Relativi Valori"; Metodologie e Strumenti per la Progettazione degli Interventi di Bonifica Ambientale, Conference proceedings, March 2006.

[38] R. Baciocchi, E. scozza, "I Principi della Procedura di Analisi di RIschio", L'applicazione della procedura di Analisi di Rischio per siti contaminati. Conference proceedings, September 2006

[39] R.Baciocchi, S.Berardi, C.Ciotti, L.D'Aprile, E.Scozza, "Criteri metodologici italiani per la conduzione di analisi di rischio da siti contaminati", 8° SIBESA, Conference proceedings, September 2006